HERRING RESEARCH AND MONITORING SCIENCE SYNTHESIS

HERRING RESEARCH AND MONITORING PROGRAM
SYNTHESIS REPORT

Exxon Valdez Oil Spill Trustee Council Program 20120111

December 12, 2019

W. Scott Pegau and Donna Robertson Aderhold, editors

Prince William Sound Science Center, Cordova, AK

With contributions from: Mary Anne Bishop, Jordan Bernard, Trevor Branch, Kristin Gorman, Maya Groner, Stormy Haught, Paul Hershberger, Dave McGowan, W. Scott Pegau, Pete Rand, Mark Scheuerell, John Trochta

HERRING RESEARCH AND MONITORING SCIENCE SYNTHESIS

HERRING RESEARCH AND MONITORING PROGRAM
SYNTHESIS REPORT

Exxon Valdez Oil Spill Trustee Council Program 20120111

December 12, 2019

W. Scott Pegau and Donna Robertson Aderhold, editors

Prince William Sound Science Center, Cordova, AK

With contributions from: Mary Anne Bishop, Jordan Bernard, Trevor Branch, Kristin Gorman, Maya Groner, Stormy Haught, Paul Hershberger, Dave McGowan, W. Scott Pegau, Pete Rand, Mark Scheuerell, John Trochta

Citation:

Pegau, W. S, and D. R. Aderhold, editors. 2020. Herring Research and Monitoring Science Synthesis. Herring Research and Monitoring Synthesis Report, (*Exxon Valdez* Oil Spill Trustee Council Program 20120111). *Exxon Valdez* Oil Spill Trustee Council, Anchorage, Alaska.

Herring Research and Monitoring
Science Synthesis

Exxon Valdez Oil Spill Trustee Council Program 20120111
Synthesis Report

Study History: The existing Herring Research and Monitoring program builds upon results from two earlier integrated herring research programs (EVOSTC programs 16120111 and 10100132). The current program consists of projects 19120111-A Program coordination, 19170111-B Annual herring migration cycle, 19120111-C Modeling & stock assessment, 19120111-D Age at reproductive maturity, 19120111-E Disease program, 19120111-F Surveys and collections, 19120111-G Adult herring acoustic surveys, and 19170115 Herring genetics.

Abstract: Each of the previous research programs produced synthesis reports. This report is meant to complement the previous efforts by focusing on different aspects of the herring research. This report describes the survey designs used within the Herring Research and Monitoring program and examines research on maturity, spawn timing, movement, and disease.

The survey design chapter describes the methods used for aerial milt surveys and methods we have tested to supplement those surveys, acoustic surveys, age-sex-size sampling, and aerial forage fish surveys. We use the age-sex-size samples and age-structure-analysis model to examine what the maturity of the fish in the pre-spawn aggregations and if fish are missing from the pre-spawn aggregations. We also examine if differential growth can be detected using herring scales. We examine how the spawn timing and location has changed over the past four decades and what factors may have influenced the changes. Changes in spawning location appear to be related to large recruit classes. We examine movement of herring after spawn and find that larger fish are more likely to move to the Gulf of Alaska. Finally, we describe the principles governing the epizootiology of Viral Hemorrhagic Septicemia virus and provide an overview of *Ichthyophonous* surveillance results.

Acknowledgements: This document is a summary of works contributed by numerous scientists with funding leveraged from both non-governmental and governmental entities to provide staff time and equipment. We wish to thank all of our partners for assistance and the Herring Research and Monitoring program scientists and staff for their thoughtful contributions and reviews of this report. We also express our appreciation to the program Science Review Panel members: Sherri Dressel, Steve Martell, and Stanley 'Jeep' Rice, for their review and guidance of the Herring Research and Monitoring Program. These findings and conclusions presented by the author(s) are their own and do not necessarily reflect the views or position of the *Exxon Valdez* Oil Spill Trustee Council.

This page intentionally left blank.

TABLE OF CONTENTS

LIST OF TABLES

LIST OF FIGURES

This page intentionally left blank

EXECUTIVE SUMMARY

This synthesis of research topics related to Pacific herring (*Clupea pallasii*) is meant to build upon earlier syntheses (Norcross et al. 2001, Pegau 2013, Herring Research and Monitoring Team 2014). The report includes sections that describe the survey designs used and research on maturity, spawn timing, movement, and disease. This selection allows the description of information from all the components of the Herring Research and Monitoring (HRM) program. There are significant differences in the development of each of the topics that leads to differences in the style of presentation. For instance, the research on spawn patterns is nearly ready to be submitted as a manuscript, whereas the work on herring movement is still in the early stages. The work presented in each section is not necessarily limited to results of *Exxon Valdez* Oil Spill Trustee Council (EVOSTC) funded research. We incorporate other findings where appropriate.

The chapter on survey designs describes efforts used in the recent past or are ongoing. We do not cover how surveys that have been discontinued were conducted. Data from the surveys are used in the Age-Structure-Analysis (ASA) model to estimate the Prince William Sound (PWS) herring population. These surveys include the aerial spawn surveys, acoustic surveys, and age-sex-size (ASL) sampling. We discuss supplemental spawn detection efforts the HRM program has tried and describe the aerial forage fish surveys that are conducted in collaboration with the Gulf Watch Alaska (GWA) forage fish program.

The aerial milt surveys provide the mile-days of milt index, which is the longest running and most consistent time series of herring abundance in PWS. As such, it is critical to maintain this index to provide necessary inputs to the assessment models. The acoustic surveys provide an independent index that measures a similar portion of the herring population. The combination of the aerial milt surveys and acoustics provides an indication if one survey has unusual values. The ASL sampling efforts inform nearly every other project in the HRM program by providing age composition and weight at age for the ASA models, estimating target strength for the acoustic survey estimates of biomass, providing vessel support for spring acoustic surveys and disease sampling, and assisting with the collection efforts for tagging and maturity studies.

Because aerial milt surveys do not include areas outside of PWS and are limited by weather, we tested the deployment of people and cameras to remote spawning locations. Neither of those approaches proved to be practical for monitoring for spawn. The use of visible remote sensing works when the skies are clear. Newer satellites with very high resolution are the most appropriate for detecting spawning events.

The forage fish surveys have been conducted since 2010 and provide information on a few different forage fish including herring. We are in the process of determining if the number of schools of age-1 herring can be used to predict the size of recruitment to the spawning stock at age-3. The aerial forage fish surveys work with the GWA forage fish project to provide an indication of the forage fish distribution in waters too shallow for that program to survey. In turn, the GWA forage fish project provides validation observations of the species identification from the aerial surveys.

In the second chapter we examine the maturity of herring. The term maturity is currently used in two manners. The first is that the herring are mature enough to spawn. The second is used in the model in that the fish are available to the ASL sampling. The percent of mature (available) herring at each age is estimated by the ASA model; however, there are no independent checks of the results. A maturity function in the ASA model uses the maturity estimates to then determine the total herring population in PWS. From the ASL data we determined that not all herring in the pre-spawning aggregations are likely to spawn. By using some crude assumptions, we estimated the percentage of the herring population not observed in the ASL samples and roughly estimated the mortality over time. These estimates are in good agreement with the maturity estimates from the ASA model.

Scale growth is examined to determine whether bimodal growth distributions occur that are hypothesized to be a result of fish not spawning able to put greater energy into growth than those that are preparing to spawn. The scale growth of four cohorts (1984, 1988, 1999, 2005) were examined to see if there is evidence of bimodal growth in male and female herring. The cohorts were chosen to include two from each time block that the ASA model currently uses. Preliminary results demonstrate that both male and female herring show indications of bimodal growth in the scale records that is most evident at the older ages (age-5 and age-6). Fewer scales were imaged at these older age classes and more scales will need to be imaged before making conclusions.

A suite of eleven model runs were used to examine the question of sensitivity of the model to different assumptions about maturity and availability. The eleven model runs were meant to bound the likely range of scenarios. The model runs were also used to examine if the maturity function should be calculated in two separate time blocks. We found that the estimated biomass is not sensitive to the range of maturity scenarios. There is no value to the model in trying to separate mature and immature fish in the ASL samples. While estimating the maturity function for two time-blocks using the ASA model provides different parameters for each time block, we did not find evidence in the residuals of a change in the maturity schedule over time. Therefore, we recommend estimating a single set of maturity parameters for the entire dataset.

The third chapter examines how spawning events have changed in space and time. The location and time of spawning plays a critical role in the survival of pelagic fish during early life stages that subsequently affects recruitment to the population. This chapter examines whether changes in spawning patterns from 1973 to 2019 provide insights on factors that are inhibiting recruitment of Pacific herring to the PWS population. Our findings show substantial changes in spatial and temporal patterns of herring spawning in PWS over the past four decades, and that these changes are likely contributing to the population's lack of recovery. We attribute major shifts in spawning distributions to changes in population demographics and fishery-related effects on local spawning aggregations. In addition, major shifts in spawn timing have coincided with large-scale changes in ocean temperatures, indicating the population is also responding to external perturbations in their environment. The current state of the population (i.e., low abundance, spatially constrained spawning habitat, and lack of a broad age structure that extends the spawning period) suggests its potential for reproductive success is greatly reduced.

The movement of herring in and out of PWS is examined in the fourth chapter. Herring are tagged with acoustic tags during the spawning period. These tags can then be detected by

acoustic receivers in the entrances, near the spawning grounds, and at locations within PWS that we expect fish may pass. The tagging effort builds upon a 2013 pilot project that established that after spawning, a majority of adult acoustic-tagged Pacific herring moved from the spawning grounds in PWS, where spawning ground acoustic arrays were located, to the entrances to the Gulf of Alaska (GOA), where the Ocean Tracking Network acoustic arrays were located.

In this effort, we analyzed herring movements over a two-year period (April 2017 through March 2019) based on herring tagged in PWS during 2017 and 2018. We modeled movement probabilities between PWS and the GOA. At both Hinchinbrook Entrance and Montague Strait, herring were more likely to migrate from PWS to GOA during the spring/summer season, while during the fall/winter season herring were more likely to migrate from GOA to PWS. At the Southwest Passages, similar patterns were not observed, suggesting that the migration pathways run primarily through Hinchinbrook Entrance and Montague Strait. We found that some fish mingle around the entrance arrays, in particular those in the Southwest Passages. We found that during spring/summer season, heavier herring were more likely to move to the entrance arrays. Smaller herring were more likely to overwinter near the spawning grounds.

The final chapter examines two common pathogens affecting herring populations, Viral Hemorrhagic Septicemia (VHS) virus and *Ichthyophonus*. It is now known that VHS virus (Genogroup IVa) is highly virulent to many species of marine fishes and it periodically causes epizootics and resulting fish kills throughout the Pacific Northwest. Efforts within the Herring Disease project have identified a series of guiding principles that govern the epizootiology of VHS virus: 1) Pacific herring are highly susceptible to VHS, 2) Pacific herring are super-shedders of VHS virus, 3) Pacific herring are a natural reservoir for VHS virus, 4) Co-factors influence the potential for VHS epizootics, and 5) Acquired resistance is a critical determinant of VHS potential.

Information from these newly articulated principles can be integrated into tools capable of assessing prior population-level impacts and forecasting future disease risk. In this context, Principle #5 is the most informative, as the immune status of individuals and populations supersedes all the principles. For example, a population of immune individuals will not experience an epizootic, even if all other disease co-factors occur simultaneously (i.e., exposure to virus, cool temperatures, elevated infection pressures, etc.). Further, with annual immunological monitoring of herring population across year classes, we can deduce if, and when, epizootics occurred. This deduced exposure history can then be paired with population assessments to assess whether the epizootic was associated with a concomitant reduction in biomass or abundance.

Ichthyophonus is perhaps the most ecologically and economically significant pathogen of wild marine fishes throughout the world, based on its low host specificity, broad geographic range, and recurring association with epizootics that result in massive fish kills and population-level impacts. Natural route(s) of *Ichthyophonus* transmission in Pacific herring remain unresolved and laboratory studies have been largely unsuccessful at demonstrating transmission by host cohabitation, immersion in parasite isolates, or feeding with infected tissues or isolates. Over broad spatial and temporal scales, the prevalence of *Ichthyophonus* infections typically increases with herring size and age. This zoographic pattern is consistent with that of a chronic infection

that accumulates in a population via recurring exposures throughout the lifetime of the host. Although *Ichthyophonus* typically persists in Pacific herring at chronic levels that accumulate in populations over time, several lines of evidence indicate that the parasite may periodically contribute to negative impacts on Pacific herring population dynamics. Investigations are currently underway to understand when the typical chronic *Ichthyophonus* infections shift to a more acute form that leads to mortality.

FUTURE DIRECTIONS

While it is important to synthesize our existing knowledge, we feel it is important to identify important gaps in our knowledge as well. What investigators in the existing program identified as top areas that could use more research are herring-salmon interactions, setting PWS information in the context of the larger GOA, and research into larval survival. Salmon hatcheries have been suggested as a cause for suppressing the herring population. Existing knowledge on this topic was covered by Pegau (2013). Interactions with salmon was studied during the Sound Ecosystem Assessment program so care needs to be taken to complement the existing research. The HRM program has focused on PWS, but there appear to be larger scale connections between herring populations. For instance, recruitment patterns in PWS and Sitka have often matched, and recruitment of herring often coincides with that of pollock. Therefore, our understanding of what is limiting recovery in PWS needs to consider larger scale processes. Finally, large recruitment can come from small spawning stocks so it is likely that issues such as larval drift and match with food sources may play a large role in the success of any given cohort. Past work has examined juvenile herring and adult herring with little effort spent researching the factors affecting larval herring.

LITERATURE CITED

Herring Research and Monitoring Team. 2014. Pacific herring in Prince William Sound: A synthesis of recent findings. Synthesis report (EVOSTC Restoration project 14120111). Prince William Sound Science Center, Cordova, Alaska.

Norcross, B.L., E.D. Brown, R.J. Foy, M. Frandsen, S.M. Gay, T.C. Kline, D.M. Mason, E.V. Patrick, A.J. Paul and K.D.E. Stokesbury. 2001. A synthesis of the life history and ecology of juvenile Pacific herring in Prince William Sound, Alaska. Fisheries Oceanography 10:42-57.

Pegau, W.S. 2013. Coordination, Logistics, Outreach, and Synthesis. Exxon Valdez Oil Spill PWS Herring Survey Final Report, (Restoration Project 10100132), Prince William Sound Science Center, Cordova, Alaska.

CHAPTER 1 PWS HERRING SURVEY DESIGNS

Stormy Haught[1], W. Scott Pegau[2], Pete Rand[2]

[1] *Alaska Department of Fish and Game, Cordova, AK*
[2] *Prince William Sound Science Center, Cordova, AK*

INTRODUCTION

Pacific herring (*Clupea pallasii*) begin sexual maturation at the end of summer and progress through winter, reaching full sexual maturity in the early spring months. As they reach maturity, herring migrate from overwintering areas and form aggregations in or near spawning habitat in shallow coastal waters, typically large bays and inlets (Hay 1985). Herring spawn primarily in the subtidal zone from about 0-4m in depth, although deeper spawning events do occur, and select for habitats with aquatic vegetation present for egg deposition (Gerke 2002). Herring spawning activity is typically conspicuous; milt concentration turns water cloudy white and the herring school attracts high concentrations of herring predators such as gulls, sea lions, and other marine mammals (Hay and Kronlund 1987). These factors make herring spawning season an ideal time to collect data regarding overall herring biomass, spawning habitat utilization, and herring predator populations in Prince William Sound (PWS). Aerial spawn surveys occur throughout the spawning period, and Age-Sex-Size (ASL) surveys target both pre-spawning and spawning herring. Herring aerial survey and ASL methods for PWS are documented in Shepherd and Haught (2019). Acoustic surveys target the pre-spawn population as well.

These surveys provide essential data inputs to the current Bayesian Age-Structure-Analysis (BASA) model used to estimate the historical biomass. The BASA model results are used by the Alaska Department of Fish and Game (ADF&G) to project pre-fishery run biomass a year ahead for management. The formulation of the BASA model is provided in Muradian et al. (2017).

AERIAL SPAWN SURVEYS

Aerial surveys in PWS to document spring herring biomass have been conducted since the early 1970s and were the primary management tool prior to the development of the first statistical catch-at-age model or age-structured-assessment (ASA) model in 1988 (Brady 1987, Funk and Sandone 1990). The surface area of herring schools observed during aerial surveys were converted to biomass by using equations developed from paired purse seine and aerial survey observations (Brady 1987, Lebida and Whitmore 1985). Herring arrive on the spawning grounds over time and pre-spawn herring may stage for several days or more prior to spawning. Because of this, the same herring may be observed during multiple aerial surveys (Brady 1987). Therefore, the biomass over several days of surveys cannot necessarily be added to estimate the total or peak biomass. Peak biomass was therefore calculated as the largest biomass observed in all areas on a single survey (Brady 1987).

The variable bathymetry of PWS herring spawning areas has a large influence on the ability to observe herring schools (Brady 1987). Herring may spawn in shallow bays (e.g., Rocky Bay),

shallow beaches (e.g., Hells Hole beach), or deep bays (e.g., Fairmont Bay). The influence of bathymetry on observer efficiency makes a biomass index less likely to be comparable across years. In the 1980s these problems with estimating biomass from aerial surveys caused the department to investigate the use of an index of spawn from observations of milt (Brady 1987, Funk and Sandone 1990). The two indices considered for spawn documented from aerial surveys were 1) discrete miles of milt over the season and 2) the sum of miles of milt for all survey days (mile-days of milt). The advantages of milt observations compared to school biomass observations are 1) herring likely spawn once each year, but a herring school may be observed for many days prior to or after spawning and 2) milt is relatively easy to observe from the air on beaches and observation efficiency is generally not influenced by ocean bathymetry (Brady 1987).

Discrete miles of milt do not account for multiple spawning events in the same area, so are unlikely to be a good index of total abundance in areas with multiple spawning event days on the same beach (Brady 1987). Mile-days of milt likely provide a better index to abundance as they account for multiple spawning events on the same beach but may be biased if the number of surveys vary significantly across years (Funk 1994). Additionally, although bathymetry will likely not influence observation of spawn, it will influence the biomass of spawning fish for each linear mile of milt observed. Willette et al. (1998) collected paired spawn deposition survey estimates and aerial survey estimates of miles of milt, and the short tons per mile of milt were much larger on Montague Island as compared to tons per mile of milt in northern or northeastern PWS.

In 2008, ADF&G began using a tablet computer and a geographic information system (GIS) application to collect aerial survey data (Bochenek 2010). Because digital maps are scalable and allow much more data to be added to a small area (contrast with the 25 paper maps used prior to 2008), and because of interest in herring predators distribution and abundance, additional effort was employed in documenting numbers and locations of predators such as Steller sea lions (*Eumetopias jubatus*), humpback whales (*Megaptera novaeangliae*), killer whales (*Orcinus orca*), Dall's porpoises (*Phocoenoides dalli*), and bird aggregations (mostly gulls) associated with herring schools or spawn. In 2001, ADF&G began extensive photo documentation of aerial survey observations, and more recently (2014) have collected video of most surveys. Photo and video documentation are now used to validate GIS collected milt extents post-season.

Aerial surveys generally begin in mid to late March or earlier if there are reports of herring aggregations, spawn, or large predator aggregations. The first survey usually covers the eastern side of PWS because the spawn timing is generally earlier on the east side (Port Gravina and Port Fidalgo), however the first survey may be expanded based on boat or pilot reports from other areas. Surveys continue once or twice a week until herring schools or spawn are detected by a survey flight or reported by other pilots or boats. Once spawning begins surveys are conducted daily in the area where spawn is detected if weather conditions are appropriate. Surveys are expanded to other portions of the PWS area (North shore, Naked Island, Montague Island, and Kayak Island) in April or based on pilot or boat reports. Survey interval, duration, and area are adjusted in-season to allow available funding to last until approximately mid-May.

ADF&G provides cooperating researchers (National Oceanic and Atmospheric Administration, Prince William Sound Science Center, ADF&G, and U.S. Geological Survey) the results of individual aerial surveys daily. Typically, electronic copies of the surveys (Figure 1-1) are provided to cooperators within 4 hours of flight completion. These surveys identify the extent of the aerial survey, locations of marine mammals, location and relative size of herring schools, and linear extent of observed herring spawn. Researchers use this information to monitor species associated with herring spawning activity and to anticipate the timing and extent of the spawning events.

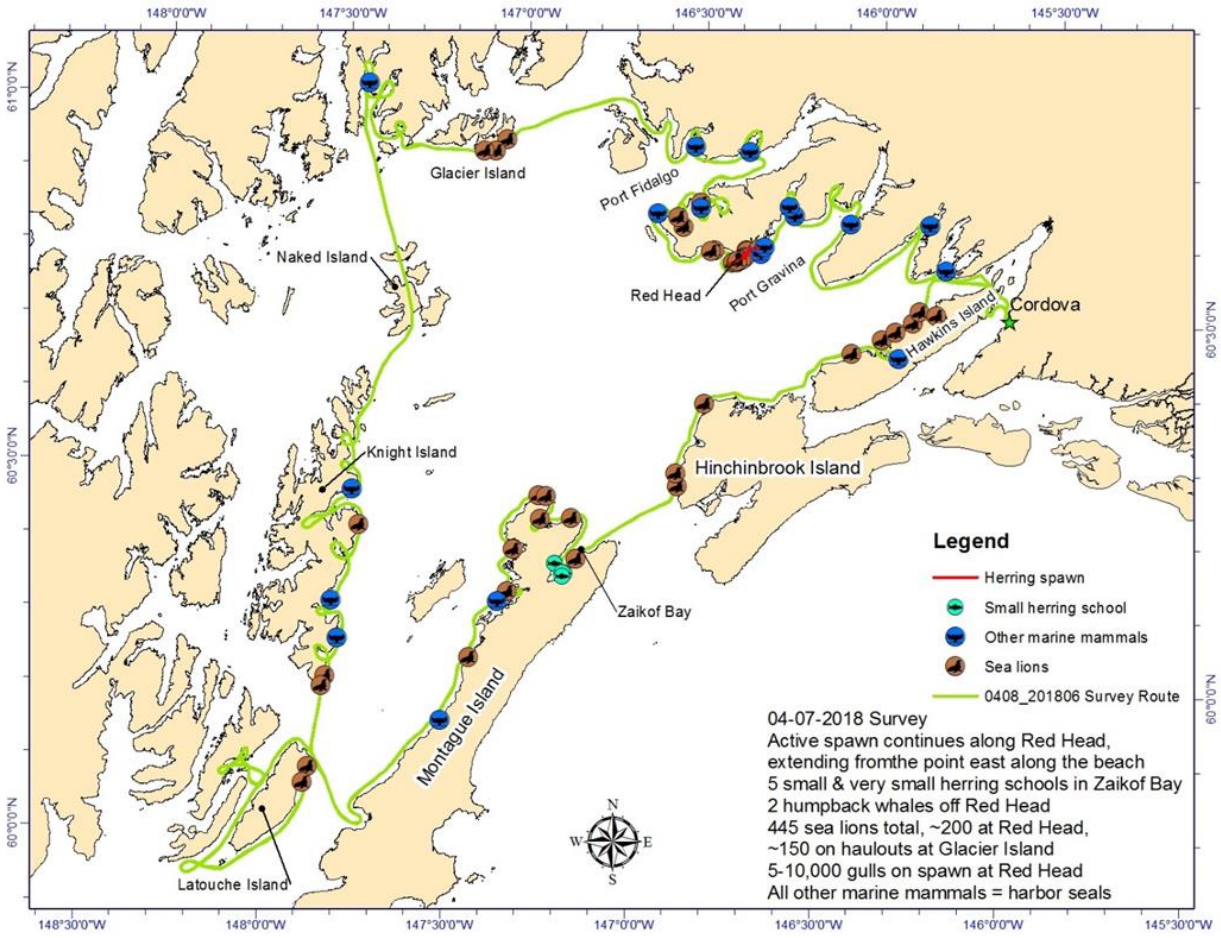

Figure 1-1. Example of a large-scale herring spawning survey flight path and the observations being collected in Prince William Sound, AK.

Surveys are conducted in a float equipped, fixed-wing aircraft flying at an elevation of ~1,200 feet. Primary and secondary observers are used for each flight. The primary observer sits in the back seat and uses a tablet computer to enter survey metadata in a spreadsheet and georeferenced survey data in an ESRI ArcPad application connected to a Bluetooth GPS (Bochenek 2010). The primary observer also attaches a camera to the inside of the back window facing out to collect either video or a still image every 1 or 2 seconds.

The secondary observer sits in the front passenger seat and reports observations to the primary observer, collects observations on paper maps as a hardcopy duplicate in case of digital failure, deploys a handheld GPS as a backup to the Bluetooth capable GPS, and takes georeferenced photos with a GPS-enabled digital single lens reflex (DSLR) camera and fast lens (F2.8) of spawning events, large biomass aggregations, and large herring predator groups. Measurements made during the survey include estimating the linear extent of milt, estimating the biomass of herring schools from surface area, estimating the number and species of marine mammals at a location, and estimating the number of birds at a location.

Herring spawn activity is located visually through discoloration of water by the presence of herring milt (Figure 1-2). The linear extent of miles of milt are estimated visually utilizing landmarks, coastal features, and detailed GIS shapefiles and are digitized directly into the ESRI ArcPad file on the survey tablet using a stylus. Spawn activity is assigned a qualitative descriptor based on density and extent of discoloration: active light, active medium, active heavy, dissipating, and drift (Biomass of individual herring schools is estimated using a surface area to short tons (st) conversion (Lebida and Whitmore 1985, Brady 1987). A sighting tube with a known focal length is used to calibrate observer estimation of surface area on a few herring schools at the beginning of each survey. Gridlines within the sighting tube provide a visual reference for known ground distances at a given elevation. Herring school sizes can then be estimated based on the surface area proximity to gridlines within the tube and are generally split into 3 classifications with corresponding biomass conversions: Small, Medium, and Large (Table 1-2). Very large and/or irregularly shaped schools are visually separated into Small size class sections and the total number of these sections enumerated for the school. Size classes are used as guidelines for estimating biomass of schools that fall in between the general classifications.

Table 1-1). These categories are recorded in the database associated with the digitized shapefile. Precise estimation for miles of milt are calculated later using ArcGIS measurement tools after the survey data has been reviewed and correlated with digital photographs and video from the survey.

Figure 1-2. Discoloration of water due to presence of milt from herring spawning activity.

Biomass of individual herring schools is estimated using a surface area to short tons (st) conversion (Lebida and Whitmore 1985, Brady 1987). A sighting tube with a known focal length is used to calibrate observer estimation of surface area on a few herring schools at the beginning of each survey. Gridlines within the sighting tube provide a visual reference for known ground distances at a given elevation. Herring school sizes can then be estimated based on the surface area proximity to gridlines within the tube and are generally split into 3 classifications with corresponding biomass conversions: Small, Medium, and Large (Table 1-2). Very large and/or irregularly shaped schools are visually separated into Small size class sections and the total number of these sections enumerated for the school. Size classes are used as guidelines for estimating biomass of schools that fall in between the general classifications.

Table 1-1.–Herring spawning activity classifications by presence and extent of milt.

CLASS	Description	Example photo
Active Light	Fish actively spawning, but little milt in the water and very light coloring. Usually some marine mammals (sea lions, harbor seals, or harbor porpoises) or sea birds associated with the spawn.	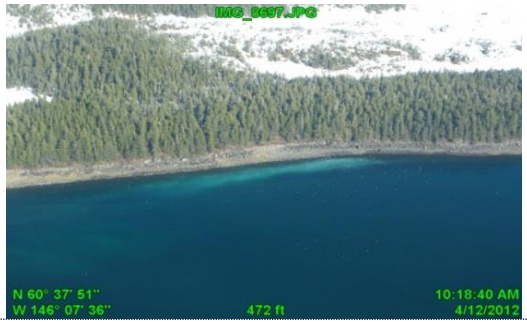
Active Medium	Fish actively spawning and moderate amounts of milt in the water and much lighter coloring. Almost always some marine mammals (sea lions, harbor seals, or harbor porpoises) or larger groups of sea birds associated with the spawn.	
Active Heavy	Fish actively spawning, and large amounts of milt in the water. The color is usually bright white to blue green. Almost always larger groups of marine mammals (sea lions, harbor seals, or harbor porpoises) or sea birds associated with the spawn.	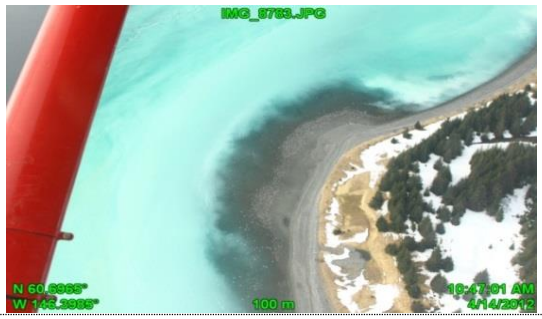
Dissipating	Milt that is likely from the previous day. Very dispersed with few marine mammals. May still be many sea birds on the beach eating eggs. Generally not included in our summary of mile-days of spawn unless we did not document the active spawn previously.	

CLASS	Description	Example photo
Drift	Areas of milt that have drifted with the current offshore or away from the areas of active spawn. For example, tides or currents regularly cause milt to drift offshore for up to a mile or more off points. Drift is not summed with active spawn for calculating the total extent of spawn.	

Table 1-2.–Herring school size class and corresponding surface area, diameter, and biomass.

Size Class	Surface Area	Diameter	Biomass
Small	1962 ft^2 (181 m^2)	50 ft (15.2 m)	10 st
Medium	7850 ft^2 (725 m^2)	100 ft (30.4 m)	40 st
Large	31400 ft^2 (2902 m^2)	200 ft (60.8 m)	160 st

Surface area of herring schools for the remainder of the survey is estimated visually without the sighting tube after calibration. Herring school observations and size estimation are entered as point data in the tablet's ArcPad application georeferenced via GPS or placed with the stylus based on landmarks and map features.

Marine mammal sightings are recorded in the tablet ArcPad application as point data and avian aggregations are recorded as line data by using GPS and spatial landmarks, identified at the species or type level (e.g., Stellar sea lion, gulls). Marine mammal abundance is directly counted for small groups (~<30) or estimated for larger groups (~>30).

After each survey all electronic data are transferred to the local Cordova ADF&G network. ArcPad data are downloaded from the tablet for processing with ESRI ArcMap. DSLR photos are transferred for editing with Adobe Lightroom. The handheld GPS is downloaded with DNRGPS software. Videos or images are downloaded from the video camera using either GoPro Quik or Garmin VIRB software. Observations on paper maps are examined for complete survey information and stored for use in post-season processing.

At the end of the survey season, milt locations, classification and lengths are adjusted by comparing data collected on the GIS application to the digital photography and video imagery. Estimates of large marine mammal aggregations (~>30) are adjusted by counting individuals from survey photographs. Georeferenced survey photographs are transformed into shapefiles.

After adjustments are complete, the individual survey GIS data are combined into shapefiles for the year and then added to the historical GIS shapefiles. These historical shapefiles allow

comparison across all years for milt observations (1973–2019), survey routes (1997–2019), sea lion location and abundance (currently 2008–2019), other marine mammals (currently 2008–2019), and birds (currently 2008–2019).

All raw and processed data and metadata are then provided to the Herring Research and Monitoring (HRM) program research workspace and the Alaska Ocean Observing System data portal for accessibility by researchers, the public, and agencies.

Supplemental Milt Detection Methods

Because aerial surveys can be limited by flight conditions and are limited in geographic coverage, we have tried a few different methods to supplement the aerial observations. We have paid particular attention to getting spawn information from Kayak Island because it is not part of the regular survey route. Our efforts include both local observations and satellite observations.

Local observers and remote cameras

Local observations that were tried included having personnel near expected spawning locations to report in spawn observations and the mounting of cameras that transmitted photographs every six hours. We sent a pair of observers with a small drone to Kayak Island. The desire being to get local observations in a greater variety of weather conditions and to be able to call in or photograph any spawn event. A remote camp was necessary because there are no facilities near the northern end of the island where most of the spawn occurs. Spawn is expected to occur in both early and mid-April. This is a cold and wet time of the year and personnel needed to cross the width of the island to be able to determine if spawn was occurring on either side. In the end the combination of the size of the area to be covered and the living conditions on the island made us to decide that the approach was not feasible for regular monitoring for spawn.

We also attempted to monitor spawn events using remote cameras. We deployed two remote camera systems that transmitted photographs by satellite to allow us to monitor likely spawn areas. The cameras were mounted at the top of approximately 30m tall bluffs that overlook the beaches on Kayak Island (Figure 1-3). We obtained photographs four times each day. Generally, the mid-day photograph was the best of the four. The large tides and extensive reefs along this shore resulted in very large changes in how much of the image covered water. Even though we know of at least one spawn event that was covered by the cameras because of aerial observations, we were not able to clearly detect spawn in any of the images. We did note large changes in bird activity that occurred after a spawn event. We believe our uncertainty in the detection of spawn is due to the low angle that the cameras had to the beach even though they were mounted on a bluff overlooking the beach. Thus, the cameras provided indirect evidence of spawn through the observation of bird activity but were not of value in knowing when a plane should be sent to cover potential spawn events.

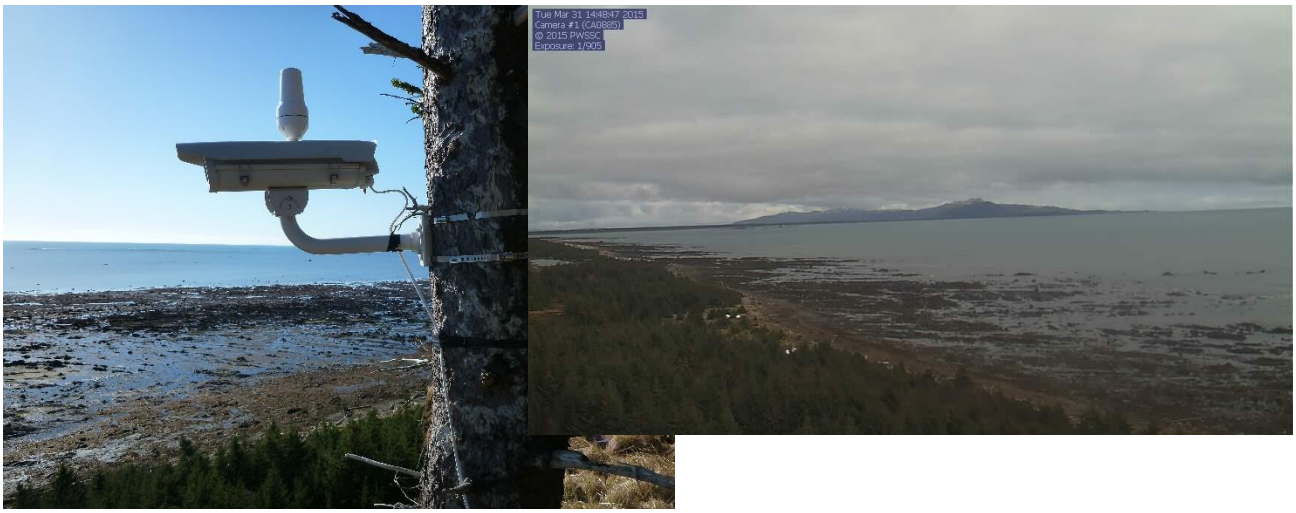

Figure 1-3. The camera as mounted overlooking a reef on Kayak Island is shown (left). An image from the camera is shown on the right.

SATELLITE IMAGERY

Satellite observations have been used for the purpose of detecting spawn to send an aircraft for direct observations and to detect spawn that may have been missed by the regular aerial surveys. True color images from satellite imaging in the visible portion of the spectrum were used. Satellites operating in the visible spectrum are not able to image the ocean through clouds, which is a major limitation for use in the northern Gulf of Alaska. Other important considerations are how often the satellite images an area and the resolution of image.

Initial efforts used MODIS imagery. The MODIS satellites are designed for ocean and terrestrial color measurements with a pixel size of approximately 1 km x 1 km. Typically the sensor would image PWS about two of every three days. Because of the low resolution of the MODIS imagery the only very large areas of spawn are detectable. The spawn at Kayak Island is one of the few that has been detected using the MODIS imagery. We did detect spawn using the satellite images and were able to fly out and confirm it (Figure 1-4).

In 2019 we tested the use of the much higher resolution planetscope satellite constellation that is available through planet.com. As with the MODIS imagery, these satellites cannot be used when clouds are present. The resolution (< 5m) of these satellites does allow for the detection of much smaller spawn events (Figure 1-5). Imagery began in 2009 so there is some ability to search for undetected spawn events in earlier years. A limitation is that the imagery is only available on a subscription basis. There is free (or low cost) high-resolution satellite imagery available for the European Sentinel Satellite system. The coverage of that system is very limited.

The high-resolution satellite imagery does allow for much greater spatial coverage than is available from aircraft but remains limited by cloud cover and temporal coverage of the area.

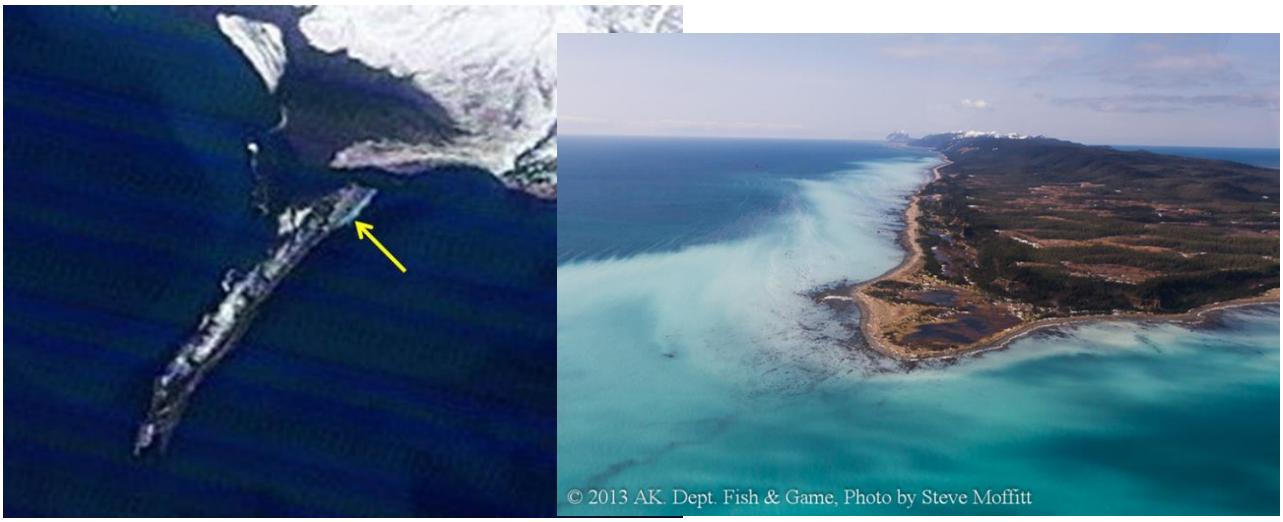

Figure 1-4. Satellite image of herring spawn off Kayak Island (left) and an aerial view of the same event (right).

Figure 1-5. Herring spawn March 31, 2019 from Knowles Head to Red Head in Prince William Sound.

ACOUSTIC SURVEYS

The objective of the acoustic survey is to provide an index of herring spawning biomass in PWS on an annual basis. The survey has been conducted in the spring (late March to early April) since 1993. The estimate of herring biomass from this survey assumes that the fish located in the pre-spawning biomass are mature. Based on data on maturity in past ASL surveys at the time of the spring acoustic surveys, the majority of the biomass measured is likely to be spawners, but immature fish do make up a component of the catch.

THREE-STAGE SURVEY DESIGN

The survey design requires flexibility to account for heterogeneity in the herring distribution from year to year. The survey is based on a three-stage survey design that is described in a number of publications (e.g., Thomas and Thorne 2003). The three stages are described in detail below:

1. *Locate aggregation(s).* We rely on several sources of information on distribution of herring to decide which regions to focus on. Traditionally there have been western and eastern spawning aggregations, with the former located mostly near the northeast coast of Montague Island (including Zaikof Bay, Rocky Bay, and Stockdale Harbor), and the latter located in Port Fidalgo and Port Gravina. Smaller aggregations have been observed in other parts of PWS, but have not been consistently surveyed, and we assume they are (collectively) a small contributor to the PWS spawning population. We rely on a combination of observations from aerial surveys conducted by ADF&G, early-season ship surveys contracted through the Prince William Sound Science Center (visual observations and ship-board sonar), and more anecdotal observations from other flights, vessels, or observations by residents of coastal communities (e.g., Tatitlek). Indicators of pre-spawn herring include direct observations of schools and foraging activity of herring predators, including whales, sea lions, and seabirds.

2. *Conduct systematic survey within the spatial sampling frame.* Once evidence of aggregations exist, cruises are planned to those regions with scientific echosounder equipment (we currently use 70 kHz and 120 kHz echosounder systems produced by Biosonics). While the surveys are typically conducted at night, daytime observations (visual, as well as ship-board sonar) are gathered to provide additional information on distribution of schools, although many herring are close to the seabed during the day and may not be detectable by sonar. The sample frame is defined to encompass the aggregation and a series of parallel zigs and parallel zags (approximately 2km separation) are charted to serve as the survey transects. The sampling frame is informed by the spatial patterns in herring schools and predators observed during the day. The largest aggregation, typically observed in Port Gravina, encompasses approximately 8 km of shoreline (from mouth of St. Matthews Bay to Red Head), and transects extend just beyond the 60m isobath (some transects pass over depths > 80 m). In Gravina we have included 8 separate transects (4 zigs and 4 zags) that add up to a total transect length of approximately 12-15km. This is equivalent to a systematic survey with evenly spaced transects within the established sampling frame. We begin the survey at dark (typically

about 10-11 PM), and the survey takes approximately 4-5 hours to complete. Conducting acoustic surveys at night is advantageous as schools are generally higher in the water column and individuals are more dispersed, which decreases the likelihood of acoustic shadowing which tends to produce bias in acoustic surveys. Our transducer is fixed down-looking on a towfin, and the towfin is towed about 1 m below the surface. Vessel speed is approximately 2-3 knots, and all ship-board lights are turned off. Sonar pulse width is set at 0.4 ms, with a ping rate of 1 per second. Similar survey designs are established in other regions to accomplish our main objective. An effort is made to repeat the survey over consecutive nights to provide an estimate of precision on our biomass estimate, although this has been difficult in recent years as herring distribution is more ephemeral and the "staging period" prior to spawning appears to now be very brief. As a result, we have not been able to obtain estimates of precision in recent years.

3. *Estimate mean target size in the surveyed aggregation.* We coordinate with another vessel (ADF&G vessel, *R/V Solstice*) to carry out the third stage involving direct capture of herring to estimate mean target size. We use an established relationship between target strength and backscatter (dB re m^{-2}, Thomas et al. 2002) that requires an unbiased estimate of the mean herring length in the surveyed aggregation, ideally collected in each region during the same night of the acoustic survey. In past surveys (particularly one conducted during daylight hours when schools are generally deeper), target strengths are adjusted to account for gas bladder compression at depth (Thomas et al. 2002). This has not been required in recent years as the mean depth of aggregations in nighttime surveys have not diverged from the depths at which the relationship was established (herring at ~ 40 m depth). ADF&G summarizes length at age and age composition of the net-captured individuals. We compute a mean length weighted by the age composition. The preference is to rely on purse seine catches, as this gear is the most effective at sampling aggregations (generally deeper, and less selective than other gear). In past years, data on sizes were obtained from other capture gear when purse-seines were not deployed or were not effective (including cast nets and multi-mesh gill nets).

DATA COLLECTION, PROCESSING, AND ANALYSIS

Acoustic data and GPS coordinates are saved during the survey as *.DT4 files on a laptop networked to the Biosonics DTX echosounder. Calibration of the system involves recording target strength (dB) of a tungsten carbide sphere suspending by monofilament at 5-10 m below the face of the transducer (at least 300 echos are recorded, recording lasts about 5 minutes). This is typically done once a season at a location near the survey area just prior to a night's survey. These calibration data are also saved in a separate *.DT4 file. Calibration results have been stable over time and no adjustments to results have been needed.

Data from each night survey are first processed using Echoview (v. 5.0) to perform vertical echointegration. This software automatically detects bottom and creates a line. Some errors in bottom detection occur, so each echogram is visually inspected, and the bottom line is adjusted accordingly. The data are filtered (-60 dB threshold) to remove smaller, non-fish targets. An image file (PNG) for each night's transect is produced from the software for use in the annual report (see example,

Figure 1-6). The echo intensity is binned in cells by depth. These calculations are performed within Echoview and the backscatter measures (area backscatter coefficient, s_a (units m^2 m^{-2}), or nautical area backscatter coefficient (s_A, NASC, units m^2 nm^{-2})) are exported in a comma delimited file. We limit the echointegration to the top 60 m of the water column. It should also be noted that the transducer is suspended approximately 1 m below the surface when the ship is underway on a transect, and we exclude data 1 m below the transducer face, the so-called blind zone due to transducer ringing and limited sampling volume. Thus, the ensonified survey area extends from ~ 2 m below the surface down to 62 m below the surface. Acoustic sampling with a transducer mounted upward-facing on the seabed near Hell's Hole in Port Gravina in 2016 indicated the herring aggregations were well below 2 m of the surface during the night, a distribution that likely limits exposure to surface herring predators (Rand 2018). This sampling, performed autonomously (i.e. no effects from the presence of a ship), indicated that our annual survey is not missing herring near surface. If deeper aggregations are encountered (particularly if any surveys are conducted during the day), we adjust the lower depth threshold to extend the survey area into deeper water.

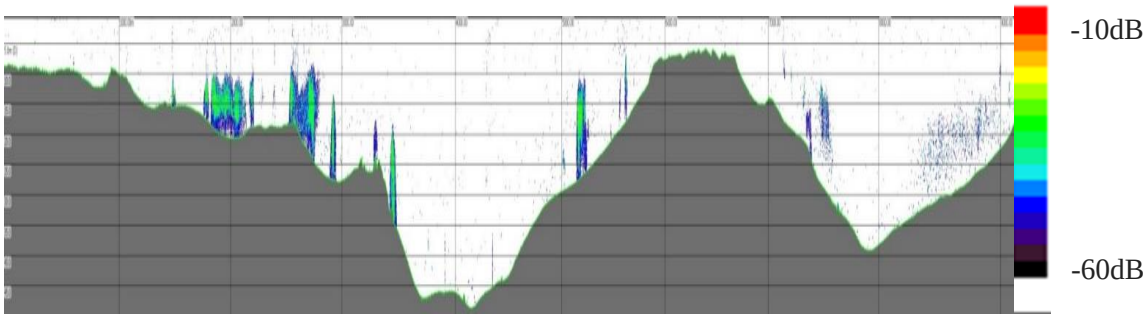

Figure 1-6. Echogram from transects conducted off Hell's Hole in Port Gravina, Prince William Sound during April 2016. Horizontal bars represent 10 m depth strata, and vertical bars represent 1 km intervals determined from GPS tracking of the vessel during the survey. Acoustic data shown are filtered by applying a minimum threshold of -60 dB.

The second and final analysis step involved uploading the output from Echoview in R statistical software to estimate the echo intensity of an individual herring target, estimate the biomass of herring along the transect, and extrapolate to the sampling frame to estimate herring biomass in the survey area. We first produce a map with the cruise track with backscatter measures represented using a false-color spectrum (Figure 1-7). This provides a plan view that highlights locations along the transect where herring schools were encountered. The R code estimates the average biomass estimate across pings along the entire transect, and this average is applied over the spatial extent of the sampling frame described above.

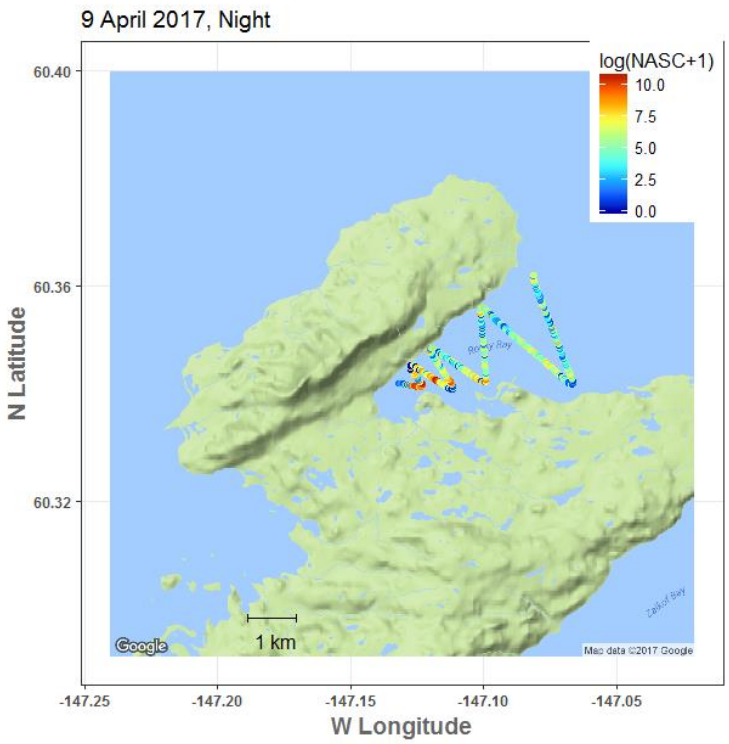

Figure 1-7. Example transect conducted in Rocky Bay in Prince William Sound in April 2017. Colors along transect reflect backscatter (NASC, defined in text) integrated from the surface to 60 m depth. Acoustic data shown are filtered by applying a minimum threshold of -60 dB.

The computation is as follows:

$$TS_w = -5.98\, log_{10}\,(L) - 24.23$$

where TS_w = target strength (dB re 1 kg herring) and L = standard length of herring (in cm). A backscatter scaler is computed as:

$$\sigma_{bs} = 10^{TS_w/10}$$

which represents the backscatter relative to 1 kg of herring (units $m^2\,kg^{-1}$).

The value of this may be adjusted in cases where herring depth distribution diverges from ~ 40 m. We then estimate average total backscatter per ping along the entire transect as:

$$\bar{s_a} = \sum_0^n s_{a,n}/n$$

where $\bar{s_a}$ is the backscatter per ping (m^2 m^{-2}), and *n* is the number of pings along the transect. Biomass is calculated as:

$$Biomass = \bar{s_a}/\sigma_{bs} * SA * 1000$$

where SA is the total survey area estimated by computing the subset of points that lie on the convex hull (chull routine in R, in m^2), and 1000 converts kg to mt.

In cases where precision of the estimate is calculated, we produce two estimates per survey-night (1 estimate derived from the transect zigs, and the other from the transect zags) and, when conducted over multiple nights, we estimate the mean and variance of biomass by considering each estimate as independent and drawn from a normal distribution. This has not been possible in recent years given the lack of evidence that the population is closed (no immigration or emigration from the survey area) over consecutive nights. Precision of the survey has been estimated during a period of overall higher abundance (CV range of 4.5-13.3% during 1993-2001, Thomas and Thorne 2003). It appears fish behavior has changed since these earlier surveys with fish likely moving in and out of the study area over multiple days, and this has frustrated efforts to estimate survey precision.

AGE, SEX, AND SIZE (ASL)

Age, sex, and size data from Pacific herring have been collected from commercial fisheries and fishery independent research projects since the early 1970s. Numerous gear types have been used to collect herring over the life of the dataset. The most commonly used gear types are an anchovy seine and cast nets. The seine is used to sample the pre-spawn population and cast nets are used to collect spawning fish.

The ASL processing methods are outlined in Baker et al. (1991) and have been followed with only a few changes through time. Samples are stratified by area, time, and gear. Sample sizes (n=450) are set to estimate the age composition of each sample to within ±5% of the true proportion 90% of the time (Thompson 1992) assuming no more than 10% of the scales are unreadable. Herring are collected in the field and frozen in large 6 mm plastic bags with labels inside the bag that document the date, time, location, gear, samplers, and the number of bags. Other information including the coordinates of the sample location are collected and added to a sample log. Often more than 450 fish are collected, so an equal number of fish are randomly selected from each bag for processing to meet the sample goal. A sixty fish sample is used for disease prevalence measurements. From the fish selected for processing, 10 fish at a time are place on a tray and their length measured to the nearest mm (standard length, tip of snout to hypural plate (Figure 1-8. Standard length (tip of snout to end of hypural plate) and fork length measurements (tip of snout to fork of tail).), whole weight to the nearest gram collected from an electronic balance, sex determined from examination of the gonads (1=male, 2=female, 3= unknown), and gonad condition estimated from examination of the gonad (scale of 1, undeveloped, to 8, recovering from spawning). All these data are collected directly into an electronic fish measuring board or measured manually and entered directly to an electronic

datasheet. The precision of length measurements collected on the electronic fish measuring board have been tested and are within ±1mm. Weights are collected with an electronic balance that is checked with calibration weights (and recalibrated if necessary) prior to each sampling event.

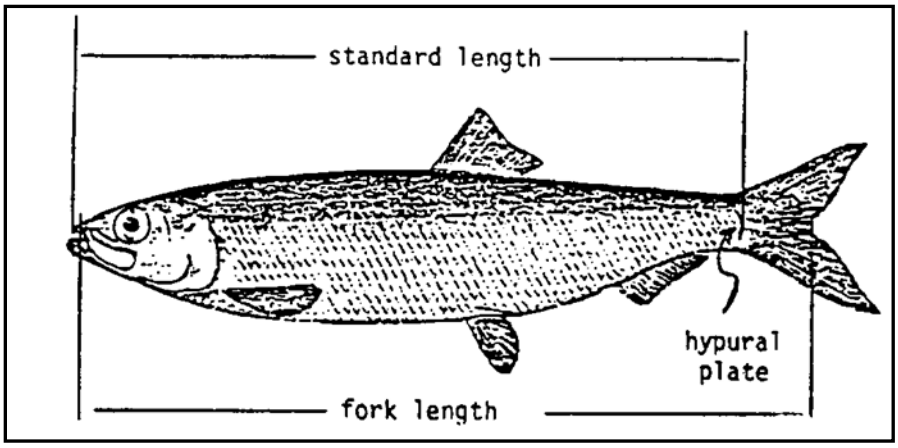

Figure 1-8. Standard length (tip of snout to end of hypural plate) and fork length measurements (tip of snout to fork of tail).

A scale is then collected from the left side of the fish from a preferred area if possible (Figure 1-9. Preferred areas for collecting scales for age from Pacific herring. Numbers are in order of preference (#1 is most preferred). Scales are collected from the left side of fish when possible.). The preferred area is above the lateral line and 3-4 rows of scales back from the operculum. This area generally has symmetrical growth patterns and distinct annuli. Scales are cleaned and placed on a pre-labeled glass microscope slide after dipping in a solution of 1:10 mucilage glue to water. A single scale from each of 10 fish is placed as two rows of 5 scales on each slide. Scales are viewed on a microfiche to ensure they are readable for age (not regenerated) and useable for measuring growth increments. If they are not useable to interpret age or measure growth increments, another scale is collected and examined. After all scales are checked they are covered with a second slide and taped together at the label end of the slide. All slides are stored in a labeled box or cabinet tray until examining for age. ADF&G currently has an archive containing approximately 210,000 scales and paired size data with most of the archive collected since 1979. Summaries of many of these data have been published (e.g., Funk and Sandone 1987, Funk and Sandone 1990, Willette et al. 1998). Scales from this archive were imaged and used in a project titled “PWS Herring Program - Scales as growth history records.”

Scales are examined for age interpretation on a microfiche reader. Scales are read by the lead ASL biologist or by a group 2 or 3 technicians. In cases of multiple readers, ages are interpreted independently and then the committee discusses any differences before agreeing on an age by consensus. The lead ASL biologist spot checks all samples to reduce the chance of reader drift in age interpretation. Ages are keyed into the spreadsheet once age interpretation from scales is completed. Age, sex, and size composition summaries that include sample size and percentage by age class and sex, mean and standard deviation by age class and sex for weight and standard

length are generated. Historical data (1973–present) are currently stored and summarized in spreadsheet form and in a web-based PWS herring relational database.

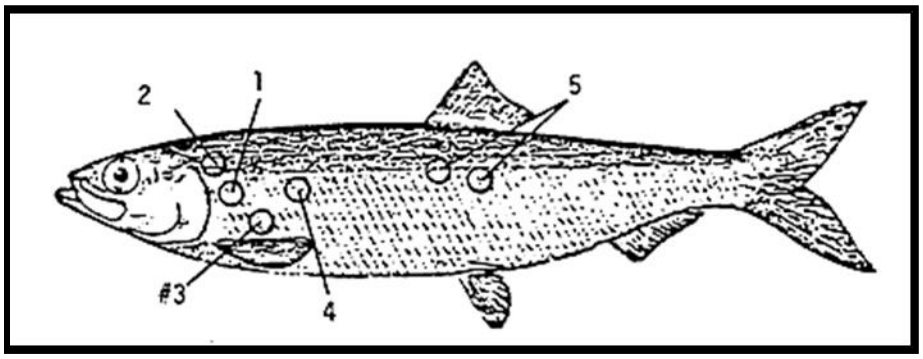

Figure 1-9. Preferred areas for collecting scales for age from Pacific herring. Numbers are in order of preference (#1 is most preferred). Scales are collected from the left side of fish when possible.

Detecting a change in the sex, age, or size composition among areas will depend on sample collection; however, annual collections have exceeded 1,000 fish per year since 1981 with a median of 5,300 fish (1982–2014). Age interpretations have been compared across areas in past (e.g., Brannian 1988).

Aerial Forage Fish Surveys

Aerial surveys of forage fish, including herring, have been conducted since 2010. One aspect of the aerial forage fish surveys is the collection of information on age-1 herring that then can be used for refining the prediction of the age-3 recruitment to the spawning population. The surveys also provide information to the Gulf Watch Alaska Forage Fish project. Coordination between the aerial surveys described here and the boat surveys of the Forage Fish project allows greater coverage than either survey could accomplish on its own and allows for validation sampling for the aerial survey identifications.

Aerial shoreline census survey methods follow those established during the Sound Ecosystem Assessment and Alaska Predator Ecosystem Experiment (Brown and Moreland 2000, Norcross et al. 1999). Aerial surveys are conducted from a Cessna 185 float plane traveling at speeds of 200-240 km/h and a target altitude of 300 m. Surveys are flown parallel to shore, but we occasionally circle back to verify observations when school densities are high. The entire PWS coastline is flown. It normally takes twelve to fourteen days, flying four to five hours in a day, to complete a survey of the entire Sound. The section of the Sound flown on any particular day depends on the weather and aircraft schedule. The completed sections are mapped on the aircraft's GPS and on a paper map to ensure there are no gaps in coverage. Surveys are flown in the month of June to reduce identification errors caused when age-0 herring and sand lance (*Ammodytes hexapterus*) become visible, typically in July.

There are two observers in the aircraft on each flight. The primary observer counts and identifies the schools while the secondary observer records the observations and looks for schools on the

other side of the plane. The primary observer is the one on the shoreline side of the plane where most schools are observed. The primary observer has at least two years of aerial survey experience. Observations during flights are collected on the location, altitude, number, and size of schools of forage fish. A GPS is used to provide position information to an electronic recording platform and paper logs are kept as a backup record. Norcross et al. (1999) contains a detailed description of the survey design and analysis of errors associated with observations.

The schools are identified by species (Pacific herring, Pacific sand lance, capelin (*Mallotus villosus*), and eulachon (*Thaleichthys pacificus*), and unknown forage fish) and herring are classified by age (1 or 2+). Age-1 herring are just over a year old in June and age-2+ herring are any herring older than one year old. Species identification is based on characteristics of the school including color, shape, location, and evidence of flashing as herring roll within a school. Herring schools tend to be round (Figure 1-10) and the tendency of individuals within schools to roll creates a telltale flash of light. Younger (smaller) herring show a finer pattern of flashing compared to older fish. Adult herring (age 2+) tend to form larger schools in deeper water than age-1 herring. Sand lance schools tend to be darker in color, irregularly shaped and in shallow areas with sand and gravel habitats (Figure 1-10; Norcross et al. 1999, Ostrand et al. 1998). Capelin tend to form large, cresent-shaped schools, whereas eulachon form very large shoals primarily associated with offshore waters and the Copper River Delta.

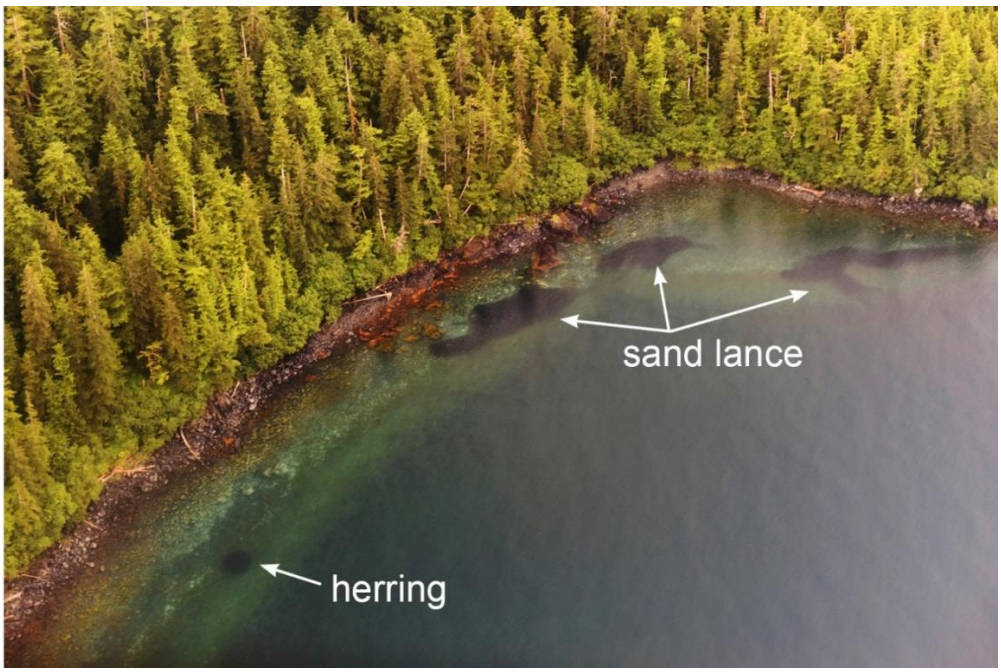

Figure 1-10. Aerial photograph of typical Pacific herring and Pacific sand lance schools along shorelines in Prince William Sound, AK. Herring schools are typically round or oval and sand lance schools are darker and irregularly shaped.

The size of schools are estimated by using a sighting tube constructed of PVC pipe with a grid drawn on mylar on the far end (see Norcross et al. 1999 for details). The focal length (F) of the tube is 210 mm, and a full tick mark on the grid is 1 cm. School size is reported as small

(diameter < 0.5 ticks), medium (> 0.5 ticks and < 1.0 ticks), and large (> 1.0 tick marks). From an observation height of 300 m this provides an equivalent surface area of < 75 m^2 for small schools, 75 – 300 m^2 for a medium school and > 300 m^2 for a large school.

The survey information is then mapped to provide an idea of the distribution (Figure 1-11). The number of schools of age-1 herring observed is tallied to provide an indication of potential future recruitment (Figure 1-12). We also provide a small-school equivalent number of schools that uses school-size weighting. The weighting being Medium = 9*Small; Large = 25*small; X-large = 36*small.

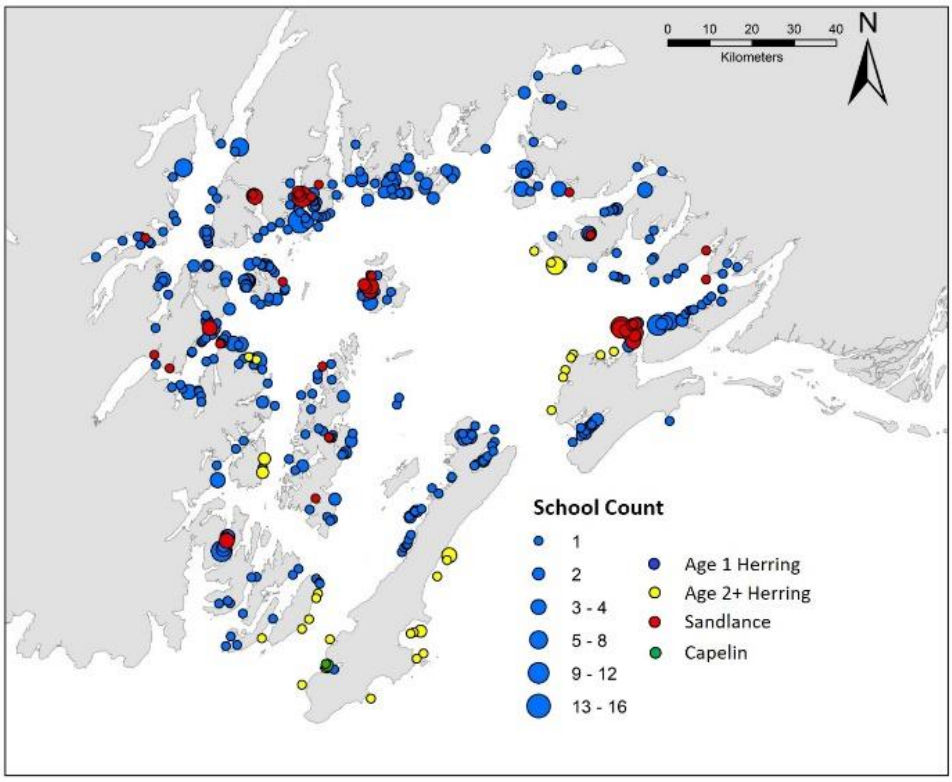

Figure 1-11. June 2019 distribution of forage fish schools in Prince William Sound, AK.

The total number of schools of age-1 herring and small-school equivalent number of age-1 herring schools was provided to the HRM population modeling team for the first time in 2019.

Validation of the aerial school identification is achieved by working with survey vessels in the GWA and HRM programs. The aircraft identifies a school and guides the survey vessel to that school to determine identification through sampling of the school. Based on validation efforts since 2015 and previous work (Norcross et al. 1999) we find that most misidentifications occur with age-0 herring and age-0 sand lance that appear in July. Even once the age-0 schools become visible to the aircraft, the error in identifying herring is between 5 and 10% and sand lance is about 20%. The sample size for identification in June is still fairly small, but as may be expected,

the herring and sand lance schools are correctly identified more often in June since there are no age-0 fish observed.

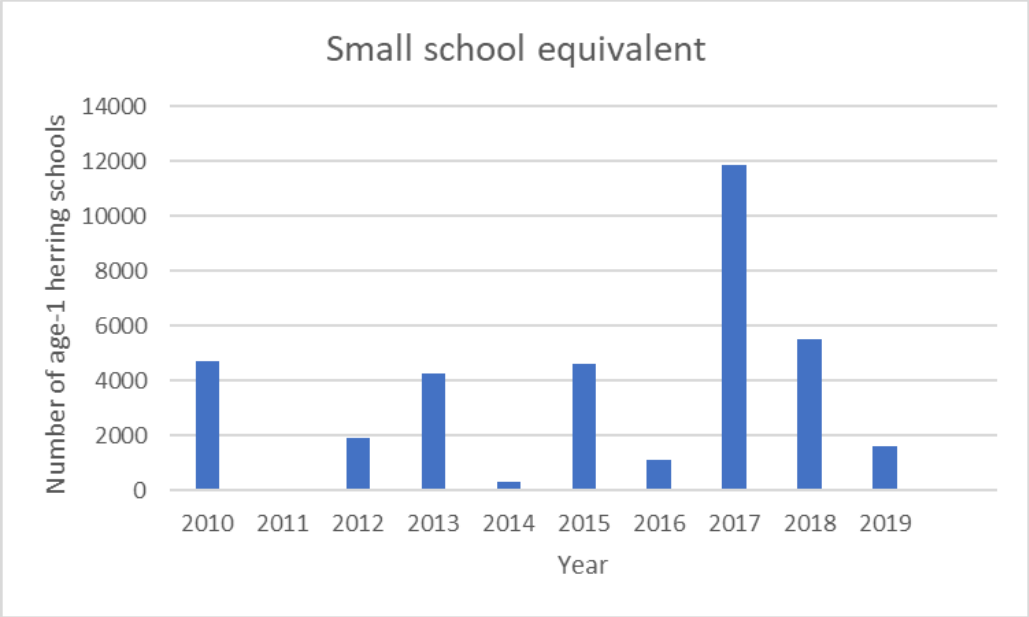

Figure 1-12. Small-school equivalent number of age-1 herring schools by year for Prince William Sound, AK. No data from 2011 are presented because there was not a complete survey.

DISCUSSION

Presented here are the surveys that are currently being conducted. Past surveys included fisheries dependent information and egg deposition surveys. The egg deposition surveys were important as they provide an anchor for the model as it estimates current herring population using the mile-days of milt and acoustic biomass estimates. In her doctoral thesis, Muradian (2015) examined the cost benefit of the different inputs to the model and determined that the existing surveys are the most cost-effective for the modeling effort.

The mile-days of milt index is the longest running and most consistent times series of herring abundance in PWS. As such, it is critical to maintain this index to provide necessary inputs to the assessment models and to meet the overall Herring Research and Monitoring program goal of improving predictive models of herring stocks through observations and research. In addition to providing a long-term index of relative abundance, the aerial survey and ASL projects inform nearly every other project in the Herring Research and Monitoring program by providing age composition and weight at age for the ASA and BASA models; estimating target strength for the acoustic survey estimates of biomass; provide vessel support for spring acoustics surveys and disease sampling; and providing timely aerial and vessel based survey observations to coordinate collection efforts for tagging and maturity studies.

The metrics generated by the aerial surveys were designed to be an index of relative abundance, comparable across the historical time series. It is important to keep these survey methods as consistent as possible to retain comparability among years. Poor weather can reduce spatial and temporal coverage of aerial surveys during some years because aerial surveys can only occur during Visual Flight Rules conditions as weather conditions allow. Despite this we make every effort to maintain consistency across years and there is not a strong relationship between survey effort and mile-days of milt (Figure 1-13). Despite the inherent issues with aerial survey data, the PWS mile-days of milt index has tracked well with other independent estimates of herring biomass (Figure 1-14).

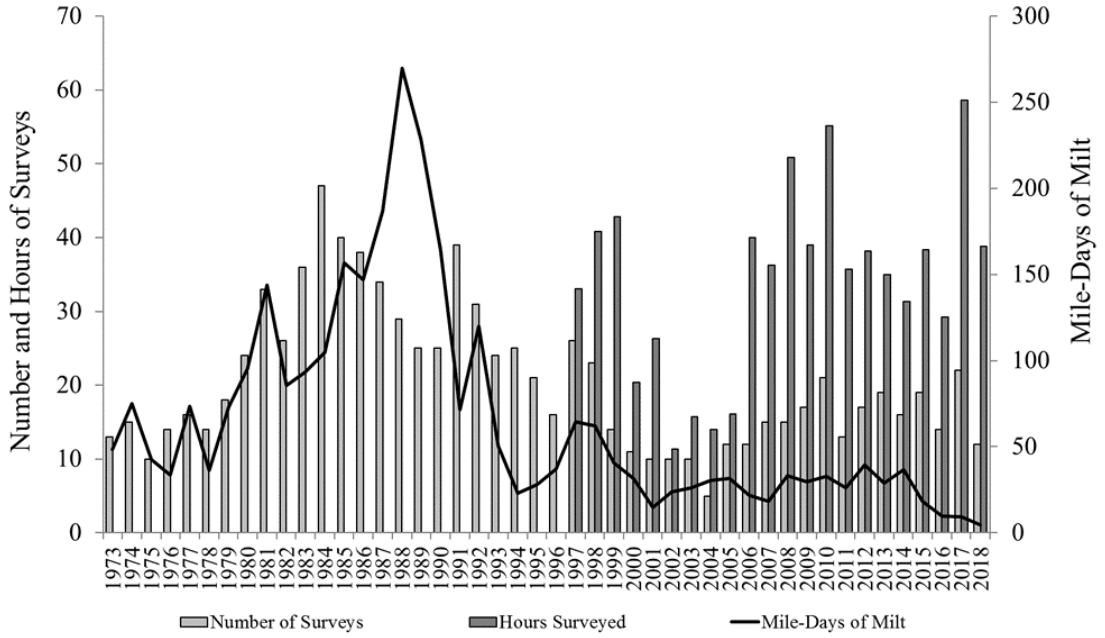

Figure 1-13. Prince William Sound herring aerial survey effort and mile-days of milt.

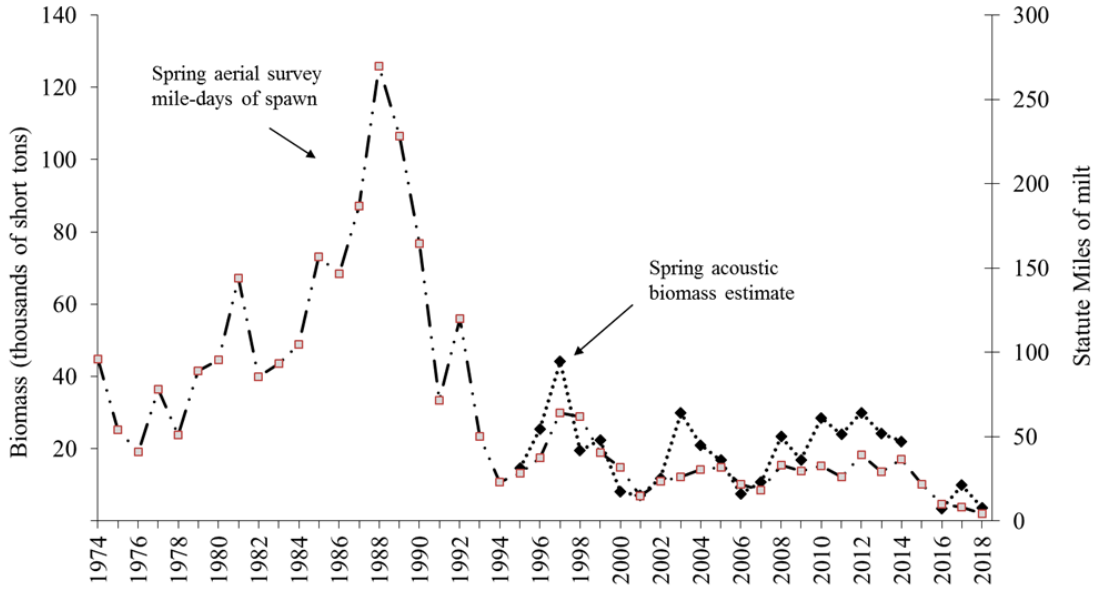

Figure 1-14. Prince William Sound mile-days of milt compared to acoustic biomass estimate.

The PWS area (including Kayak Island) is heavily trafficked by boat and airplane. We have regular communication with air taxis, private pilots, fishers, subsistence users, and other Herring Research and Monitoring projects (acoustics, tagging, disease, and ASL surveys) during PWS herring spawn timing. Many PWS commercial herring permit holders live in Cordova and the general interest in, and subsistence value of, PWS herring among residents is high. Considering the amount of air and vessel traffic in the Sound, and the general interest in herring and in ADF&G's herring monitoring program, it is unlikely that significant spawning events, similar in magnitude to those observed in the Port Gravina and Hawkins Island areas in recent years, would go unobserved and unreported. However, we undoubtedly miss small, short-timed "spot spawning" events. As remote imaging technology improves, continued investigations into supplemental milt detection methods may provide valuable insights into the frequency and magnitude of otherwise unobserved spawning events.

We also continue to explore options to supplement the existing aerial survey effort to ensure we are not missing spawn events and learn how we might be able to detect spawn near PWS, such as at Kayak Island more often.

The acoustic surveys are meant to provide an index of the pre-spawn aggregation biomass because this is the time that the herring are the most congregated. It is shown in the maturity chapter that not all herring are present in the pre-spawn aggregations and thus the acoustic survey should be considered an index of the spawning population. Because the location of the fish not in the pre-spawn aggregation is not known, the expansion of the acoustic surveys to provide an index of total biomass is not practical.

The aerial surveys of juvenile herring provide the only index of potential recruitment. We are just now beginning the process of determining how well the index predicts future recruitment.

Given the wide range of recruitment success each year, we have high hopes that this index will be better than assuming that recruitment will be the median value of recruitment during the past ten years.

REFERENCES

Baker, T.T., J.A. Wilcock, and B.W. McCracken. 1991. Stock assessment and management of Pacific herring in Prince William Sound, 1990. Alaska Department of Fish and Game, Division of Commercial Fisheries. Technical Fisheries Data Report No. 91-22, Juneau.

Bochenek, R.J. 2010. PWS herring data portal, Exxon Valdez Oil Spill Restoration Project Final Report (Restoration Project 090822), Axiom Consulting & Design, Anchorage, Alaska.

Brady, J.A. 1987. Distribution, timing, and relative biomass indices for Pacific Herring as determined by aerial surveys in Prince William Sound 1978 to 1987. Alaska Department of Fish and Game, Division of Commercial Fisheries, Prince William Sound Data Report 87-14, Anchorage.

Brannian, L. K. 1988. Precision of age determination and the effect on estimates of abundance and mortality among Pacific herring. Alaska Department of Fish and Game, Division of Commercial Fisheries, Regional Information Report 2A88-11, Anchorage.

Brown, E.D., Moreland, S.M., 2000. Ecological factors affecting the distribution and abundance of forage fish in Prince William Sound, Alaska: An APEX synthesis product. Restoration Project 00163T. Final Report. Fairbanks, AK 79 pp.

Funk, F. 1994. *Forecast of the Pacific herring biomass in Prince William Sound, Alaska. 1993*. Alaska Department of Fish and Game, Commercial Fisheries Management and Development Division.

Funk, F. and G. J. Sandone.1987. Stock assessment of Prince William Sound herring 1973-1987, using cohort analysis. Fisheries Bulletin. D. o. C. F. Alaska Department of Fish and Game. Juneau, AK, Alaska Department of Fish and Game.

Funk, F., and G. Sandone. 1990. Catch-age analysis of Prince William Sound, Alaska, herring, 1973–1988. Fishery Research Bulletin No. 90-01, Juneau.

Gerke, B.L. 2002. Spawning Habitat Characteristics of Pacific Herring (*Clupea pallasi*) in Prince William Sound, Alaska. Master of Science thesis, University of Alaska Fairbanks.

Hay, D.E. 1985. Reproductive biology of Pacific herring (*Clupea harengus pallasi*). Can. J. Fish. Aquat. Sci. 42 (Suppl. 1):111-126.

Hay, D. E. and A.R. Kronlund. 1987. Factors affecting the distribution, abundance, and measurement of Pacific herring (*Clupea harengus pallasi*) spawn. Can. J. Fish. Aquat. Sci. 44:1181-1194.

Lebida, R.C. and D.C. Whitmore. 1985. Bering Sea herring aerial survey manual. Bristol Bay Data Report, No. 85-02. Alaska Department of Fish and Game, Division of Commercial Fisheries, Anchorage, Alaska.

Muradian, M.L., 2015. *Modeling the population dynamics of herring in the Prince William Sound, Alaska* (Doctoral dissertation). University of Washington.

Muradian M., Branch TA, Moffitt SD, and P. Hulson. 2017. Bayesian stock assessment of Pacific herring in Prince William Sound, Alaska. PLoS ONE 12(2): e0172153.

Norcross, B., Brown, E.D., Foy, R.J., Frandsen, M., Seitz, J., Stokesbury, K., 1999. *Exxon Valdez* Oil Spill Restoration Project Final Report- Juvenile Herring Growth and Habitats-Restoration Project 99320T-ch10 juvenile herring growth.

Ostrand, W.D., Coyle, K.O., Drew, G.S., Maniscalco, J.M., Irons, D.B. 1998. Selection of forage fish schools by murrelets and tufted puffins in Prince William Sound, Alaska. Condor 100:286–297.

Shepherd, C.S., and S. Haught. 2019. Pacific herring aerial surveys and age, sex, and size processing in the Prince William Sound Area, 2018-2021. Alaska Department of Fish and Game, Regional Operational Plan ROP. CF.2A.2019.05, Cordova.

Thomas, G.L, J. Kirsch and R.E. Thorne 2002. Ex situ target strength measurements of Pacific herring and Pacific sand lance, North American Journal of Fisheries Management 22:1136-1145.

Thomas, G. L. and Thorne, R.E. 2003. Acoustical-optical assessment of Pacific herring and their predator assemblage in Prince William Sound, Alaska. *Aquatic Living Resources* 16:247-253.

Thompson, S. K. 1992. Sampling. New York, Wiley-Interscience; John Wiley & Sons, Inc.:39-40.

Willette, T.M., G.S. Carpenter, K. Hyer, and J.A. Wilcock. 1998. Herring natal habitats, *Exxon Valdez* Oil Spill Restoration Project Final Report (Restoration Project 97166), Alaska Department of Fish and Game, Division of Commercial Fisheries, Cordova, Alaska.

This page intentionally left blank

CHAPTER 2 MATURITY

W. Scott Pegau[1], John Trochta[2], Kristen Gorman[1], Trevor Branch[2]

[1] *Prince William Sound Science Center, Cordova, AK*
[2] *University of Washington, Seattle, WA*

INTRODUCTION

Maturity has two definitions in the context of this work. The first is whether a fish is likely to spawn. The second is whether a fish is observed in the sampling of the spawning aggregation. The second definition is more of an operational definition that is used by the Age-Structure-Analysis (ASA) model to convert from spawning biomass to total biomass and may be better termed availability. As we will show, there are some fish that are observed in the pre-spawning and spawning aggregations that are not likely to spawn and not all fish are observed in the pre-spawning aggregations.

In this chapter we examine the maturity of Pacific herring (*Clupea pallasii*) in the pre-spawning and spawning aggregations from samples collected for age-sex-size (ASL) analysis. We then use the ASL data to determine if the pre-spawning and spawning aggregations represent the total population of herring at a given age, or if there is a need for an availability function in the ASA model. The purpose of the availability function is to extrapolate to the total population at each age from the observed spawning population. We find that there are immature fish collected in the ASL samples and that not all fish are available to ASL sampling. A percentage of age-3 and age-4 fish do not appear to be part of the pre-spawning or spawning populations.

The scale growth of four cohorts (1984, 1988, 1999, 2005) are examined to see if there is evidence of bimodal growth in male and female herring. The cohorts were chosen to include two on from each time block that the ASA model currently uses. Preliminary results show that both male and female herring show indications of bimodal growth in the scale records that is most evident at the older ages (age-5 and age-6). Fewer scales are imaged at these older age classes and more scales will need to be imaged before making conclusions.

A suite of eleven model runs are used to examine the question of sensitivity of the model to different assumptions about maturity and availability. The eleven model runs are meant to bound the likely range of scenarios. The model runs are also used to examine the assertion by Hulson et al. (2007) that the maturity function should be calculated in two separate time blocks. We find that the estimated biomass is not sensitive to the range of maturity scenarios. There is no value to the model in trying to separate mature and immature fish in the ASL samples. We do not find evidence in the residuals of a change in the maturity schedule as suggested by Hulson et al. (2007).

MATURITY MEASURES AND ESTIMATES FROM THE AGE-WEIGHT-LENGTH SAMPLES

Much of the existing information on Pacific herring in Prince William Sound (PWS) comes from Alaska Department of Fish and Game's (ADF&G's) age-weight-length (AWL) database. This database extends back to 1973 and the age-structure information input into the ASA model is based on the AWL sampling. The database includes information on sampling time, location, and sampling gear. Since 2009, ADF&G has included an estimate of the maturity of herring using the maturity stages as described in Hay (1985): (1) Undeveloped, (2) Starting, (3) Developing, (4) Maturing, (5) Mature, (6) Ripe, (7) Spent, and (8) Recovering. In this text we will consider maturity indices 1-3 as immature and 5-8 as mature. We will explore how best to classify maturity index value of 4. We use the information in the AWL, including maturity index, to examine the maturity of the pre-spawning aggregation and estimate the number of fish not observed in those aggregations.

MATURITY OF FISH SAMPLED

From 2009 to 2018 there were 35 seine net samples collected during the pre-spawning time period (March and April). These samples were intended to collect pre-spawn herring for ASL analysis. The maturity index by age in those samples is provided in Figure 2-1. It can be seen that most of the age-1 and age-2 fish are immature and fish age-5 have a higher maturity index (MI) that indicates they are likely to spawn. As expected, the age-3 fish have a mixed MI. The age-4 fish are generally mature or ripe, but still have a significant proportion of fish that are maturing.

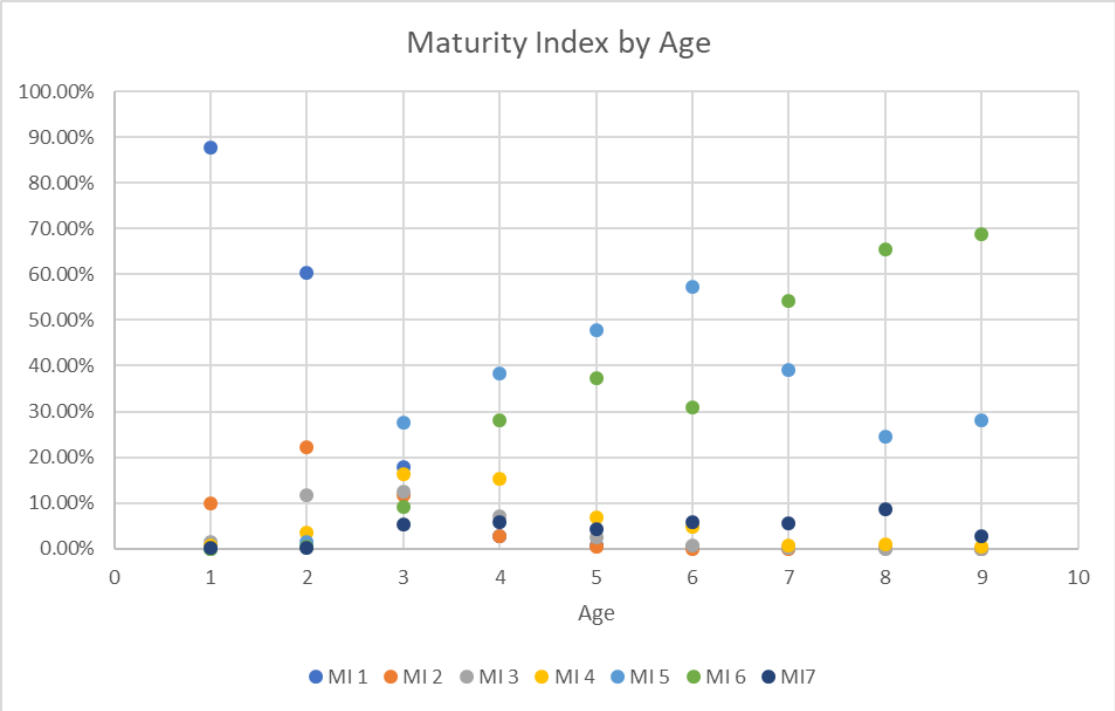

Figure 2-1. Maturity index by age of herring sampled by the seine net in Prince William Sound, AK.

It is known that the spawning and nursery grounds overlap and there may be some seine sets that captured immature fish in a nursery area rather than those in the pre-spawning aggregations. Each sampling event was examined to see if there were unusual numbers of age-1 and age-2 fish, or unusual levels of immature fish in a sample. Five samples were identified to have unusual numbers of age-1 or age-2 fish using a criterion of greater than 60% of the fish caught being age-1 or age-2. These same five samples were identified as being the only ones with more than 75% of the sample having a MI <4. Excluding the five samples dominated by young, immature fish eliminated 1,803 fish from the analysis, of which 398 were age-3 and older and 198 were MI 4 or greater. This left thirty samples consisting of 11,099 fish in the analysis of age versus maturity index of seine samples (Table 2-1). The number and maturity of the fish in the five samples excluded from consideration are provided in **Error! Reference source not found.**. While some older mature fish were excluded, they are proportionally much less prevalent than in the samples dominated by older, more mature fish.

Table 2-1. Number of fish collected by seine by age and maturity index. Fish older than 10 are not included.

Age	Maturity index							
	1	**2**	**3**	**4**	**5**	**6**	**7**	**Grand Total**
1	1	3		1				5
2	94	198	37	28	36	11		404
3	274	213	249	538	1101	351	8	2734
4	28	24	46	314	998	784	18	2212
5	3	3	13	129	1166	917	10	2241
6	2		6	65	863	454	8	1398
7	1			7	440	614	5	1067
8		2		3	169	460	2	636
9					92	223		315
10					39	48		87
Grand Total	403	443	351	1085	4904	3862	51	11099

It is clear from **Error! Reference source not found.** that there are few mature age-2 fish and few fish age-6 and above that are immature. It is difficult to tell if a fish of MI 4 may complete maturation and spawn that year or if it should be considered an immature fish. **Error! Reference source not found.** provides the percentage of fish sampled that have an index value greater than 3 or 4 to demonstrate the impact of setting an index of 4 as mature versus immature. This is most important to age-3 and age-4 fish. If a MI of 4 is likely to spawn, then nearly all age-4 fish caught are likely to spawn. But about 27% of the age-3 fish caught should be considered immature. If a fish with a MI of 4 is immature, then nearly half of the age-3 fish are immature.

Table 2-2. Number of fish collected by seine by age and maturity index in the five samples excluded from further analysis.

Age	Maturity index							
	1	**2**	**3**	**4**	**5**	**6**	**7**	**Grand Total**
1	251		3					254
2	1061	59	11	9	9	1	1	1151
3	119	20	28	43	50			260
4	8	12	22	26	42			110
5	2	4	2	4	2			14
6			3	1	8	1		13
8					1			1
Grand Total	1441	95	69	83	112	2	1	1803

Table 2-3. The percentage of fish by age caught by the seine that are above a maturity index (MI) of 3 or 4.

Age	% >MI 3	% >MI 4
2	18	12
3	73	53
4	96	81
5	99	93
6	99	95
7	100	99
8	100	99
9	100	100
10	100	100

Examining the variability between years shows a wide range of the percentage of fish with a MI of <4 captured in the seine each year (Table 2-4). The purse seine samples in 2009 had unusually high levels of immature fish as both age 3 and 4.

Table 2-4. Observed immature (maturity index < 4) in seine samples. In 2011 there were less than 10 age-3 fish captured; hence no value is provided.

Year	2009	2010	2011	2012	2013	2014	2017	2018
Number of age-3	535	1167	6	429	35	32	210	325
Number of age-4	433	398	142	106	385	361	96	291
Immature age-3	52%	25%		29%	0%	13%	0%	10%
Immature age-4	12%	5%	1%	5%	0%	0%	0%	6%

If the seine samples represented the entire population in PWS, the percentage of immature fish in Table 2-2 could be considered the appropriate numbers for the maturity schedule used by the ASA model. The samples with large numbers of age-1 and age-2 fish that were excluded from the analysis also contained a higher percentage of immature age-3 fish. This indicates that the seine samples should not be considered representative of the entire population and the numbers in Table 2-3 likely represent the maximum percentage of mature fish at each age. What remains unclear is which MI represents fish likely to spawn. It is highly unlikely that fish with a MI less than four will spawn, but it isn't clear if a MI of four (maturing) represents fish likely to spawn that season.

One check on whether a fish is likely to be mature is to compare the age composition of the seine samples to those collected by cast nets. The cast net samples are from areas with active spawning. The MI shows that there are immature fish caught with the cast nets but they represent no more than 5% of the total fish caught. The purse seine samples tend to have a greater percentage of age-3 fish, which leads to a lower percentage of age-5 and older fish (Table 2-5). Removing the age-3 fish from consideration provides closer agreement in the age composition (Table 2-6). The best agreement between the cast net and seine samples is achieved if a MI of 4 (maturing) is considered immature for age-3 and age-4 fish. It is reasonable to believe that younger fish have a more difficult time becoming fully mature in time to spawn. It is also possible that the cast net sampling ended before the age-3 and 4 fish were able to fully mature and spawn and therefore are underrepresented in the cast net samples, or that there is a gear selectivity issue (small fish able to fall out of the cast net).

Table 2-5. The age composition of fish caught by cast net and seine.

Gear	Cast net	Seine maturity >3	Seine maturity >4
Age-3	8.9%	18.0%	13.2%
Age-4	19.0%	19.1%	16.2%
Age-5	25.2%	20.0%	18.9%
Age-6	14.7%	12.5%	11.9%
Age-7	13.0%	9.6%	9.5%
Age-8	8.0%	5.7%	5.7%

Table 2-6. The age composition of fish caught by cast net and seine after excluding age-3 and younger fish.

Gear	Cast net	Seine maturity >3	Seine maturity >4
Age-4	21.3%	26.6%	22.6%
Age-5	28.2%	27.9%	26.3%
Age-6	16.5%	17.5%	16.7%
Age-7	8.9%	8.0%	7.9%
Age-8	5.0%	4.0%	4.0%

From the maturity index data, it is evident that there are immature fish within the pre-spawning aggregations. Since seine samples that primarily caught immature fish within the region have a different percentage of immature fish, it is likely that the pre-spawning biomass does not represent the total population in PWS. It is likely that fish with a MI of 4 are not likely to spawn that year, but this may be a result of incomplete cast net sampling late in the spawning season.

ESTIMATION OF FISH NOT SAMPLED

Another issue of interest is whether the spawning aggregations represent the entire population of PWS or if large portions of the population are missing during the surveys. This is of particular interest for immature fish that may not have joined the spawning aggregations. An estimate of the missing fish can be made using the age structure data from the AWL database. The approach used provides an estimate similar to the maturity variables estimated in the ASA model with two simplifying assumptions and without using all of the data input into the ASA model. The first assumption is that the population is stable through the time period. This means that recruitment is constant and equal to mortality. The second assumption is that mortality is constant in time and across ages. The combination of assumptions imply that the age structure is constant in time and therefore the percentage of the population in each age class is constant. This allows us to analyze the data using percentages of the population observed.

Based on these assumptions we averaged the percentage of fish in each age class collected by all types of gear each year from 2000 to 2015. We did not include more recent years because the population declined substantially after 2015. There was one strong recruit year in the time series, but its effect was minimized by the long period used in the averaging. Furthermore, removing the effect of that strong cohort would have reduced the years used in the analysis in half. We then fit an exponential function to the proportion of age-5 through age-8 fish (Figure 2-2). The exponential fit provides an estimate of mortality and the deviation from the fit gives an estimate of the percentage of the age-3 and age-4 fish not observed. This approach leads to an estimated annual mortality rate of 27% with approximately 42% of the age-3 fish and 8 percent of the age-4 fish unaccounted for in the sampling. The fit has an error margin of +- 5%.

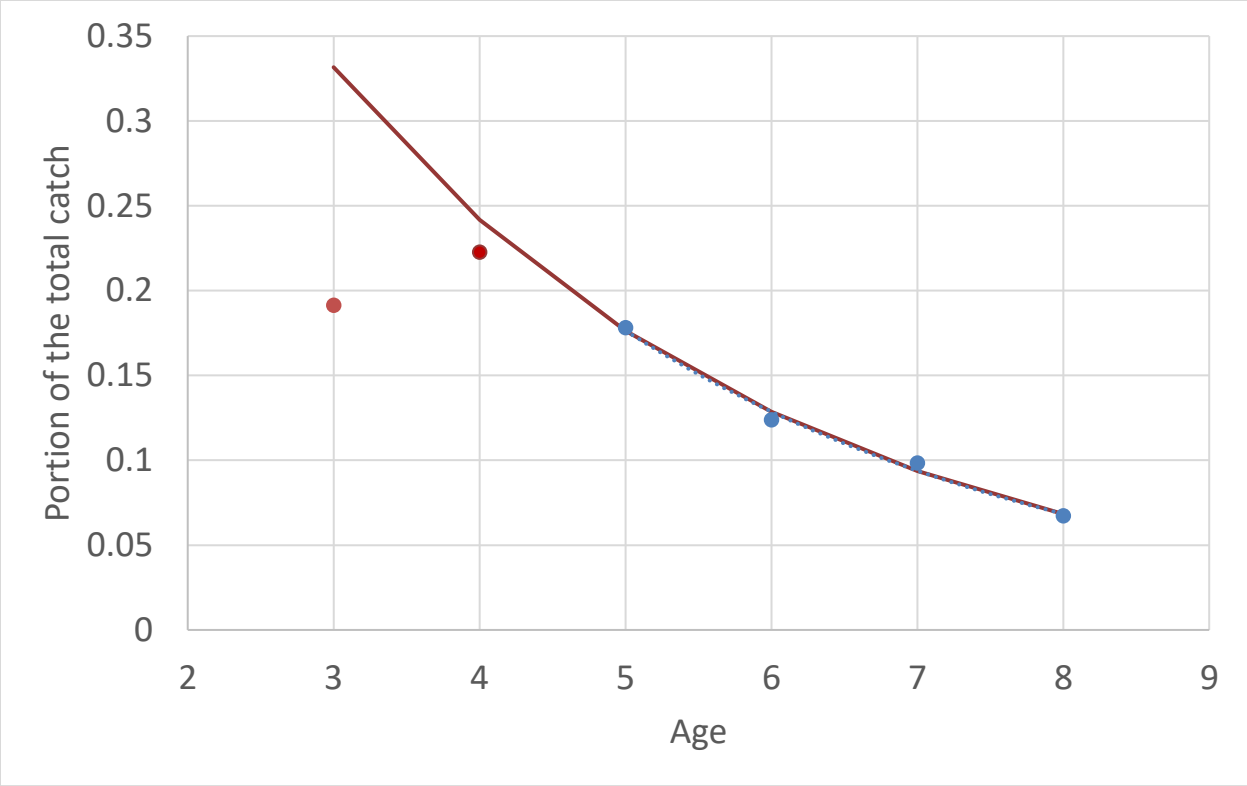

Figure 2-2. The percent of the total catch by age. An exponential function was fit to the age-5 through age-8 data (blue dots) and the solid red line shows that function. The age-3 and age-4 percentages are shown as orange dots.

Sub-setting the data and repeating the fit provides a remarkably consistent annual mortality estimate of 25-30%. If it is assumed that the age-4 fish have all recruited and the exponential fit is extended to include age-4 fish, then the mortality estimate drops from 27% to 26% and the r^2 of the fit does not significantly change (0.991 to 0.992). However, the estimated proportion of age-4 fish still slightly higher than observed percentage of age-4 fish.

Because we found that there is a different age structure in the seine samples than from the cast net, we repeated the analysis by gear type (Figure 2-3). Separated, the two data sets give the annual mortality estimates of 27% and 32%. The cast net samples have proportionally fewer age-3 and age-4 fish than the seine. Most likely this is a result of the immature fish observed in the seine samples not being present in the cast net samples.

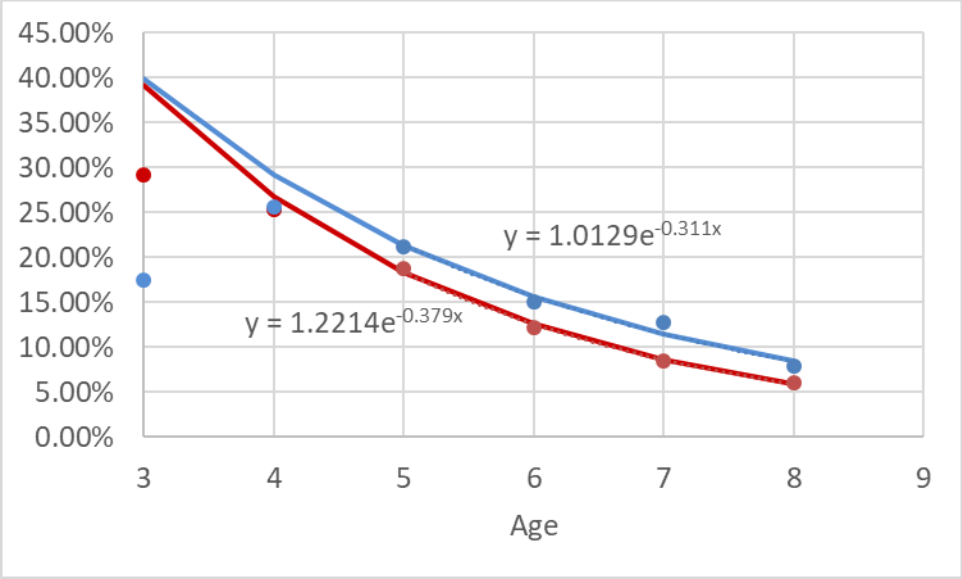

Figure 2-3. The percent of the total catch by age. An exponential function was fit to the age-5 through age-8 data. The blue line and dots represent the cast net data and the red the seine samples.

DISCUSSION

The work presented here is based on several simplifying assumptions and should only be taken as a general indication of the maturity and percentage of fish that are not observed. The data show that there are immature fish in the pre-spawning aggregations and that the overlap between the location of the pre-spawning and nursery aggregations allows some sampling of primarily immature fish. Seine sampling of the pre-spawning biomass catches more age-3 fish, many of which have a maturity index that indicates they are not likely to spawn, than are caught using a cast net in active spawning areas. Even after correcting the seine samples for maturity the cast net samples have proportionally fewer age-3 fish, which suggests that there is a sampling bias towards early in the season when younger fish are less likely to spawn (Lambert 1987).

It is unlikely that any fish sampled with a MI of 3 or less will spawn, and it is highly likely that fish with a MI of 5 or higher will spawn. The difficult MI to assess is what is the likelihood that a fish with a MI of 4 will spawn. Our work suggests that age-3 and age-4 herring with a MI of 4 are unlikely to spawn. However, if there is a temporal bias to the cast net sampling it could produce this result. We find that approximately 47% of the age-3 fish and 9% of the age-4 fish in the pre-spawning aggregations are immature when using a MI of 5 as the minimum for a mature fish.

Examining the age structure of the samples between 2000 and 2015 indicates that the annual mortality is between 27 and 32%. Projecting the curves to age-3 and age-4 fish indicates that we do not sample the full age-3 population and may be missing a small portion of the age-4 fish. Based on our simplified analysis of the age-structure data, it appears that the percentage of age-4 fish not observed in the pre-spawning or spawning biomass is likely to be between 3 and 10%. The percentage of age-3 fish not observed is between 39 and 52%. If we assume all of the

missing fish are immature, then the total percentage of immature fish is the combination of the missing fish and the percentage of the observed fish that are not mature, or roughly 67-75% of age-3 fish and 12-18% of the age-4 fish do not spawn.

The model uses data on the number of fish that are observed in the pre-spawning or spawning population, not the number of fish that will actually spawn, and uses a function to estimate the total population. This means that we expect that the model numbers will be most similar to our percentage of observed fish (48-61% of age-3 fish and 90-97% of age-4). In the same period the model's 95th percentage estimates of observed age-3 fish is 55-76% and the age-4 observed estimate is fixed at 90%. The model fixes the percent of age-4 fish as observed at the low end of our estimated range of unobserved fish. This will in turn cause the model's age-3 percentage of fish observed to be higher than ours.

Combining age-structure from different types of sampling gear is likely to be a source of error in the age-structure data used by the model because of the different age structures from the different sampling techniques. It remains to be seen if the potential error is of the same magnitude as that from the number of fish caught each year or the timing of sampling. It is important to be able to collect fish using both the seine and cast nets. We are not always able to collect seine samples and thus are dependent on cast net samples to fill out the age structure. The cast net samples also provide the best measure of the age-structure of the fish that are spawning. It is important that the sampling continue throughout the spawning events. The cast net samples don't provide a good measure of the weight of the herring because many have spawned and thus the seine net samples are needed to understand how environmental conditions impact herring condition. We should consider if it is necessary to correct for the differences in the sampling techniques. If so, how best to combine data from the two approaches to provide a consistent measure of the population. This can be done by only using herring with a maturity index of 5 or higher from the seine samples. This will keep the estimate closest to the spawning population and reduce the impact of the balance of the sampling techniques and the changes in the proportion of immature herring among years. The issue being that this information is not available for all years and changing the data included in the time series may require the time series to be broken into two separate time series.

MATURITY BASED ON SCALES

INTRODUCTION

Reproductive maturity schedules are key demographic parameters included in stock assessment models such as the ASA. At the individual level, age at maturity can shape overall lifetime reproductive success (Bernardo 1993, Stearns 1992), and therefore, contribute to stock productivity. There is some evidence that age at maturity for herring might vary with population size. For example, Engelhard and Heino (2004) showed that during a period of low stock abundance for Norwegian spring-spawning herring, age at maturity was considerably reduced while length at maturity moderately increased, in comparison with time periods before and after the population collapse. Such dynamics may be important for Pacific herring of PWS given the population crash by the mid-1990's following the *Exxon Valdez* oil spill. Hulson et al. (2008) reported the original ASA model for PWS herring, noting that maturity schedules appeared to

have changed before and after 1997 (Table 2-7). Further, the current BASA model (Muradian et al. 2017) estimates two different sets of maturity parameters before and after 1997 (Table 2-7, see also maturity section in this report by Trochta and Branch). Empirical tests of the maturity schedules estimated by the PWS herring ASA models is of interest, particularly if methods allowed for understanding both past and present maturity schedules.

Table 2-7. Reproductive maturity parameterization used in former and current (Bayesian) ASA models for Pacific herring in Prince William Sound, AK. Values for Muradian et al. (2017) are median percent spawning and associated credible intervals.

Age	% Spawning 1980-1996	% Spawning 1997-2004	Reference
3	27	48	Hulson et al. 2008
4	89	75	Hulson et al. 2008
5	100	100	Hulson et al. 2008
	1980-1996	**1997-2012**	
	39 (28, 56)	49 (37, 66)	Muradian et al. 2017
	80 (62, 97)	90	Muradian et al. 2017
	100 (assumed)	100 (assumed)	Muradian et al. 2017

Approaches for studying maturity in herring have typically relied on either direct measures of gonad maturation such as a gonad-somatic index, Hjort criteria, and histology of ovaries (Hay and Outram 1981, Hay 1985), or indirect measures of past spawning history as might be inferred by scale growth (Engelhard et al. 2003, Vollenweider et al. 2017). As noted in the chapter section on AWL, capturing fish from the spawning population does not allow for direct measurements of fish that have not recruited - although some immature fish were collected with the PWS spawning population. This issue of sampling the entire population is particularly difficult for herring because finding fish of specific age cohorts outside the spawning event is particularly difficult except for age-0 herring that use protected nursery bays. The use of scale growth patterns is one alternative that potentially circumvents the need to sample herring at specific ages for the study of maturity because scales provide a complete lifetime record of growth for individual fish that can be sampled from the spawning population once they have recruited. For Norwegian spring-spawn herring, the scale growth technique has been used to examine age at maturation (Engelhard et al. 2003). This approach relies on the fact that as herring grow over their lifetime, scale growth is proportional to body growth. Thus, when herring invest more energy in gonad development during reproduction, it reduces the energy available for body growth and therefore should be reflected in scale growth patterns. In this way, scale growth can potentially be used a proxy for age-specific maturity schedules. Pilot work as part of the Herring Research and Monitoring program by Vollenweider et al. (2017) concluded that scale growth patterns in PWS herring could be used to discern spawning activity.

The purpose of the current analysis is to explore ADF&G's herring scale growth library (Moffitt 2017) and assess whether there is evidence for bimodal distributions of herring scale growth as individual cohorts of herring move through time from age-1 through age-6. The analysis reported

here considers two cohorts of PWS herring before and after the 1997 break point as estimated by the ASA. The basic prediction is that unimodal scale growth distributions would be expected for age-1 and age-2 herring. As herring mature, bimodal distributions are expected for ages 3-5. By age-6, unimodal scale growth distributions are expected as all fish should be recruited by this age. This idea was tested using ADF&G's scale growth library (Moffitt 2017). Because the analysis does not include any information on scale growth changes directly in relation to known spawning activity, i.e., histology, the analysis here is meant to explore the scale growth library to understand bimodal patterns in scale growth as a single cohort of fish matures over time. At this point, results cannot be used to say anything specific about direct spawning activity, but simply the presence or absence of bimodal patterns in scale growth for specific cohorts of PWS herring.

METHODS

Four cohorts of PWS pacific herring were considered in analyses – 1984, 1988, 1999, and 2005 representing two cohorts before and after the 1997 breakpoint as estimated by the ASA. Scale growth information for these cohorts from age-1 through age-6 were obtained from ADF&G's scale growth library (Moffitt 2017). Data were collated from age-4, age-5, and age-6 fish, respectively, from the years 1988-1990, 1992-1994, 2003-2005, and 2009-2011 to produce each cohort's dataset. Histogram and density plots were created for males and females separately from each cohort to help identify which age group might be predicted to show bimodal distributions in scale growth. Additionally, a Gaussian mixture model was used to detect bimodal distributions in annual scale growth using the *mixtools* package (Benaglia et al. 2009) in the R language environment (R Core Team 2018). The mclust package (Scrucca et al. 2016), also implemented in R was used to conduct likelihood ratio tests and Bayesian clustering analysis of the mixture models produced by the *mixtools* package.

RESULTS

Histograms, density plots, and mixture model results are show in Figure 2-4 through Figure 2-11 for female and male cohorts of Pacific herring for 1984, 1988, 1999, and 2005, respectively. Sample sizes for each age group are noted in histogram and density plots. Sample sizes specific to the Bayesian clustering analysis are noted for each Gaussian mixture model plot.

Density plots suggest that age 5 female herring in 1988 might be composed of two groups based on scale growth due to the apparent bimodal distribution (Figure 2-4). Gaussian mixture model results indicate that females age-4 to age-6 show bimodal distributions in scale growth based on likelihood ratio tests (LRT: $p \leq 0.05$). Bayesian clustering analysis indicated that only age-5 females in this cohort can be distinguished into two groups based on scale growth (Figure 2-4).

Density plots suggested that age 3 male herring in 1986 might be composed of two groups based on bimodal scale growth (Figure 2-5). Likelihood ratio tests were significant for male herring age-3 to age-5 in the 1984 cohort (LRT: $p \leq 0.05$). Bayesian clustering analysis only distinguished age-4 and age-5 males as having bimodal scale growth. However, the sample sizes in each group show only a small number of males belonging to groups with larger scale growth (i.e., 1 or 2 individuals) (Figure 2-5).

Density plots did not show any obvious sign of bimodal distributions in scale growth, with the possible exception of age 4 females from the 1988 cohort (Figure 2-6). Likelihood ratio tests were all non-significant except for age-4 females (LRT: $p = 0.5$). However, the Bayesian clustering analysis detected no bimodal distributions for any age class in the 1988 female cohort.

Density plots suggested that age-2 male herring from the 1988 cohort make show bimodal distributions in scale growth (Figure 2-7). Likelihood ratio tests and Bayesian clustering analysis did not detect bimodal distributions in scale growth for any age class of males from the 1988 cohort (Figure 2-7).

Density plots for female Pacific herring from the 1999 cohort did not obviously suggest any group might show bimodal scale growth distributions, possibly with the exception of age-6 female herring from 2004 (Figure 2-8). The likelihood ratio test for age-6 female herring was significant indicating evidence for bimodal scale growth. However, the Bayesian cluster analysis grouped all ages into one group for females of the 1999 cohort (Figure 2-8).

Density plots did not obviously suggest any age group of male herring from the 1999 cohort would show bimodal scale growth distributions (Figure 2-9). Likelihood ratio tests were significant ($p < 0.05$) for age 1 and age 6 male herring, which was also confirmed by the Bayesian clustering analysis (Figure 2-9).

Density plots suggested that age 3 and age 4 female herring from the 2005 cohort might show bimodal distributions in scale growth (Figure 2-10). Likelihood ratio tests and Bayesian clustering analysis were only significant for age-6 female herring in 2010 (Figure 2-10).

Density plots appeared to indicate that age-2 male herring from the 2005 cohort might show bimodal distributions scale growth (Figure 2-11). The likelihood ratio test was significant ($p< 0.05$) for age 1 male herring in 2005 only, but this result was not supported by the Bayesian clustering analysis. All other age groups showed unimodal scale growth patterns (Figure 2-11).

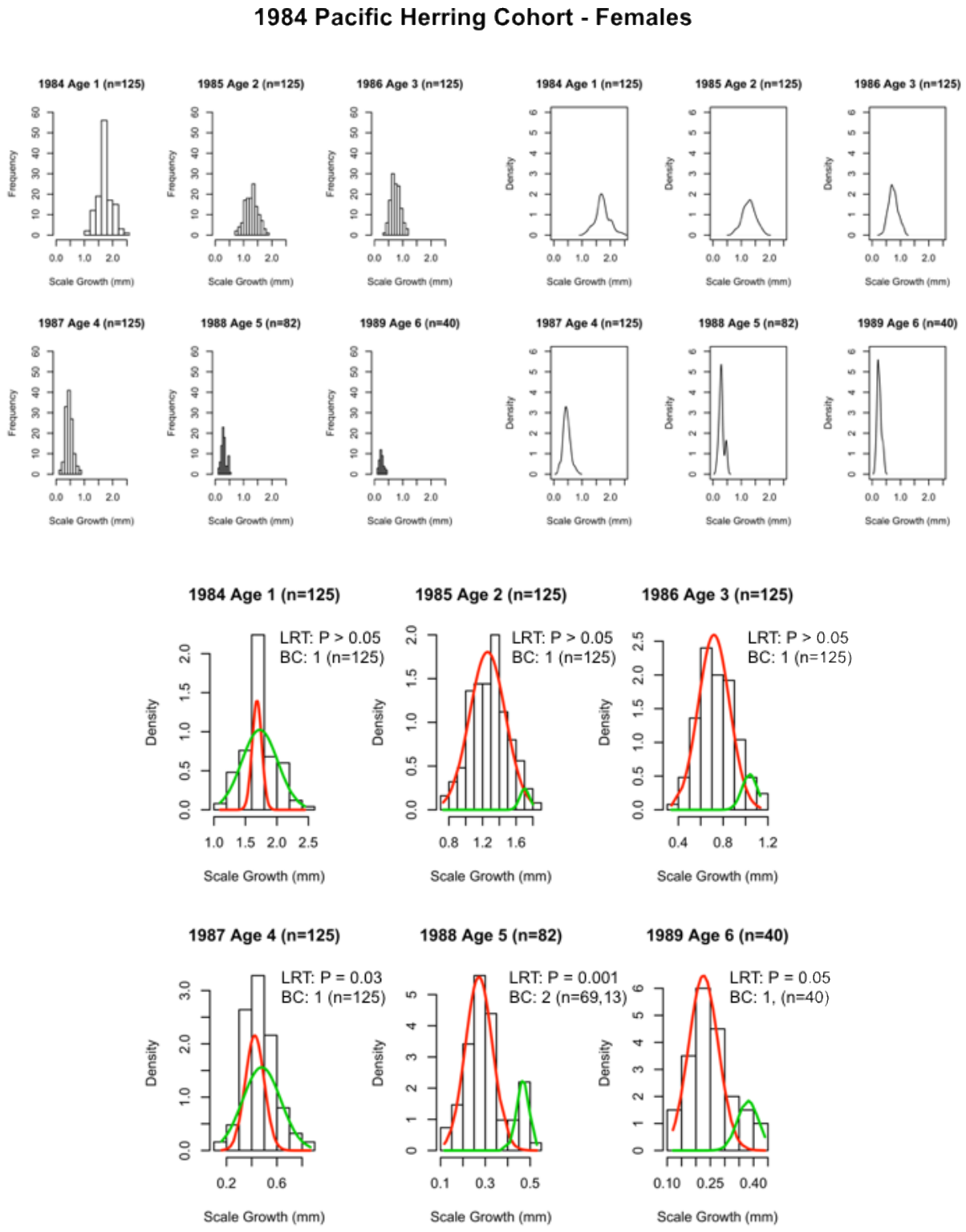

Figure 2-4. Scale growth histograms, density plots, and Gaussian mixture models results for female Pacific herring of the 1984 cohort in Prince William Sound, AK.

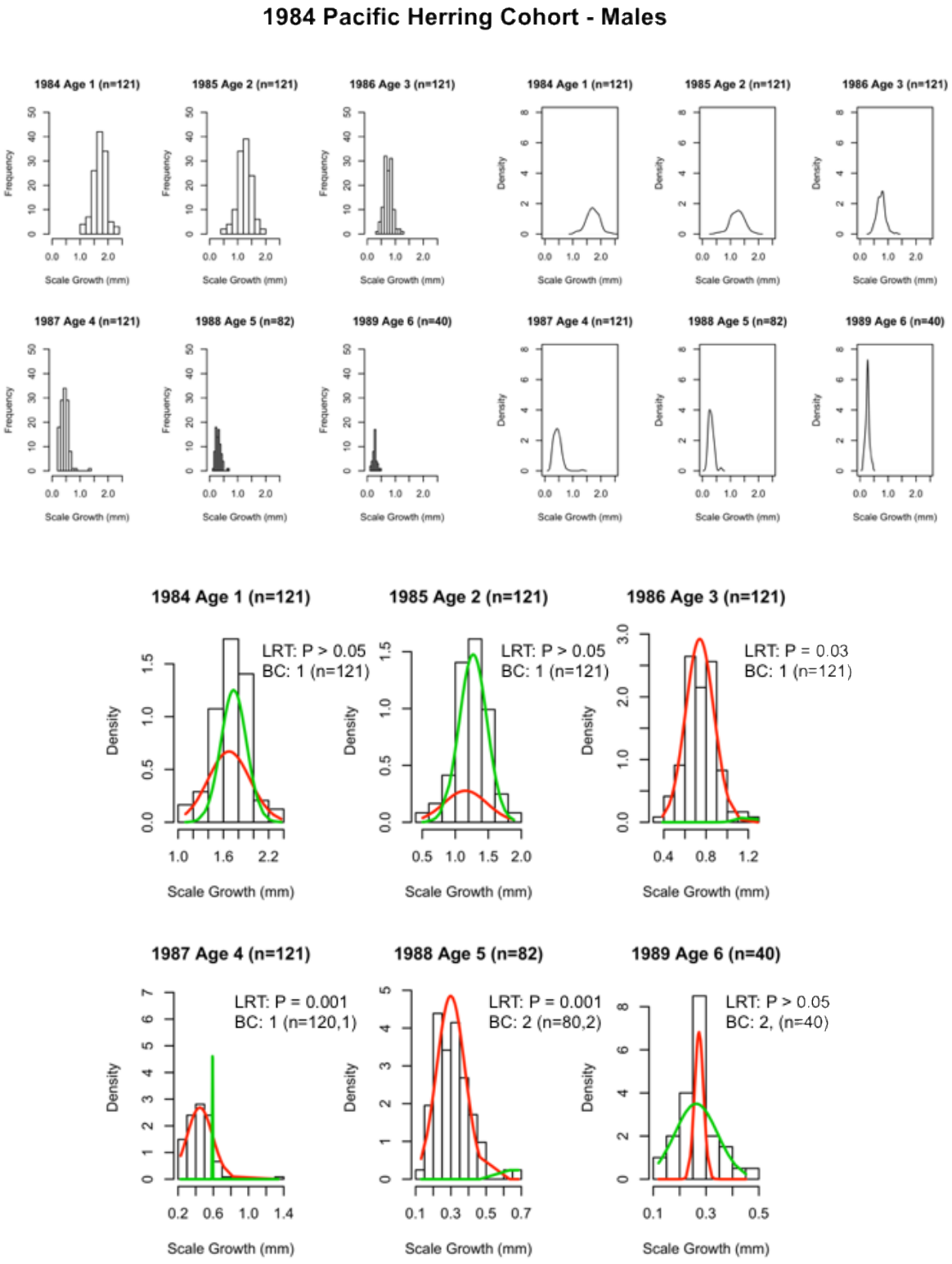

Figure 2-5. Scale growth histograms, density plots, and Gaussian mixture models results for male Pacific herring of the 1984 cohort in Prince William Sound, AK.

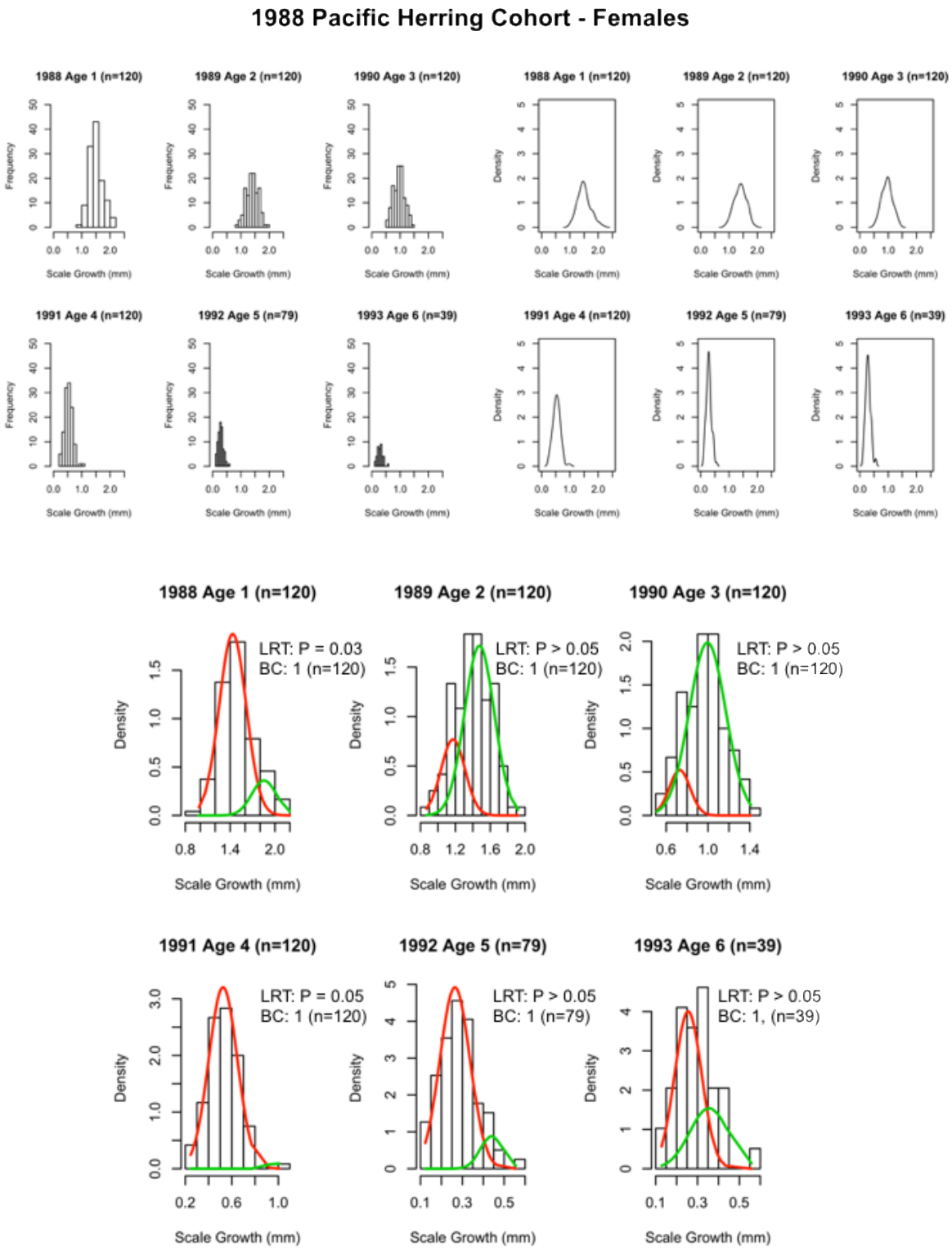

Figure 2-6. Scale growth histograms, density plots, and Gaussian mixture models results for female Pacific herring of the 1988 cohort in Prince William Sound, AK.

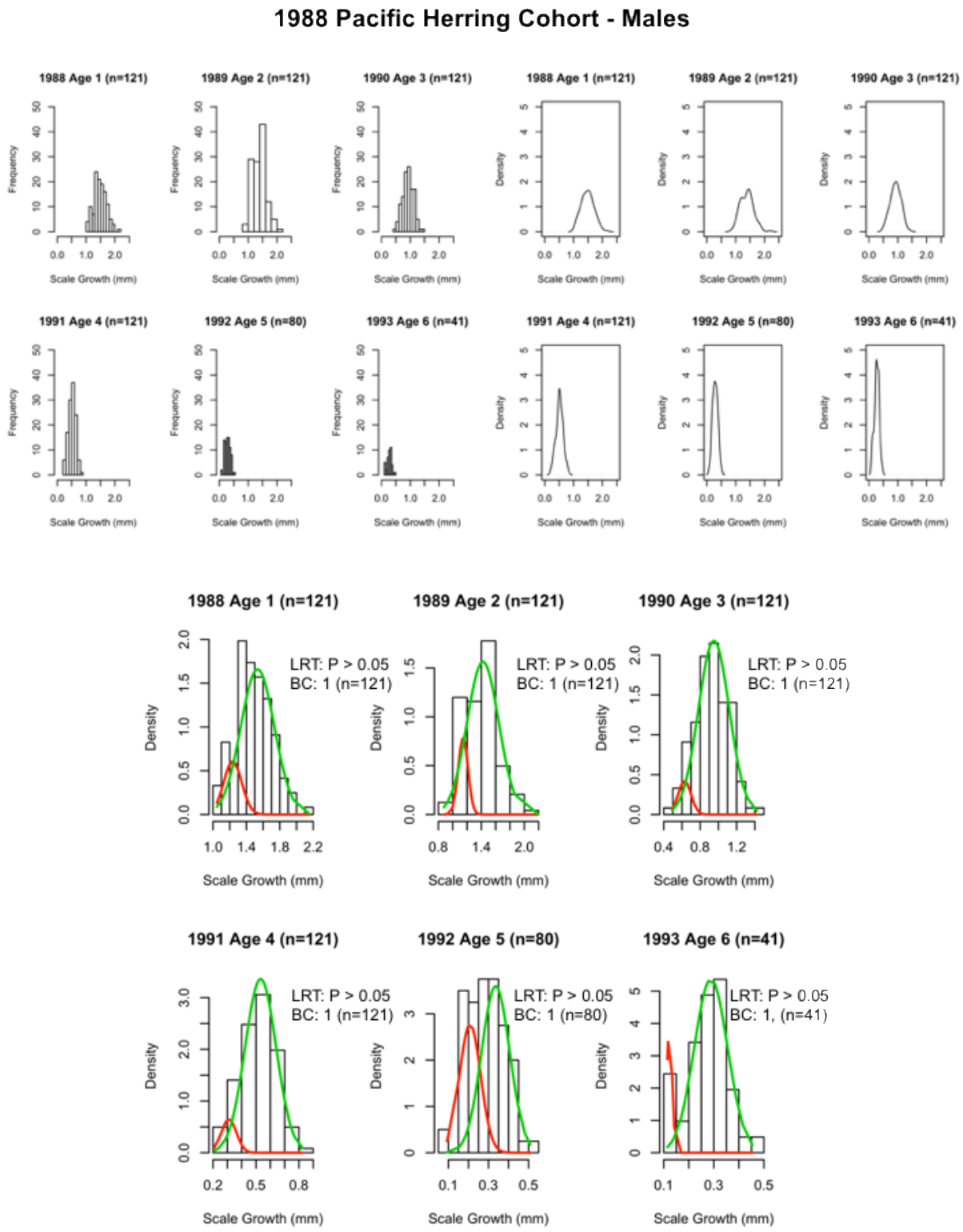

Figure 2-7. Scale growth histograms, density plots, and Gaussian mixture models results for male Pacific herring of the 1988 cohort in Prince William Sound, AK.

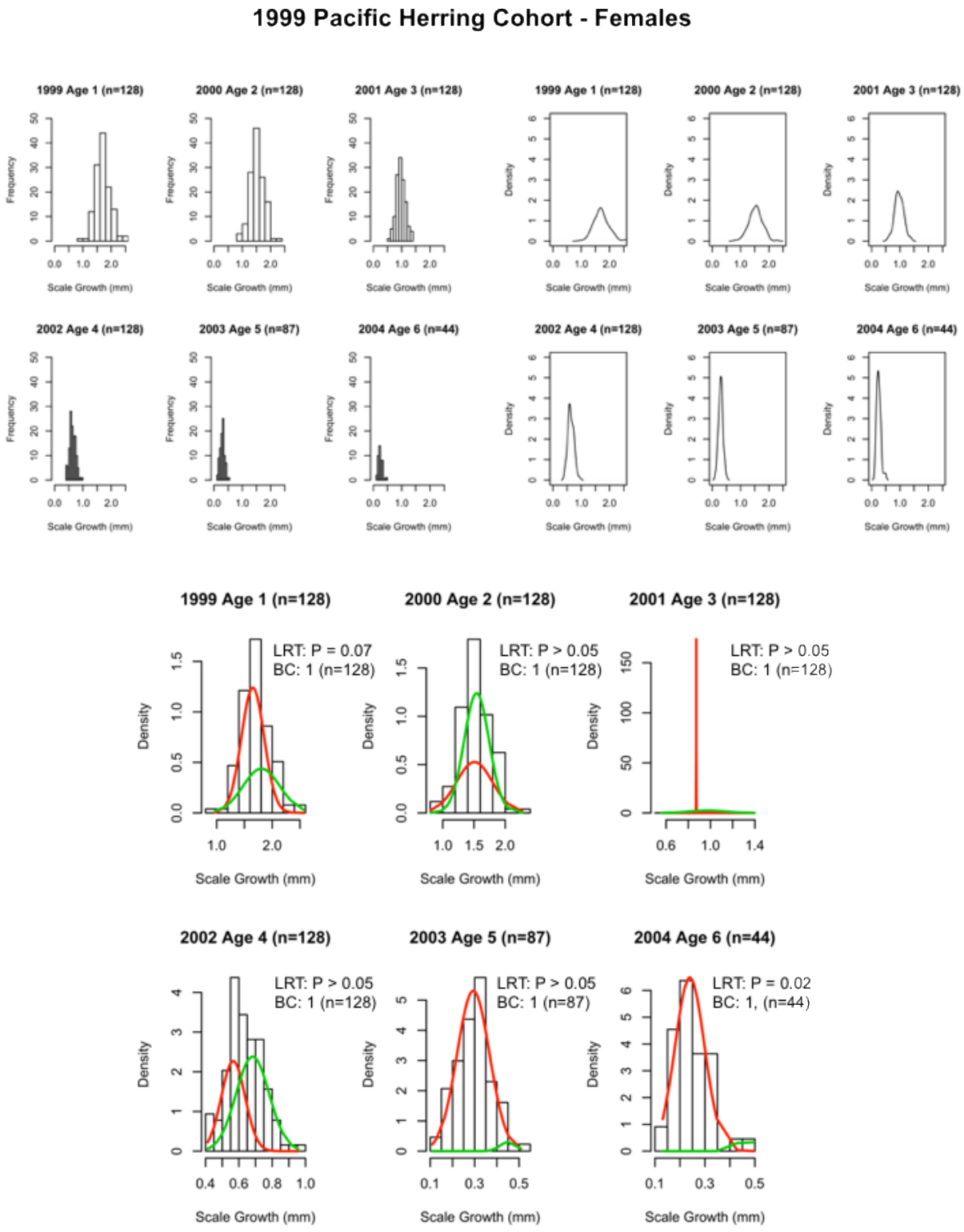

Figure 2-8. Scale growth histograms, density plots, and Gaussian mixture models results for female Pacific herring of the 1999 cohort in Prince William Sound, AK.

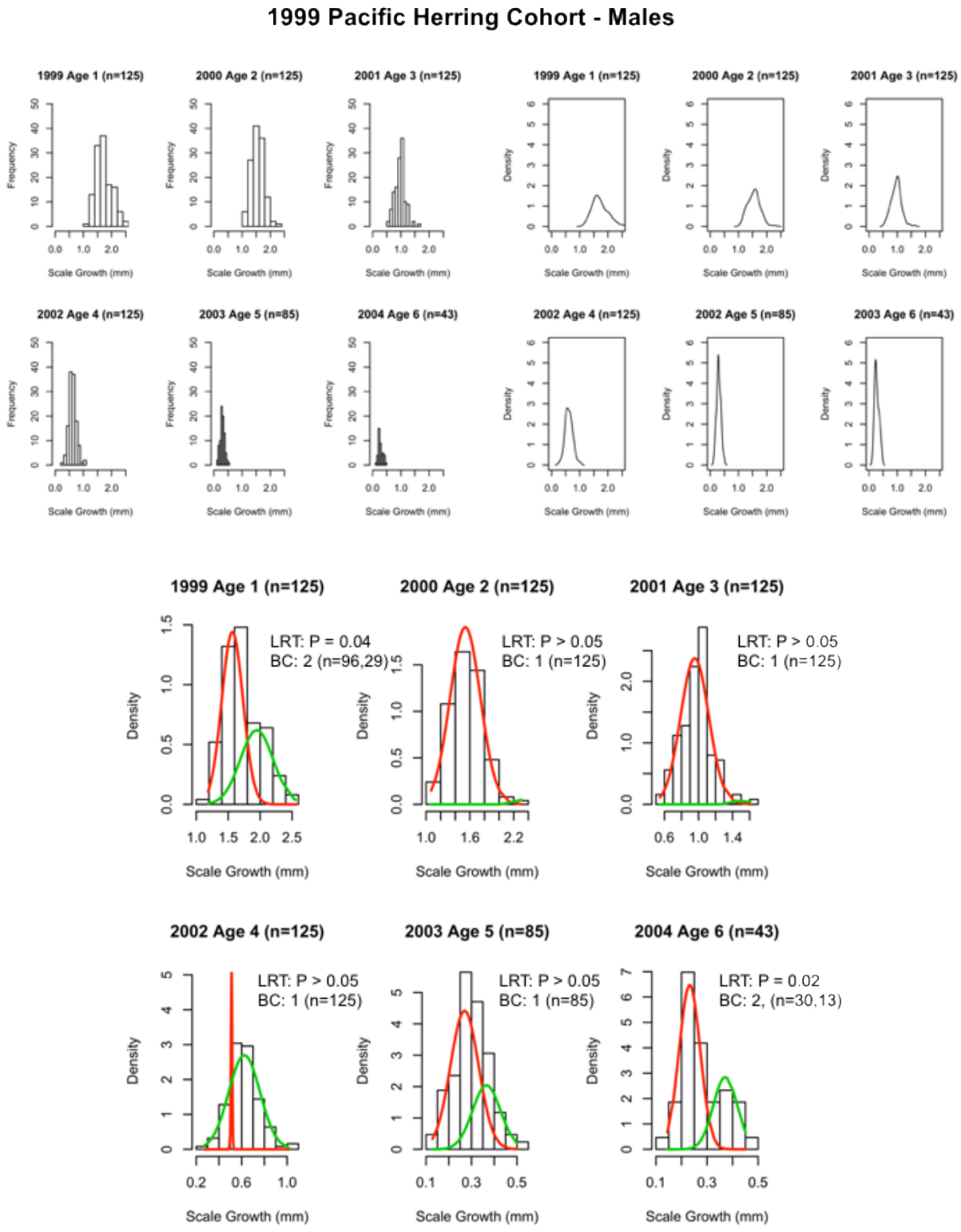

Figure 2-9. Scale growth histograms, density plots, and Gaussian mixture models results for male Pacific herring of the 1999 cohort in Prince William Sound, AK.

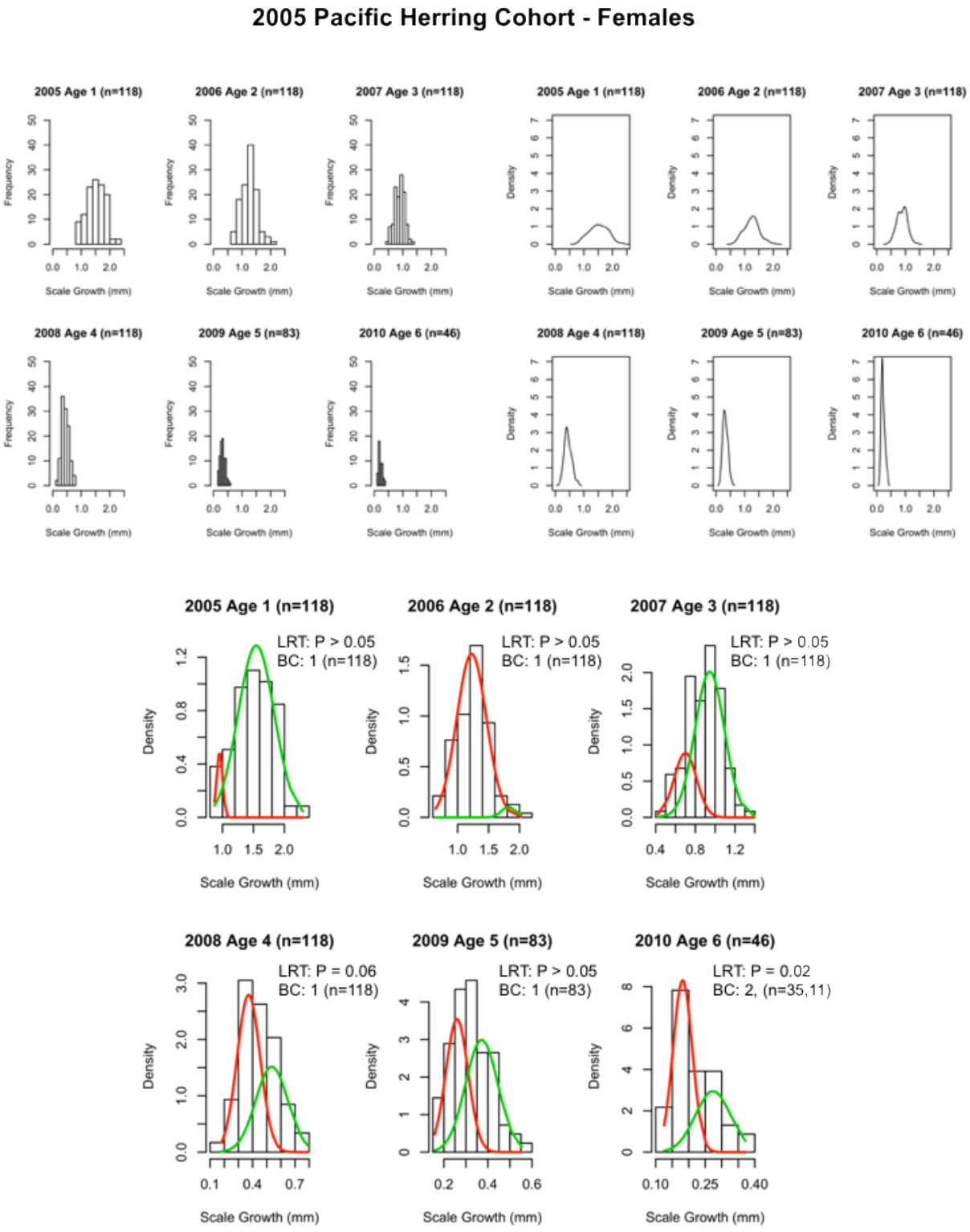

Figure 2-10. Scale growth histograms, density plots, and Gaussian mixture models results for female Pacific herring of the 2005 cohort in Prince William Sound, AK.

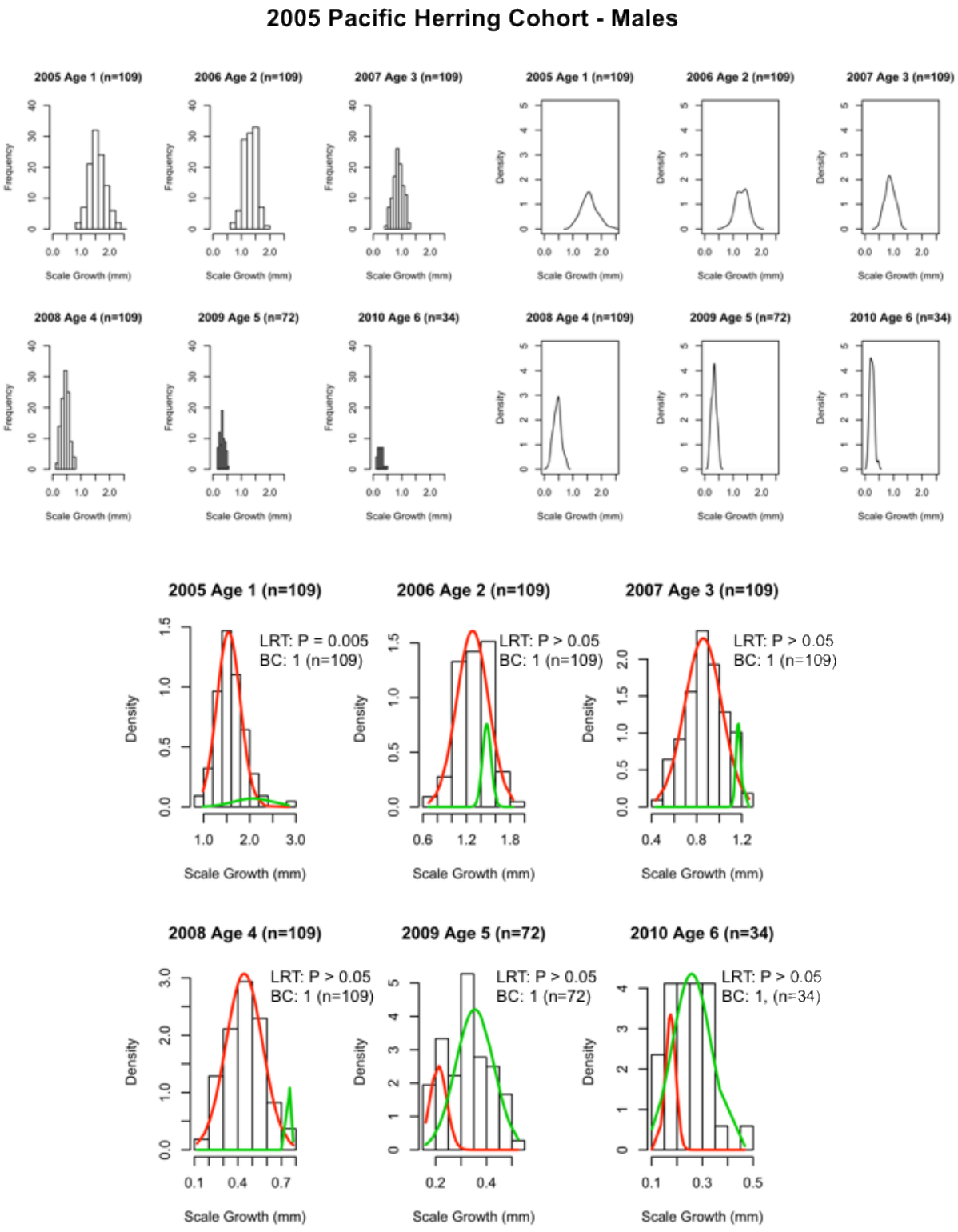

Figure 2-11. Scale growth histograms, density plots, and Gaussian mixture models results for male Pacific herring of the 2005 cohort in Prince William Sound, AK.

DISCUSSION

This preliminary analysis demonstrates some evidence for bimodal distributions in scale growth of specific cohorts of PWS herring as they mature over time. Of interest is the fact that bimodal distributions were detected for both female and male herring. There was no strong evidence that younger fish show unimodal distributions in scale growth that then diverges into bimodal distributions in older fish as bimodal distributions in scale growth were detected in several age-1 groups (1988 females, 1999 males, and 2005 males). Age-2 groups did not exhibit any evidence for bimodal distributions in the dataset. Only one age-3 group had evidence of bimodal scale growth distributions (1986 males). Several age-4 groups showed bimodal distributions for scale growth (1987 females and males, and 1991 females), as well as age-5 and age-6 groups (age-5: 1988 females and males; age-6: 1989 females, 2004 females and males, 2010 females). Clearly, this analysis indicates the presence of bimodal distributions in scale growth for PWS Pacific herring, which confirms the conclusion by Vollenweider et al. (2017). It would be useful to increase the sample sizes of scale growth measurements for future analysis for all age groups. Additional sample sizes may help resolve long-term shifts in bimodal scale growth, in addition to considering more cohorts before and after 1997.

MODEL TREATMENT OF MATURITY

The Bayesian ASA (BASA) model (Muradian et al. 2017) is adapted from the model described by Hulson et al. (2007). The model described by Hulson et al. includes a "maturity" function that estimates the total number of fish at each age from the observed number of fish at each age within the pre-spawn and spawning population as measured in the ASL samples. As described earlier, this definition is better considered an "availability" function because it estimates the proportion of fish available to the ASL sampling.

An updated version of BASA has been developed and made available on the Alaska Ocean Observing System Research Workspace (Branch et al., Research Workspace). Included in BASA is a maturity function as described by Hulson et al. (2007) that the model estimates as the proportion of all fish available to the acoustic (pre-spawn) and milt (post-spawn) surveys. Importantly, this maturity function implies that only mature fish are observed, and no immature fish are included.

The issue with estimating maturity in this manner is that there is no actual maturity information given to the model. BASA is able to estimate "maturity" at age-3 relative to maturity at age-4 because it treats maturity more like selectivity in the seine and cast net sampling. Because fits to the age composition, as well as acoustic survey and milt survey data, are assumed to be indices of spawners, not immature fish, then any discrepancy in the youngest age compositions is treated as percent mature.

For example, age-5 fish are assumed to be fully accounted for and so the expected total number of age-4 fish the prior year should be determined from:

Eq. 1 $$\widehat{N}_{4,y-1} = \frac{\widehat{N}_{5,y}}{S}$$

Where $\widehat{N}_{5,y}$ is the number of age-5 fish expected in year y, $\widehat{N}_{4,y-1}$ is the number of age-4 fish at year y minus one, and *S* is the annual survival rate. However, if the observed number of age-5 fish ${N^{obs}}_{5,y}$ is consistently greater than the preceding year's age-4 cohort and/or the predicted age-5 fish from the survival curve, then some age-4 fish must be missed by sampling and can be calculated by:

Eq. 2 $${N^{miss}}_{4,y-1} = \frac{{N^{obs}}_{5,y} - \widehat{N}_{5,y}}{S}$$

Where ${N^{miss}}_{4,y-1}$ is the number of age-4 fish missing in year minus one. BASA implicitly calculates maturity to then be:

Eq. 3 $$Mat_4 = \frac{\widehat{N}_{4,y-1}}{{N^{miss}}_{4,y-1} + \widehat{N}_{4,y-1}}$$

Where Mat_4 is the mature proportion of age-4 fish, or those age-4 fish in the spawning aggregations sampled by surveys and therefore selected by the survey because they are available to the survey gear. When correcting Eq.1 to fully account for all age-4 fish:

Eq. 4 $$\widehat{N}_{4,y-1} = \frac{\widehat{N}_{5,y}}{S \cdot Mat_4}$$

It is possible to project back to the number of age-3 fish that must have existed the prior year by following Eq. 1-4. Again, the discrepancy between the observed number of age-3 fish in a year to the estimated number of age-4 fish (the true value) provides the mature proportion of age-3 fish in the model.

BASA does not annually estimate the maturity function as suggested in Eq. 1-4, rather, it estimates the maturity in time blocks. However, this method raises another issue. Age-3 maturity for each of two time periods and age-4 in the first time period are estimated, and age-4 in the second time period is fixed (Table 2-8). For age-5 and older the maturity is set to 1.0 in all years. These two time periods were established with an earlier version of the ASA model (Hulson et al. 2007). Hulson et al. state that an "analysis of residuals suggested that maturity changed before and after 1997" without showing these results and further acknowledge "it remains unresolved whether there was a shift in maturity during the late 1990s." This vague justification for the establishment of two maturity periods within the model begs the question of whether a break in maturity does exist or whether a change in selectivity of age composition sampling and/or availability of spawner groups occurred instead. Regardless, the model does converge and provide two very different sets of maturity parameters for the two periods.

Table 2-8. 2018 Bayesian Age-Structure-Analysis maturity parameter estimates.

	Median	Lower 95th	Upper 95th
Proportion mature at age-3, 1980-96	0.36	0.28	0.46
Proportion mature at age-4, 1980-96	0.92	0.76	1
Proportion mature at age-3, 1997-2018	0.64	0.55	0.76
Proportion mature at age-4, 1997-2018	0.9	0.9	0.9

Current maturity assumptions within BASA suggest model mis-specification that may bias estimates. As we showed earlier, there are immature fish being counted in the acoustic surveys and the age-structure estimate includes immature fish that would not be able to contribute to the milt surveys. While there is a maturity estimate for the pre-spawning population surveyed by the acoustics, it is not straightforward to include these maturity data in the model, because the percentages counted are not a reflection of numbers in the whole population. Without maturity data representing the whole population, all we can do is ask how much of a difference the maturity schedule makes to model estimates by running a sensitivity analysis.

EFFECT OF CHANGING MATURITY ASSUMPTIONS ON MODEL RESULTS

We developed a subset of BASA models that bound the potential effects of mis-specifying maturity on key model outputs:

Model 1: The current version of BASA in which two sets of mature proportions (1980-1997 and 1998-2018) are estimated. The mature spawning biomass is fit to the acoustic and milt survey data.

Model 2: Mature proportions are fixed to hypothesized lower bounds over the entire modeling time frame (1980-2018). The proportions are: 0.5 for age-3, 0.8 for age-4, 0.9 for age-5, and 1.0 for age-6+. Mature biomass is then fit to the acoustic and milt survey data.

Model 3: Mature proportions are fixed to hypothesized upper bounds as: 0.8 for age-3, 0.95 for age-4, and 1.0 for age-5+. Mature biomass is fit to the acoustic and milt survey data.

Model 4: Similar to Model 2 except that total age-3+ herring is fit to the acoustic and milt survey data.

Model 5: Similar to Model 3 except that total age-3+ herring is fit to the acoustic and milt survey data.

Model 6: True mature proportions are fixed to the lower bounds as stated in Model 2, but now estimate mature proportions of the sampled population by fitting to the data from Table 2-3 (% MI>4) using a logistic likelihood function. With the estimated maturity of the sampled fish, we can then calculate the proportion of immature fish

that are available for sampling with the seine nets at each age. The resulting biomass that is fit to the age composition and acoustic data is the model predictions for available fish (i.e., mature fish + availability*immature fish) at each age.

Model 7: Same as Model 6 except that true mature proportions are fixed to the upper bounds from Model 3.

Model 8: A selectivity curve is directly estimated for fitting to the age composition data (selectivity*total population) from the seine and cast nets. The estimated selectivity is then used to calculate how many fish are missing from the spawning aggregations/sampled fish. We assume the sampled fish have fixed mature proportions equal to those calculated from Table 2-1 (as shown in Table 2-3 with MI>4), while the missing fish have fixed mature proportions from Table 2-2. The fixed mature proportions in the sampled and missing/unsampled populations are the same across all years. The resulting mature biomass that is fit to both the milt and acoustic data is derived from the mature numbers from both sampled and unsampled populations (e.g., (selectivity*mature in sampled fish + (1-selectivity) *mature in unsampled fish)*total fish*weight).

Model 9: Similar to Model 1 except that one maturity schedule (1980-2018) is estimated. The mature spawning biomass is fit to the acoustic and milt survey data.

Model 10: Similar to Model 1 except that early period maturity is estimated (1980-2008) while the later period (2009-2018) is fixed to 0.53 for age-3 and 0.91 for age-4. The fixed maturity during 2009-2018 corresponds to seine samples from the pre-spawning aggregations with a maturity index greater than 4. The mature spawning biomass is fit to the acoustic and milt survey data.

Model 11: Similar to Model 1 except that early period maturity is estimated (1980-1999) while the later period (2000-2018) is fixed to 0.29 for age-3 and 0.85 for age-4. The fixed maturity during 2000-2018 corresponds to the combination of missing fish and observed fish that are not mature as estimated from the simplified age-structure analysis fitting an exponential decay (Figure 2-2). The mature spawning biomass is fit to the acoustic and milt survey data.

Summary values of spawning biomass and recruitment estimates show minor differences between models (Figure 2-12). Estimates are from the recent time period to determine the implications of maturity information on BASA output that has the most relevance for current management. The base model (Model 1) has a slightly lower 2013-2018 mean biomass compared to most other models, albeit with a posterior median well within the 95% credibility intervals for the other models, implying this difference is negligible. The 2018 biomass estimate was slightly lower from Models 6 and 7 which fit to the maturity data from the seine net sampling, while the

between-model differences were again negligible. Negligible differences are also seen in median recruitment estimates from recent years (2013-2018) and across all years.

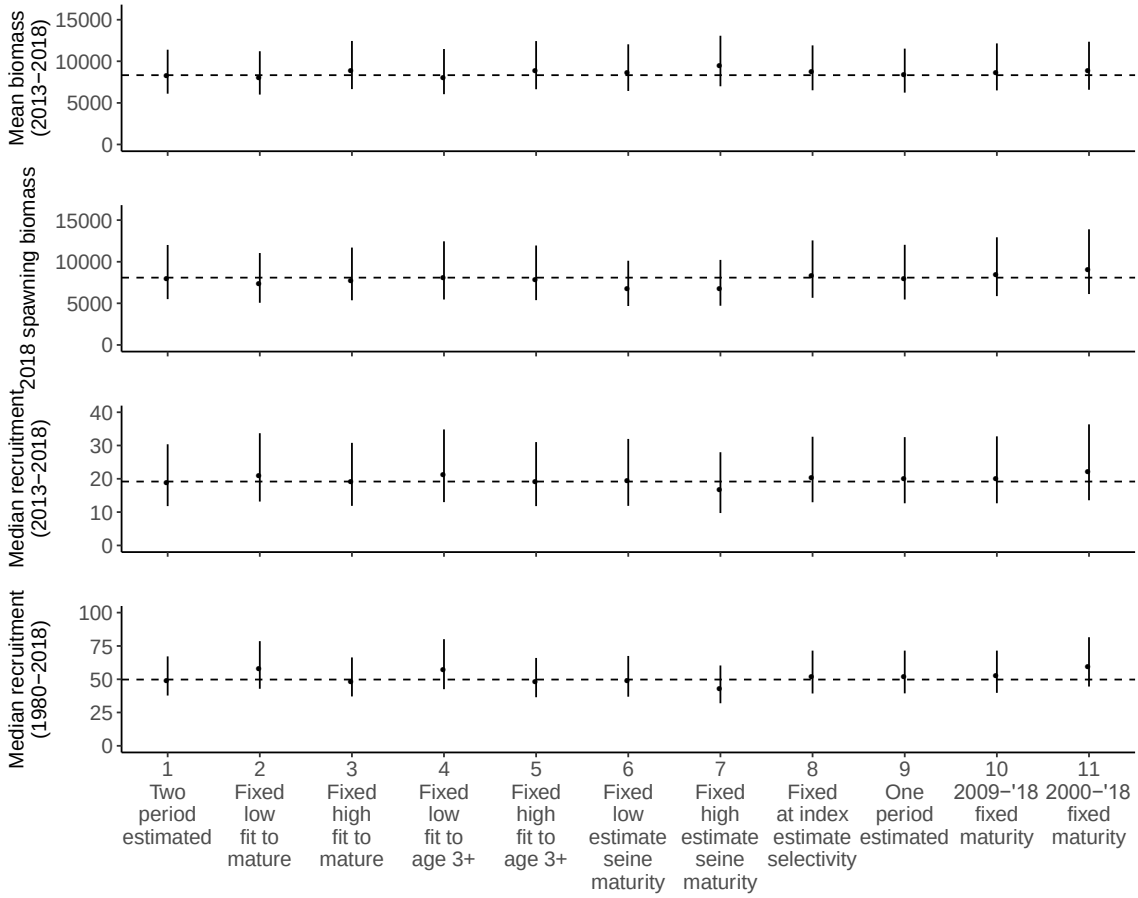

Figure 2-12. Summary values of key management estimates from the Bayesian Age-Structure-Analysis. The median (point) with 95% credibility intervals are shown for each model.

Age-specific estimates of the different availability parameters (Figure 2-13) generally agree with the results presented in Figure 2-12. Incorporating maturity information into Models 6-8 produced different age-specific values amongst models, as would be expected. For Models 6 and 7, the estimated sampled mature proportions converged on the same values because they are fit to the percent of fish with MI >4 shown in Table 2-3, estimating approximately 53% mature age-3, 79% mature age-4, and 93% mature age-5 in both models. When fixing true maturity to the observed maturity values from Table 2-1 and Table 2-3 and estimating seine selectivity (Model 8), the model estimates that nearly 57% of age-3 fish are selected while age-4+ are nearly fully selected. The 95% credibility intervals of the selected proportions of these fish (50-60% for age-3 and 91-100% for age-4) well agrees with the range of observed age-3 and age-4 fish estimated from Figure 2-2 and Figure 2-3 (48-61% of age-3 and 90-97% of age-4). Maturity over the entire modeling period (Model 9) was estimated at 55% age-3 (41-71% interval) and 92% age-4 (79-99% interval). These values closely matched selectivity estimates from Model 8 and were similar

to maturity estimates from Model 1, particularly for the 1998-2018 time period. Fixing model maturity to the maturity based on MI>4 from the 2009-2018 seine samples while estimating maturity in the years prior (Model 10) resulted in BASA estimates similar to the fixed values between the two time periods (age-3 = 56% and age-4 = 95%, with 42-69% and 85-100% intervals respectively). Model 10 maturity values also closely matched estimates from Models 1, 8, and 9. The 1980-1999 estimated maturity greatly differed from the fixed maturity during 2000-2018 (determined from an exponential fit of the pooled age composition data from 2000-2015) in Model 11, though agreed with values from Models 1 and 8-10.

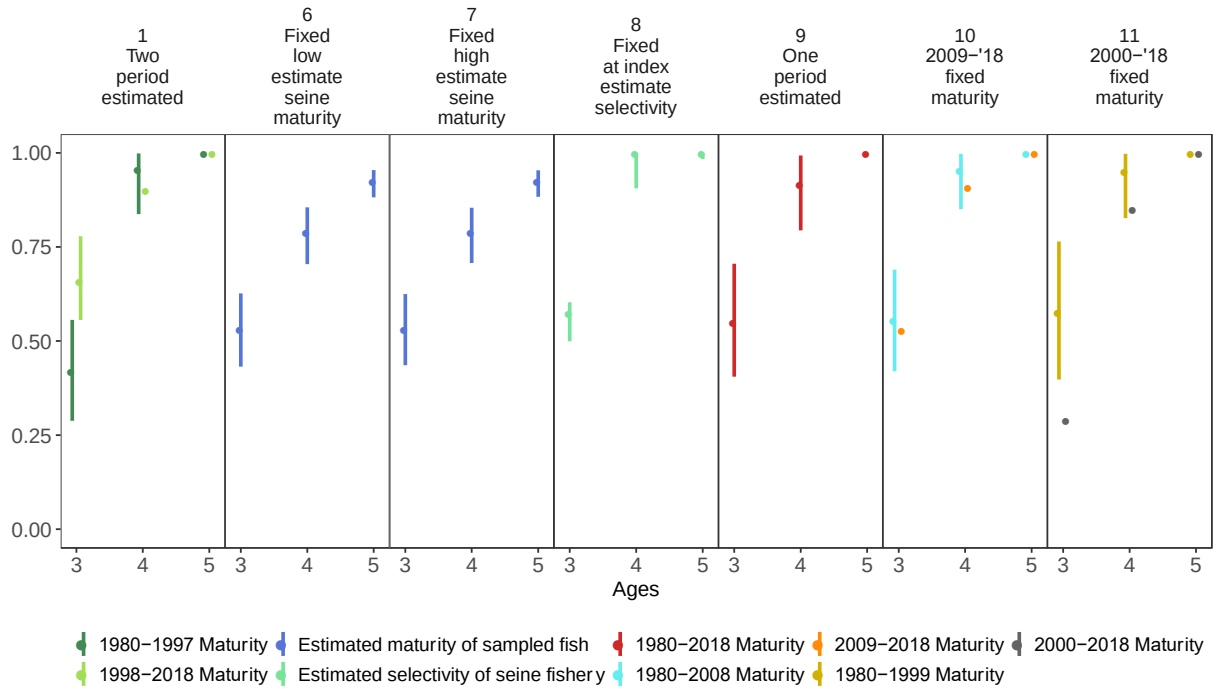

Figure 2-13. Key age-specific estimates of the availability of pre-spawning herring to surveys. The names of the estimated parameters as are color coded.

We also included BASA in which maturity is estimated for a single period (Model 9) to investigate differences noted by Hulson et al. (2007), where they observed a change in the residual patterns around 1997. A look at the residuals in age composition of the seine fishery survey from Model 1 and Model 9 (Figure 2-14) do not reveal any stark changes in the residual patterns between models, and thus the past justification for two periods of different maturity values no longer seems valid. Additionally, there is no observable change in residuals before and after 1997 in the model with one-period of estimated maturity.

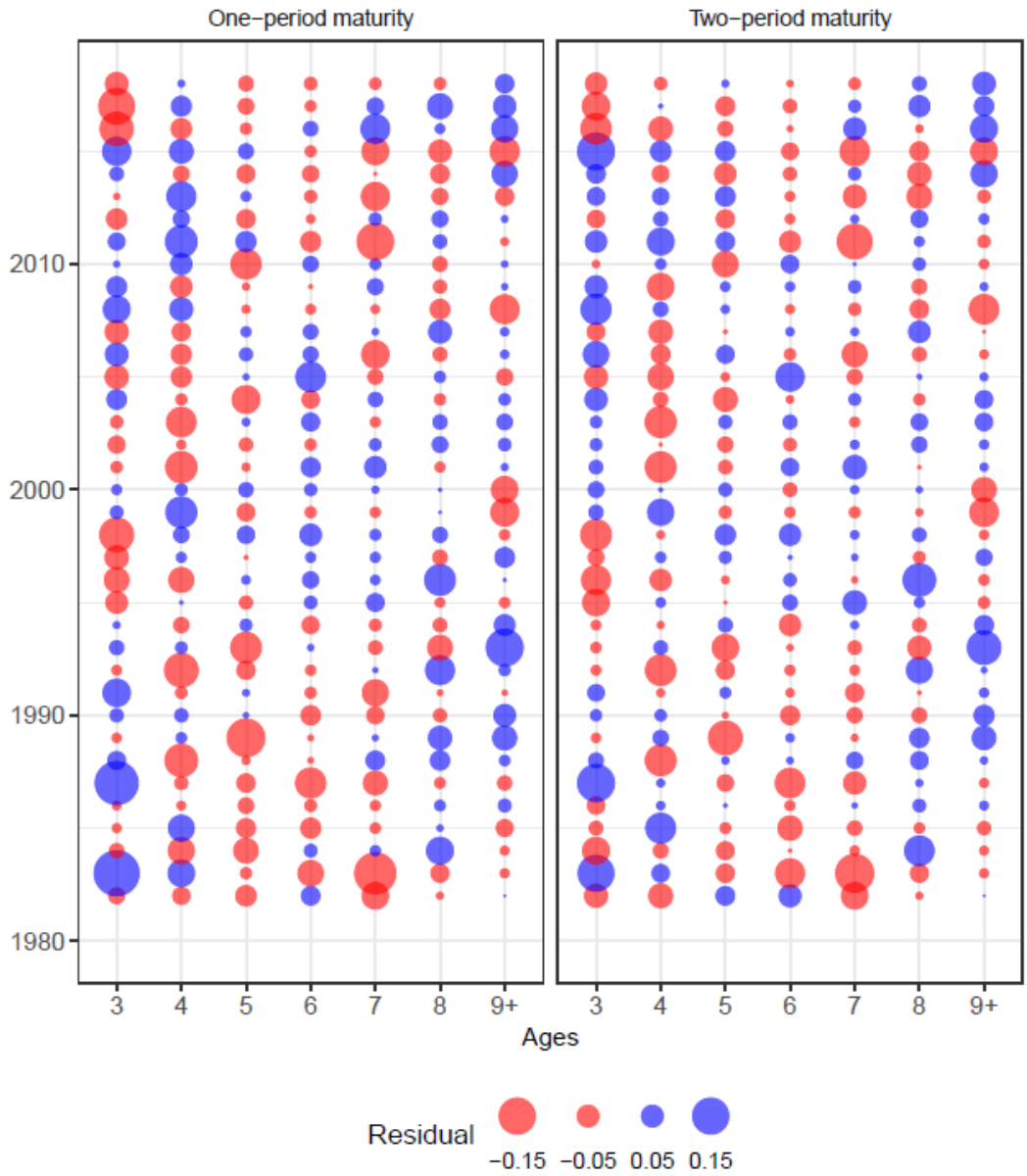

Figure 2-14. Comparing residuals (i.e., the difference between the predicted age composition, expressed as the median of the posterior distribution, and observed age composition in the seine net fishery) between models that estimate two periods (left) and one period (right) of maturity. Red circles denote negative residuals and blue are positive, while sizes show magnitude.

Modeling Implications

Different maturity assumptions, whether fixing different maturity values, fitting different aggregations of fish to survey data, or changing model structure, yielded negligible differences in results compared to the current BASA model. BASA estimates currently used by management to inform the status of PWS herring all show similarly low recent spawning biomass and similar mean recruitment estimates. These negligible differences result even despite the incorporation of the maturity information from seine samples, which BASA fits well. BASA also accurately estimates age-specific availability compared to estimates from the preceding analysis on the raw data. Furthermore, we find no basis for justifying the inclusion of two "maturity periods" in the current BASA.

Maturity remains a key uncertainty in herring biology, and BASA in particular, although not a major sensitivity. The true definition of "maturity" estimates in the current version of BASA (Model 1) likely lies somewhere between availability, the percent of stock available to the sampling gear (which differs between seine and cast nets, and likely fishery catches), and biological maturity, the proportion of all fish in the entire population that is capable of spawning at each age. Both availability and/or maturity are also likely time-varying as suggested by Table 2-4. Despite the lack of accurate information on maturity and availability, BASA still produces stable estimates of biomass and recruitment. However, we have neither shown nor tested maturity assumptions on forecasting or estimation of biological reference points, neither of which is currently implemented in BASA or used by management. Moving forward, we recommend that the base model should only estimate one set of maturity parameters that apply to the entire time period, together with a small set of scenarios for maturity to conduct as sensitivity tests of different assumptions about maturity and availability during pre-spawning. In other words, the specific scenario we recommend as the base case is Model 9. Simplifying this component of the model will improve model stability, in which further changes to BASA (unpublished results) have resulted in estimation issues with these parameters (e.g., overparameterization). The model checks conducted here offer a simple framework for investigating maturity uncertainty in future assessments.

References

Branch, T.A., Muradian, M., Pegau, W.S., Trochta, T., & Moffitt, S. Using Bayesian Age-Structured-Analysis (ASA) Model for Herring Population Dynamics in Prince William Sound, EVOS Herring Program. Research Workspace. 10.24431/rw1k1t.

Benaglia, T., D. Chauveau, D. Hunter, and D. Young. 2009. mixtools: An R Package for Analyzing Finite Mixture Models. Journal of Statistical Software, University of California, Los Angeles 32:1-29.

Engelhard, G. H., U. Dieckmann, and O. R. Godo. 2003. Age at maturation predicted from routine scale measurements in Norwegian spring-spawning herring (Clupea harengus) using discriminant and neural network analyses. Ices Journal of Marine Science 60:304-313.

Engelhard, G. H., and M. Heino. 2004. Maturity changes in Norwegian spring-spawning herring before, during, and after a major population collapse. Fisheries Research 66:299-310.

Hay, D. E. 1985. Reproductive biology of Pacific herring (Clupea harnangus pallasi). Canadian Journal of Fisheries and Aquatic Sciences 42:111-126.

Hay, D. E., and D. N. Outram. 1981. Assessing and monitoring maturity and gonad development in Pacific herring. Canadian Technical Report of Fisheries and Aquatic Sciences:i-v, 1-31.

Hulson, P.-J. F., S. E. Miller, I. I. T. J. Quinn, G. D. Marty, S. D. Moffitt, and F. Funk. 2008. Data conflicts in fishery models: incorporating hydroacoustic data into the Prince William Sound Pacific herring assessment model. Ices Journal of Marine Science 65:25-43.

Lambert, T. C. 1987. Duration and Intensity of Spawning in Herring Clupea-Harengus as Related to the Age Structure of the Mature Population. Marine Ecology-Progress Series 39:209-220.

Moffitt, S. D. 2017. Exon Valdez Lomg-Term Herring Restoration and Monitoring Program: Scales as growth history records. Exxon Valdez Long-Term Herring Research and Monitoring Final Report (Restoration Project 13120111-N), Alaska Department of Fish & Game, Cordova, Alaska.

R Core Team. 2018. R Foundation for Statistical Computing, Vienna, Austria., Vienna, Austria.

Scrucca, L., M. Fop, T. B. Murphy, and A. E. Raftery. 2016. mclust 5: clustering, classification and density estimation using Gaussian finite mixture models. The R Journal 8/1, pp. 205-233.

Vollenweider, J., J. Maselko, and R. Heintz. 2017. *Exon Valdez* Lomg-Term Herring Restoration and Monitoring Program: What is the age at first spawning for female herring in PWS? Exxon Valdez Long-Term Herring Research and Monitoring Final Report (Restoration Project 13120111-J), Auke Bay Labs, Alaska Fisheries Science Center, NOAA Fisheries, Juneau, Alaska.

This page intentionally left blank

CHAPTER 3 MULTI-DECADAL SHIFTS IN THE DISTRIBUTION AND TIMING OF PACIFIC HERRING SPAWNING IN PRINCE WILLIAM SOUND, ALASKA

David W. McGowan[1], Trevor A. Branch[1], Stormy Haught[2], and Mark Scheuerell[3]

[1] *School of Aquatic and Fishery Sciences, Box 355020, University of Washington, Seattle, WA*
[2] *Alaska Department of Fish and Game, Division of Commercial Fisheries, PO Box 669, Cordova, AK*
[3] *U.S. Geological Survey Washington Cooperative Fish and Wildlife Research Unit, School of Aquatic and Fishery Sciences, Box 355020, University of Washington, Seattle, WA*

ABSTRACT

The location and time of spawning plays a critical role in the survival of pelagic fish during early life stages that subsequently affects recruitment to the population. This study examines if changes in spawning patterns from 1973 to 2019 provide insights on factors that are inhibiting recruitment of Pacific herring (*Clupea pallasii*) to the Prince William Sound (PWS) population. Our findings show substantial changes in spatial and temporal patterns of herring spawning in PWS have occurred over the past four decades, and that these changes are likely contributing to the population's lack of recovery. We attribute major shifts in spawning distributions prior to the population collapse in 1993 and in the late 1990s to changes in population demographics and fishery-related effects on local spawning aggregations. For the past two decades, the concentration of spawning towards the Southeast Shore region has coincided with declines in population abundance to current record lows, and there are indications that this region may be an ecological sink compared to other areas of PWS. In addition, major shifts in spawn timing have coincided with large-scale changes in ocean temperatures, indicating the population is also responding to external perturbations in their environment. The current state of the population (i.e., low abundance, spatially constrained spawning habitat, and lack of a broad age structure that extends the spawning period) suggests its potential for reproductive success is greatly reduced.

INTRODUCTION

The location and time of spawning plays a critical role in the survival of pelagic fish during early life stages that subsequently affects recruitment to the population. For herring (*Clupea* spp.), spatial differences among spawning sites can influence egg mortality rates (Rooper et al. 1999, Shelton et al. 2014, Keeling et al. 2017) and the transport and/or retention of larvae in nursery areas (Sinclair and Tremblay 1984, Cowan and Shaw 2002). Temporal shifts in spawning can affect the duration of egg and larval stages (Houde 2016), predation risk, and the availability of prey to larvae during the critical early feeding period (Cushing 1990).

To increase opportunities for the offspring of Pacific herring to survive early life stages, a typical herring population will collectively release batches of eggs over a period of days to months across numerous sites. Given that individual herring are one-time batch spawners, staggered spawning by the population in time and space has the effect of hedging against uncertainty of when and where conditions will be optimal for egg and larval survival. The adaptability of

herring to their local environment is evident by the diversity of spawning areas and timing among and within populations (Hay et al. 2009, Siple and Francis 2016). Spatial and temporal diversity in spawning among metapopulations buffers the larger population from abundance fluctuations (i.e., the portfolio effect, Schindler et al. 2010); herring spawning that is broadly distributed in space and time increases population resilience to annual to decadal frequency perturbations in their environment that impact reproductive productivity (Hay 1985, Lambert 1987, Siple and Francis 2016). Accordingly, declines in the number or diversity of spawning sites, or temporal shifts in the onset or duration of spawning may reduce a population's long-term productivity.

Herring exhibit interannual fidelity to spawning areas (Hay et al. 2001, Ware and Schweigert 2001, Flostrand et al. 2009). Unlike salmonids and other species that return to natal spawning sites, herring are hypothesized to select spawning areas the first time they reproduce by either dispersal or learned behavior (i.e., by following older herring), and then return to that spawning area in successive years (MacCall et al. 2018). MacCall and colleagues demonstrated that if spawning habitat is first selected by young herring via following older fish, spatial reorganization of a population that undergoes fishing may lead to long-term declines in the population's productivity. This outcome results from local depletion of a metapopulation by the fishery (Okamoto et al. 2018), which subsequently decreases the probability that first-time spawners encounter older fish with knowledge of migratory routes to spawning sites used by the depleted metapopulation (Corten 2002) and leads to declines in the diversity and total number of utilized spawning sites. In the absence of fishing, it is plausible that other natural processes that result in high mortality of a metapopulation, such as a disease outbreak or localized predation, could have similar impacts on productivity of the overall population.

In the Northeast Pacific, interannual variations in herring spawn timing have been primarily attributed to population demographics and temperature (Hay 1985, Ware and Tanasichuk 1989). Gonad maturation rate is determined by fish weight and daily temperature (Ware and Tanasichuk 1989), resulting in earlier spawning by larger fish and/or during warm years. In populations comprised of multiple cohorts, spawning may be staggered in discrete waves where older (larger) fish tend to spawn first and younger (smaller) fish spawn during subsequent waves (Hay 1985, Ware and Tanasichuk 1989). If the age composition of a population is truncated or dominated by one age class, the spawning period duration is likely shorter. State-dependent life history modeling also suggests that variations in food availability to adult herring may result in shifts in spawn timing in order to optimize their own fitness at the expense of their offspring (Ljungström et al. 2018).

This study examines if changes in spawning patterns provide insights on factors that are inhibiting recruitment to a once-thriving herring population in PWS. Herring are a key forage species in this ecosystem, where they have supported a commercial fishery for more than a century (Muradian 2015). The population collapsed in 1993 (Quinn et al. 2001), just a few years after the 1989 *Exxon Valdez* oil spill (EVOS), and has yet to recover to pre-1993 abundance levels (Figure 3-1). Hypotheses vary on the primary causes of the initial population collapse (Hulson et al. 2008, Thorne and Thomas 2008, Pearson et al. 2012) and continued low population size and poor recruitment (Deriso et al. 2008, Pearson et al. 2012, Ward et al. 2017). There have not been any high recruitment events since 1988 (Muradian et al. 2017), creating uncertainty as to which conditions will be favorable to the population's long-term recovery.

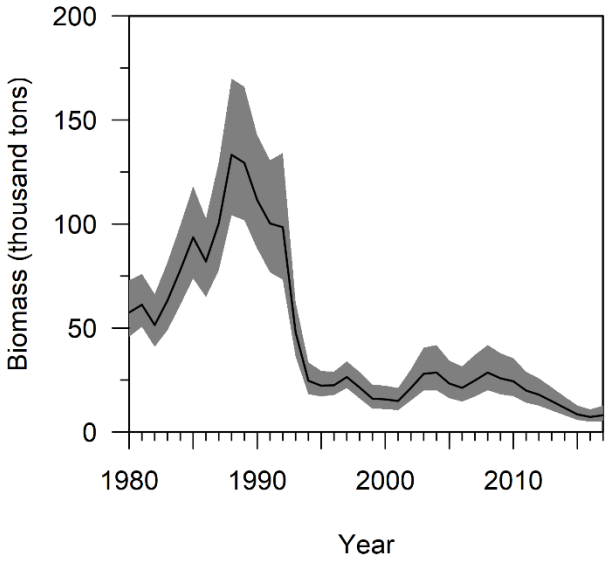

Figure 3-1. Estimated median herring spawning biomass (solid line) and 95% confidence interval (shaded area) for the Prince William Sound management area from 1980 to 2017 (J. Trochta per. comm. 16 May 2019).

Given the critical nature of the timing and location of spawning in both the match-mismatch theory and the portfolio effect, we investigated how these have changed over time. We examined the following aspects: 1) decadal and interannual shifts in distribution of spawn locations from 1973 to 2019; 2) interannual shifts in spawn timing from 1980 to 2019; and 3) the spatial structure of spawning areas based on spawn timing trends.

METHODS

DATA COLLECTION

Observations of active herring spawning were collected during aerial surveys conducted by the Alaska Department of Fish and Game (ADF&G) in the PWS management area between 1973 to 2019. Active herring spawn was quantified based on the length of milt clouds along the coastline per day (hereafter mile-days of milt) following Shepherd and Haught (2019). Mile-days of milt is used as a key index of relative abundance for PWS herring in the fisheries stock assessment model (Muradian et al. 2017). Mile-days of milt was measured by using aerial surveys that were flown between late-March and mid-May (Table A1 in the Appendix). The ADF&G aerial survey is a non-random survey that attempts to conduct a total count of all spawning within PWS. At the start of the period, scheduled surveys were flown once or twice per week, and then flown more frequently when spawning or pre-spawning herring aggregations were first observed (up to twice a day if funding was available). Surveys ended when there were no observed spawning and no anecdotal reports of spawning in PWS. Surveys were flown along the coastline at an altitude of approximately 460 m (1500 ft) for up to 5 hours, covering approximately 800 km (~500 mi) per survey.

There have been notable changes in survey coverage during the study period. Prior to 1981, survey coverage was limited to the eastern Sound from lower Valdez Arm to Port Gravina, and

the southern Sound along the northern coasts of Hawkins and Hinchinbrook Islands and Northeast Montague Island (Figure 3-2). The survey domain was expanded west along the north shore from Valdez Arm to Esther Island in the 1980s, and in the western Sound to include Perry, Naked, and Knight Islands. Starting in 2007, surveys also have been flown over Kayak Island in most years.

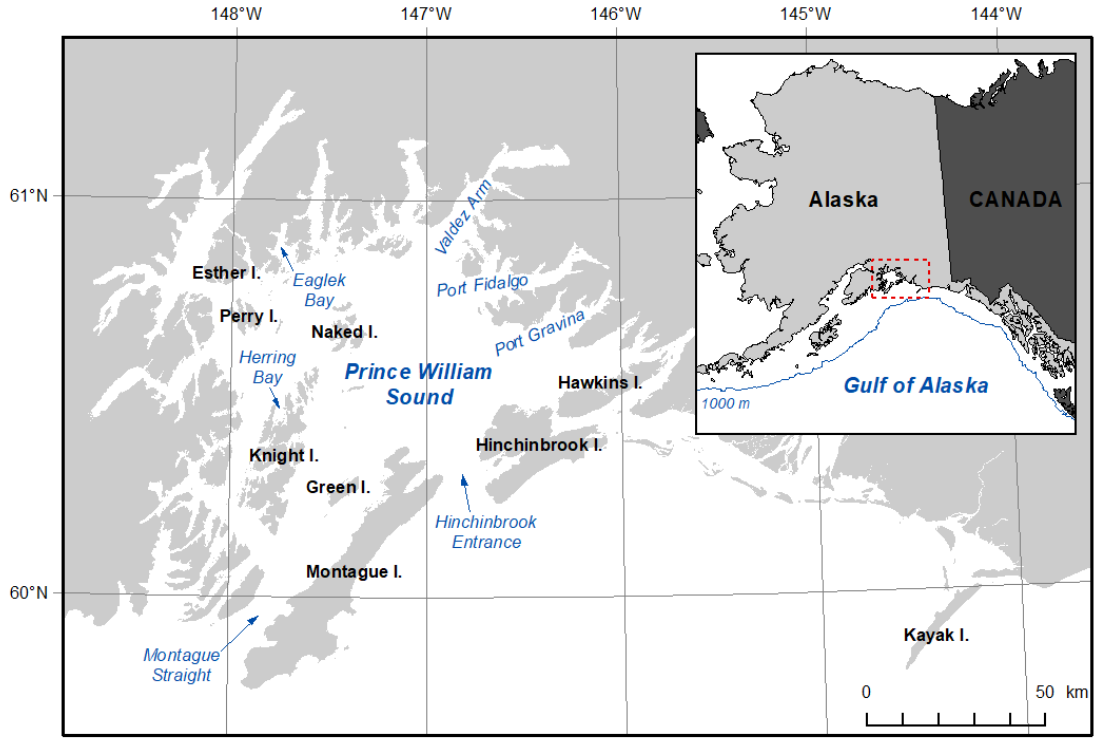

Figure 3-2. Prince William Sound management area. The red box within the inset map of the Northeast Pacific outlines the study area. Key bathymetric (blue text) and geographic (black text) features mentioned in text are labeled.

Prior to 2008, most surveys were conducted by a single observer in addition to the pilot who photographed and recorded all spawn observations on paper maps (Brady 1987). Since 2008, two observers have conducted surveys and all spawn observations have been digitally recorded as polylines using Esri ArcPad (Esri Inc., Redlands, CA) with a Bluetooth GPS for georeferencing (Shepherd and Haught 2019). Post-processing of digital data entailed using photographs to adjust the lengths of spawn events (MDM) in ArcGIS (Esri Inc., Redlands, CA). Prior to 2008, spawn observations were recorded on paper maps and later digitized as polylines in ArcGIS to make all survey data from 1973 to 2018 publicly available through the Alaska Ocean Observing System (https://portal.aoos.org, Bochenek 2010). Survey coverage was digitized into one of two formats in ArcGIS: either as polygons recorded in historical logbooks (1973 to 1999), or as polylines recorded as georeferenced flight paths (1997 to 2019). Processed survey data from 1973 to 2018 were downloaded from the Alaska Ocean Observing System (Haught and Moffitt 2018), and combined with survey data from 2019.

SPATIAL ANALYSIS

Survey coverage and spawning data were partitioned into 10 × 10 km grid cells. ArcGIS polylines and polygons that occurred in two or more grid cells were split into segments at the borders of each cell. Polyline segments for mile-days of milt (i.e., spawning) were assigned values equivalent to the length of the segment within the grid cell. Grid cells were assigned binary values for survey coverage (1 = coverage, 0 = no coverage) based on the presence/absence of either a survey coverage polygon or polyline segment by year and day of year. MDM polyline segment values were summed within each grid cell by observation. Grid cells were grouped into the following regions (Figure A1 in the Appendix) based on ADF&G herring districts within the PWS management area (cf. Appendix G4. in Russell et al. 2017): Montague Island; Southeast Sound; Northeast Sound; North Shore; Naked Island; and Kayak Island.

Spatial patterns of herring spawning were characterized at decadal and interannual scales across the PWS area and by region from 1973 to 2019. To examine decadal spatial patterns, MDM values for observation i were summed within each grid cell *j* by decadal period *k* (i.e., 1970s, 1980s) as:

(3-1) $$\mathrm{MDM}_{j,k} = \sum \mathrm{MDM}_{i,j,k}$$

$\mathrm{MDM}_{j,d}$ values were plotted by decade as quantiles in 20% increments to highlight cells where herring spawning was concentrated during each period. To examine interannual spatial patterns, MDM values for observation *i* were summed within each grid cell *j* by year *t* as:

(3-2) $$\mathrm{MDM}_{j,t} = \sum \mathrm{MDM}_{i,j,d,t}$$

where *d* is the day of year. Quantiles for $\mathrm{MDM}_{j,t}$ values were calculated in 20% increments for all years combined and plotted as heat maps by year and grid cell. Grid cells with positive survey coverage values for each year were identified in the heat map to indicate interannual changes in the survey domain. To show interannual spatial variations in cumulative spawn, $\mathrm{MDM}_{j,t}$ values were summed across grid cells within each region (Figure A1) by year.

To quantify interannual changes in how evenly distributed spawning was across PWS, we used an index of spatial dispersion (Payne et al. 2005) adapted from Pielou's (1966) species evenness index that is based on Shannon's species diversity index (Shannon and Weaver 1949):

(3-3) $$D_t = \frac{-\sum_{j=1}^{s} p_{j,t} \ln(p_{j,t})}{\ln(s)}$$

where $p_{j,t}$ is the proportion of total spawn (MDM) in each grid cell in a given year, and *s* is the number of grid cells in which active spawning was observed during the study period. Index values D_t range from 0 (all in one grid cell) to one (evenly distributed across all grid cells). Although not all grid cells were surveyed each year, under this approach we assume that all grid cells were either directly sampled by the survey or indirectly via other methods (e.g., other aircraft or vessels) each year. Given that the ADF&G aerial survey is a non-random survey that attempts to conduct a total count of all spawning within PWS, anecdotal reports of the presence

of pre-spawning herring aggregations or spawn events would typically have resulted in an ADF&G survey flight being conducted in that area. While it likely that a small proportion of total spawn is not observed each year, the dispersion index should be sufficiently robust to quantify relative changes in evenness given the high proportion of sites (> 50%) that are sampled each year (Payne et al. 2005).

Changes in spawning distributions were compared to age composition data and commercial landings. Age composition data from commercial and survey catches used in the stock assessment model were provided by J. Trochta, while geo-referenced commercial landings for the sac-roe fishery from 1980 to 1998 were accessed from the AOOS website. Commercial landings were summed with each region in PWS and from the Gulf of Alaska shelf.

TEMPORAL ANALYSIS

Interannual variations in spawn timing were examined across PWS and by region from 1980 to 2019, excluding observations from the 1970s and the Kayak Island region due to survey coverage gaps in space and time. MDM values for observation *i* were summed within each region *n* by day of year *d* in year *t* as:

$$\mathrm{MDM}_{n,d,t} = \sum \mathrm{MDM}_{i,n,d,t} \quad \textbf{(3-4)}$$

where *j* are grid cells within *n* (see Figure A1). Survey coverage and spawn events (scaled by $\mathrm{MDM}_{n,d,t}$ values) were plotted by day of year and year for each region and all regions combined. A time series of spawn timing was calculated for each region based on the day of year when 50% of total MDM for that year had been observed, which corresponds with the peak of spawning activity in most years (Figure A2 in the Appendix).

To quantify spatial and temporal shifts in spawn timing for PWS herring, multivariate autoregressive state-space (MARSS) models were fitted to time series of spawn timing for each region. The MARSS framework consists of separate observation and process models, allowing total variance in each time series to be partitioned into observation (i.e., sampling error) and process (i.e., environmental perturbations) variance (Holmes et al. 2012). The MARSS process model was fitted in the following matrix form:

$$\mathbf{x}_t = \mathbf{B}\mathbf{x}_{t-1} + \mathbf{w}_t, \text{ where } \mathbf{w}_t \sim \mathrm{MVN}(0,\mathbf{Q}) \quad \textbf{(3-5a)}$$

$$\mathbf{x}_t = \mathbf{x}_{t-1} + \mathbf{u} + \mathbf{w}_t, \text{ where } \mathbf{w}_t \sim \mathrm{MVN}(0,\mathbf{Q}) \quad \textbf{(3-6b)}$$

where $\mathbf{x}_t$ represents true spawn timing (i.e. hidden states), an $m \times 1$ vector for spawning area m in year t, estimated by a 1st-order autoregressive process where $\mathbf{B}$ is an $m \times m$ matrix with values that represent the strength of the autoregressive process for each state along the diagonal and zeroes elsewhere, and $\mathbf{w}_t$ is an $m \times 1$ vector for process errors drawn from a multivariate normal (MVN) distribution with mean vector $\mathbf{0}$ and variance-covariance matrix $\mathbf{Q}$. Equation (**3-5**a is a mean-reverting stationary process (an unbiased random walk when $\mathbf{B} = 1$, or a stationary autoregressive process when $\mathbf{B} \neq 1$), while Equation **Error! Reference source not found.**b is a biased (non-stationary) random walk ($\mathbf{B}$ is fixed as 1) where $\mathbf{u}$ is an $m \times 1$ vector that represents the estimated bias. We fit different models to evaluate the data support for three different

assumptions of how process variance was structured: process errors are assumed to be 1) not correlated among the trajectories with equal variances (same q value on the diagonal and zeroes elsewhere); 2) not correlated with unequal variances (unique q_m values on the diagonal and zeroes elsewhere); or 3) correlated with equal variances (same q value on the diagonal and the same g value elsewhere).

$$\mathbf{y}_t = \mathbf{Z}\mathbf{x}_t + \mathbf{v}_t, \text{ where } \mathbf{v}_t \sim \text{MVN}(0, \mathbf{R}) \quad \textit{(3-7)}$$

Equation (**3-7** is the MARSS observation model, where $\mathbf{y}_t$ is an $n \times 1$ vector for the observed time series of spawn timing in PWS region n, $\mathbf{Z}$ is an $n \times m$ matrix containing 0s and 1s that maps each of the times series of observed spawn timing onto an associated true spawn timing $\mathbf{x}_t$ for each spawning area, and $\mathbf{v}_t$ is an $m \times 1$ vector for sampling errors for each time series drawn from a MVN distribution with mean vector $\mathbf{0}$ and variance-covariance matrix $\mathbf{R}$. Given that there are regional differences in weather conditions, topography, and currents that potentially affect sampling efficiency of the aerial survey, we assumed sampling errors have unequal observation variances (i.e., unique r_n along the diagonal of $\mathbf{R}$) and they are not correlated among the time series (i.e., 0s in the off-diagonals of $\mathbf{R}$).

We evaluated 14 hypothesized spawning area configurations among the five PWS regions, where each model was modified to associate one or more of the observed time series to a corresponding process in $\mathbf{x}_t$. The hypothesized spawning areas differed from each other by the number of estimated states and/or which time series were associated to the same process. For example, m = 1 when the data from all regions are treated as observations of a single spawning area, and m = 5 when each region is modeled as an independent spawning area. This approach is similar to other analyses that have inferred population structure of marine mammals (e.g., Ward et al. 2010, Holmes et al. 2014) and herring (Siple and Francis 2016) among multiple monitoring sites.

For each of the 14 spawning area configurations, we fit nine models in which the parameterization of **Q** was changed to test the three assumptions of process errors for three model structures: an unbiased random walk (Equation **Error! Reference source not found.**a, **B** is fixed at 1), a biased random walk (Equation **Error! Reference source not found.**b), and a stationary autoregressive process (Equation **Error! Reference source not found.**a, **B** is estimated). Models were fit within the R statistical environment version 3.4.3 (http://www.R-project.org; R Core Development Team 2015) using the 'MARSS' package version 3.10.10 (Holmes et al. 2018). Maximum likelihood estimates for parameters were obtained using the expectation-maximization algorithm (Holmes 2013).

We evaluated all 126 models for convergence, and used standard diagnostic plots (i.e., residual scatterplots, autocorrelation function plots) to verify that the residuals were normally distributed and not autocorrelated in time. Model fit was approximated using Akaike's Information Criterion for small sample size (AICc), with the most parsimonious models determined by the lowest AICc value (Burnham and Anderson 2002). Models with ΔAICc < 2 were considered statistically similar (Burnham and Anderson 2002).

RESULTS

SPATIAL PATTERNS

Coverage of the herring spawning season by the ADF&G aerial survey expanded and contracted over the 45-year study period. In the 1970s, survey coverage was primarily focused in the Northeast Shore region, with flights over all other regions occurring during less than 30% of the mean days sampled per year (Table 3-1). Coverage was expanded across PWS in the early 1980s (Table A1), with flights occurring over all regions within PWS on more than 50% of the days sampled per year (Table 3-1). Throughout the 1980s, sampling effort was at its highest (mean ± 1 SD, 30.2 ± 6.2 d sampled yr^{-1}) as the population was at its peak (Figure 3-1). Survey effort was gradually reduced through the 1990s (20.9 ± 5.3 d sampled yr^{-1}) and the early 2000s, reaching a low of only 6 days sampled in 2004, but has since increased in the past decade (16.8 ± 3.3 d sampled yr^{-1}). Despite the reduced sampling effort, survey coverage in the 1990s and 2000s remained above 40% for all regions in PWS, except in four years (1995, 1996, 1999, and 2000). In the 2010s, all regions in PWS were covered each year but sampling effort was concentrated over the Southeast Shore and Northeast Shore regions while effort over the other regions was more variable. The Kayak Island region was not included in the survey domain until 2007 (one flight was conducted in 1982). It has since been sampled 1 to 3 d yr^{-1}, except in 2010 and 2016 when no flights were conducted.

There have been pronounced decadal shifts in the distribution of herring spawning within PWS. In the 1970s, spawning was concentrated in the Northeast Shore region, and to a lesser extent in the Montague Island and Southeast Shore regions (Figure 3-3, Figure 3-4). This pattern largely reflects the survey's unbalanced coverage of all PWS regions during this period (Table 3-1, Figure 3-4A). Throughout the 1980s, spawning was widely distributed across all regions within PWS (Figure 3-3). The total cumulative spawn for all regions increased from 68.9 (SD 20.7) mile-days of milt yr^{-1} in the 1970s (Table 3-2) to a peak of 271.0 mile-days of milt in 1988 (Figure 3-4B). Following brief increases in spawning in the Southeast Shore and Montague Island regions in 1979-81, a sustained increase in spawning was first evident in the North Shore and Naked Island regions during the early 1980s, followed by increases in the Montague Island and Northeast Shore regions a few years later (Figure 3-4B). Sharp declines in spawning in the North Shore and Naked Island regions in 1990 and the Northeast Shore region in 1991 (Figure 3-4B) preceded the population's collapse in 1993 (Figure 3-1). In contrast, there was little change in spawn activity in the Southeast Shore region during the population's expansion, with this area accounting for less than 10% of the annual total spawn in all but one year (1984) prior to the population's collapse in 1993 (Figure 3-4).

Table 3-1. Mean days of survey coverage (1 SD) summarized by decade and region within Prince William Sound.

Decade	All regions		Montague Island		Southeast Shore		Northeast Shore		North Shore		Naked Island		Kayak Island	
	Mean	SD	Mean	SD	Mean	SD	Mean	SD	Mean	SD	Mean	SD	Mean	SD
1970s	13.6	2.4	3.6	1.8	3.3	3.6	11.9	3.4	3.7	2.8	0	0	0	0
1980s	30.2	6.2	19.3	5.0	19.8	5.9	26.4	6.5	20.6	6.3	15.8	9.9	0.1	0.3
1990s	20.9	5.3	17.8	5.3	15.7	4.7	17.1	6.0	13.3	8.6	12.5	8.3	0	0
2000s	11.7	3.1	8.6	2.3	11.1	2.5	9.7	2.2	5.5	1.6	6.4	2.5	0.7	1.2
2010s	16.8	3.3	8.6	4.1	16.3	3.2	14.6	3.3	4.0	2.1	5.3	3.4	1.7	1.2

Table 3-2. Total spawn (mean mile-days of milt year^{-1}) summarized by decade and region within the Prince William Sound management area. – indicates little to no survey coverage.

Decade	All regions		Montague Island		Southeast Shore		Northeast Shore		North Shore		Naked Island	
	Mean	SD	Mean	SD	Mean	SD	Mean	SD	Mean	SD	Mean	SD
1970s	68.9	20.7	6.2	7.1	5.5	13.8	56.6	15.0	–	–	–	–
1980s	151.5	62.0	32.6	27.2	8.4	7.5	56.5	29.1			12.9	13
1990s	66.1	44.2	32.0	15.2	8.1	6.3	21.6	26.6			0.6	1.4
2000s	26.7	7.2	6.9	4.0	11.7	6.1	5.5	3.1			0.4	0.7
2010s	42.9	27.1	1.7	2.8	24.5	19.2	10.9	14.2	0	0	0	0

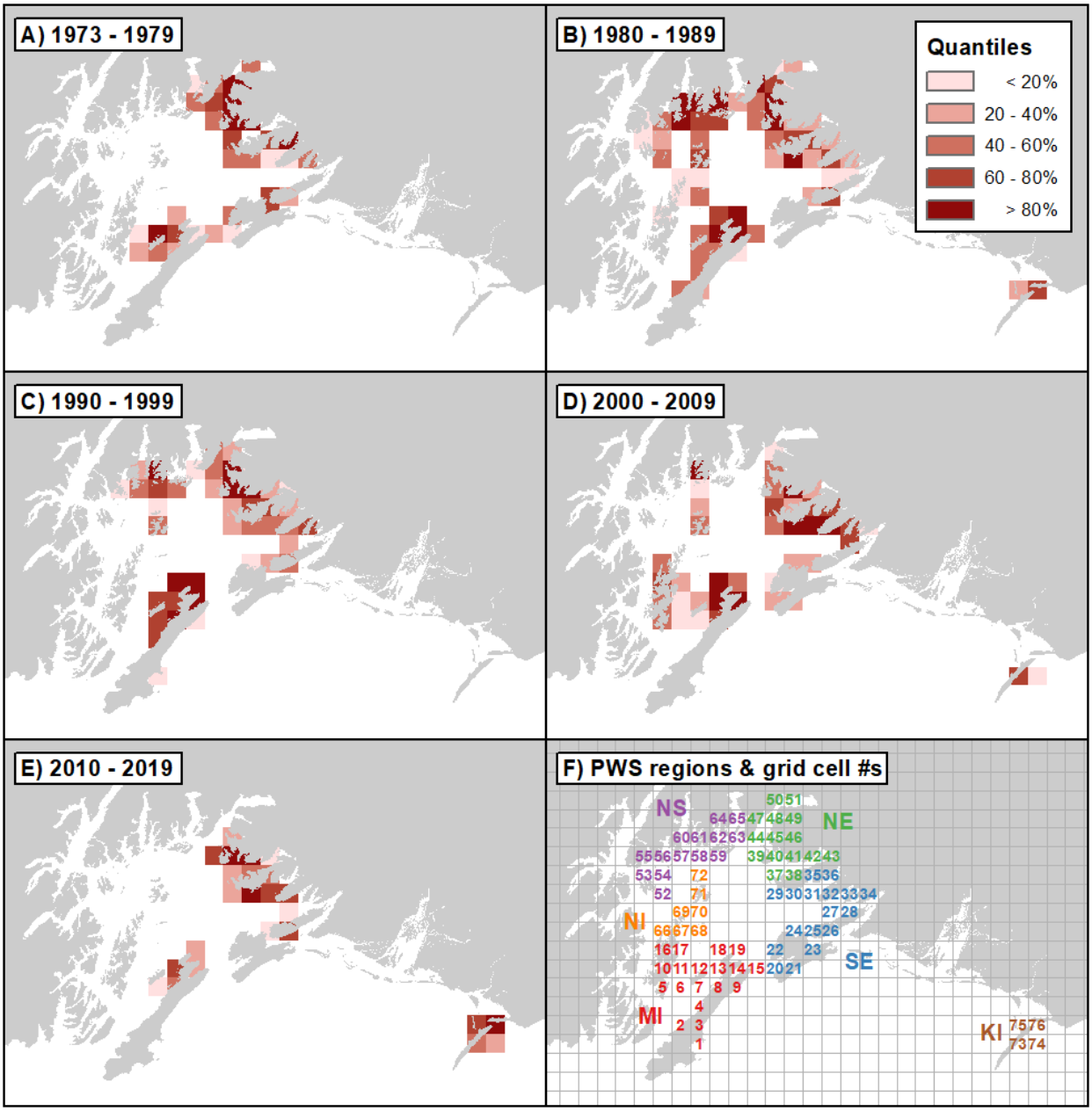

Figure 3-3. Distribution of spawning from 1973 to 2019 by decade. Spawn patterns are represented as quantiles of mile-days of milt (MDM) that were summed within each 10×10 km grid cell by decade (plots A-E). In plot F, grid cell numbers (1-76) are grouped into the following regions: MI = Montague Island; SE = Southeast Shore; NE = Northeast Shore; NS = North Shore; NI = Naked Island; KI = Kayak Island.

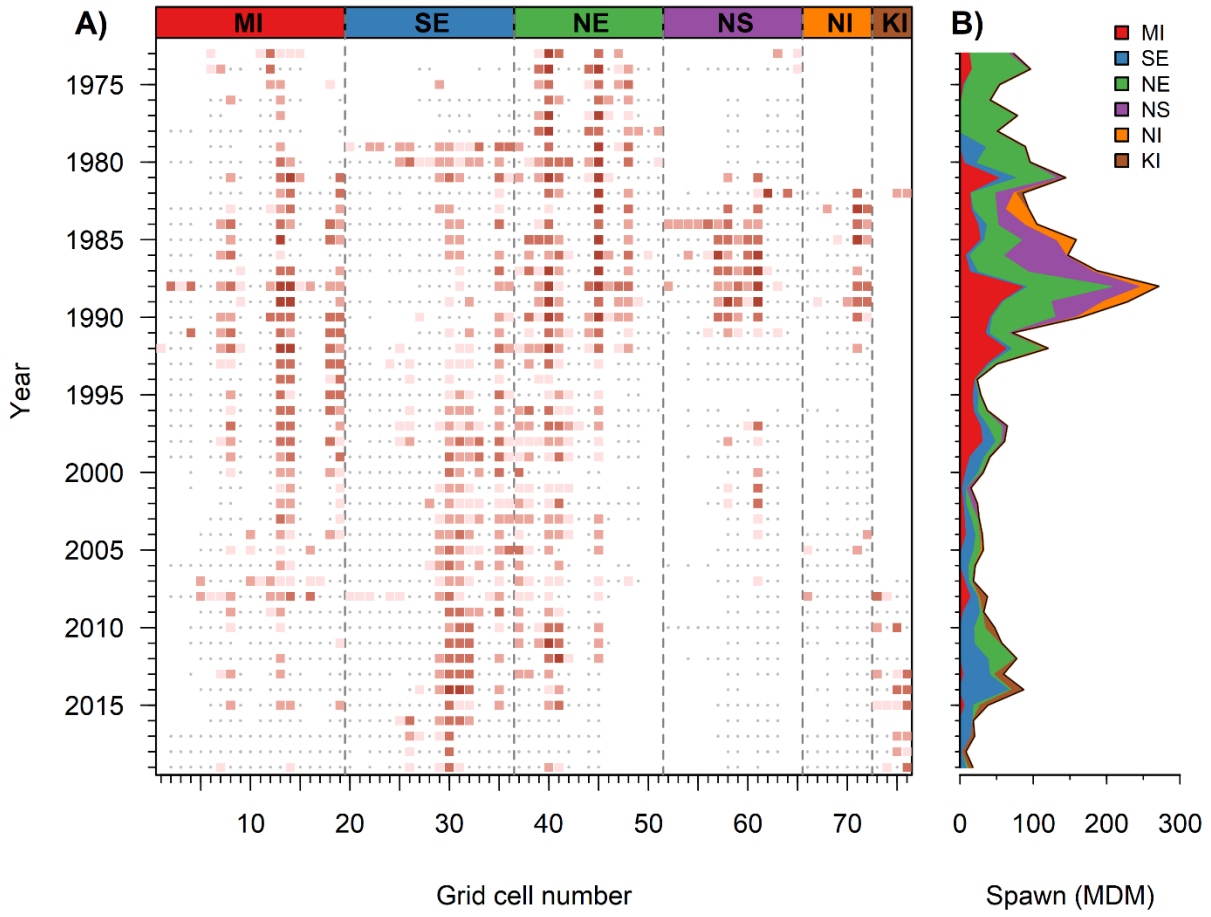

Figure 3-4. Distribution of spawning from 1973 to 2019 by year. Spawn patterns are represented as (A) quantiles of mile-days of milt (MDM) by 10×10 km grid cell and year (note, quantiles were calculated across all years), and as (B) cumulative spawn within each region (MI = Montague Island; SE = Southeast Shore; NE = Northeast Shore; NS = North Shore; NI = Naked Island; KI = Kayak Island). Grid cell numbers (1-76) correspond with cell locations identified in Figure 3-3.

Following the population collapse, the distribution of herring spawning locations within PWS contracted towards the Southeast Shore region over the next three decades (Figure 3-3). Spawning activity in the North Shore and Naked Island regions effectively ceased, with only intermittent spawning in the 1990s and 2000s, and the last observed spawning event occurring in 2008 (Figure 3-4). In the Northeast Shore region, the distribution of spawning locations contracted southward around Port Fidalgo (Figure 3-2) as the total spawn declined to less than 20 mile-days of milt (MDM) yr^{-1} until 2010 (Figure 3-4). Spawning activity in the Northeast Shore region briefly increased from 2010 to 2012 (range 21.8 to 30.8 MDM yr^{-1}) but has since declined to less than 6.2 MDM yr^{-1}. Throughout the 1990s, the Montague Island region accounted for at least half of the cumulative spawn for all regions in most years, but spawning activity has steadily declined within this region since 1999 (Table 3-2, Figure 3-4B). And for the first time

since the survey began, no spawning activity was observed in both the Northeast Shore or Montague Island regions from 2016 to 2018 (Figure 3-4).

In contrast to the other regions within PWS, spawning activity within the Southeast Shore region began to increase in the mid-1990s (Figure 3-4B), and has accounted for the highest annual cumulative spawn among the regions for the past two decades (Table 3-2). The spatial dispersion index shows that the distribution of spawning remained similarly dispersed across PWS in the decade prior to and after the population collapse (Figure 3-5). This suggests that increases in spawning activity in the Southeast Shore region during the 1990s and 2000s offset declines in activity within the other regions with regard to the proportional utilization of available habitat. The concentration of spawning in the Southeast Shore region over the past decade, especially in the past 4 years when the dispersion index declined sharply (Figure 3-5), coincides with the current decline in spawning biomass (Figure 3-1). This shift towards the Southeast Shore region over the past three decades indicates that PWS herring have largely abandoned the primary spawning habitat used during the population's expansion in the 1980s and are currently only using a small number of spawning locations.

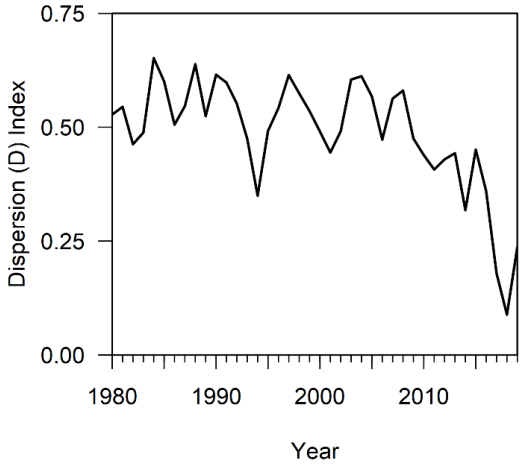

Figure 3-5. Spawning area dispersion index. D values range from 0 (aggregated in one grid cell) to 1 (evenly distributed across all grid cells).

Age composition data used in the stock assessment model was examined relative to the timing of changes in spawning distributions. The rapid increase in population size during the 1980s (Figure 3-1) primarily resulted from production by the 1976, 1980, 1981, and 1984 year classes (cohorts identified by birth year) (Figure 3-6).

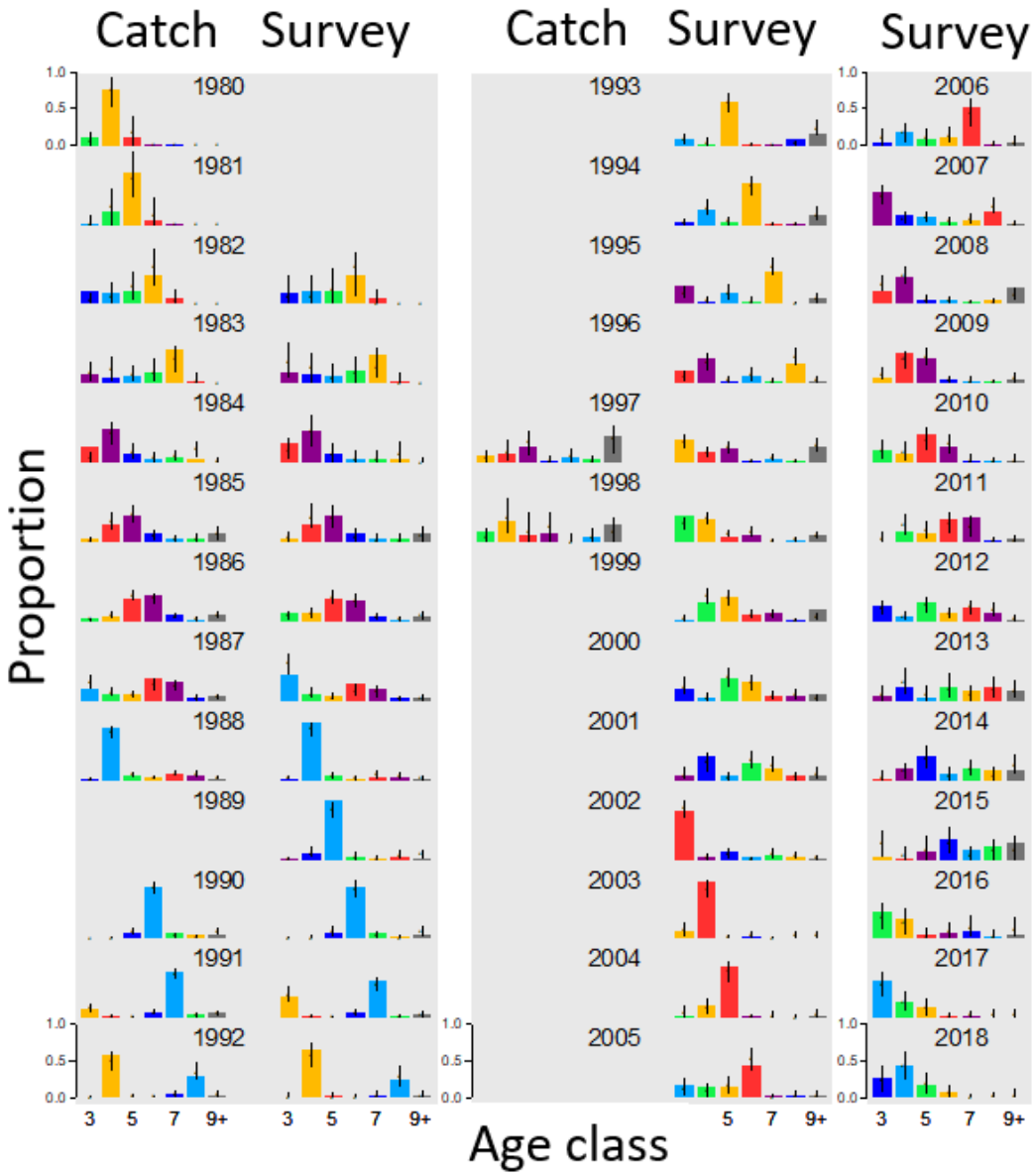

Figure 3-6. The 2018 Bayesian age-structured assessment model fits to the age composition data from purse-seine catches and from the Alaska Department of Fish and Game herring-spawn survey (data from all sampling gears combined). Colors track individual cohorts over time, while points and lines indicate the model posterior median and 95% posterior intervals (Source: J. Trochta unpublished data).

Spawning production declined rapidly in the early 1990s as these year classes, particularly the 1984 cohort, aged out of the population. Prior to the population collapse, the 1988 cohort was the last strong year class to recruit to the spawning population. Preliminary examination of age composition data summarized for each region (not shown) indicates that the 1988 cohort became the dominant year class for spawning aggregations in the Montague Island region in 1991 where spawning production remained relatively stable, while the 1984 cohort remained the dominant year class in the North Shore and Northeast Shore regions where spawning declined sharply from

prior years (Figure 3-4B). The next year, spawning ceased in the North Shore region, while stabilizing (albeit for only one year) in the Northeast Shore region and increasing in the Montague Island region where the 1988 cohort established itself as the dominant year class across all PWS through the mid-1990s (Figure 3-6). In 1993, the extended period of low spawning activity in the Northeast Shore began while spawning production remained stable in the Montague Island region until the 1988 cohort began to age out of the population in the late-1990s. With no strong year classes following behind the 1988 cohort, spawning declined to consistently low levels in the Montague Island by 2000 as spawning in the Southeast Shore region began its slow increase over the next two decades largely due to production by the 1999 cohort. The brief increase in spawning in the early 2010s in the eastern PWS regions resulted from the combined production of multiple weak year classes from 2004 to 2007, rather than from a strong cohort.

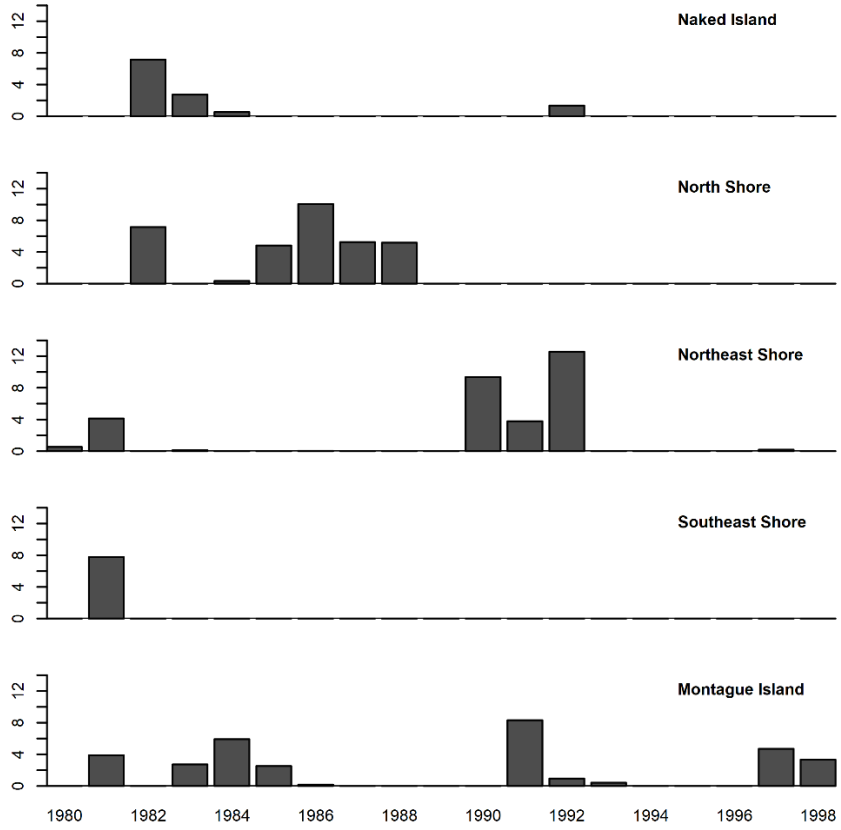

Figure 3-7. Commercial landings for herring sac-roe and gillnet fisheries from 1980 to 1998 in Prince William Sound by region (MI = Montague Island; SE = Southeast Shore; NE = Northeast Shore; NS = North Shore; NI = Naked Island) and in the adjacent Gulf of Alaska waters.

Changes in spawning distributions also were compared to the distribution of commercial landings for the sac-roe fishery from 1980 and 1998 (Figure 3-7). In the 1980s, herring were harvested in the North Shore, Naked Island, and Montague Island regions. The fishery shifted to the Northeast region from 1990 to 1992, preceding the sharp decline in spawning activity in this

region in 1993. The fishery also was active in the Montague Island region from 1991 to 1993, and again from 1997 to 1998 (note the fishery was closed from 1994 to 1996). It's notable that the sharp decline in spawning in the Montague Island region in 1999 also occurred after multiple years of fishing, similar to the Northeast Shore region earlier in the decade.

TEMPORAL PATTERNS

Herring spawn timing was highly variable in PWS from 1980 to 2019 (Figure 3-8).

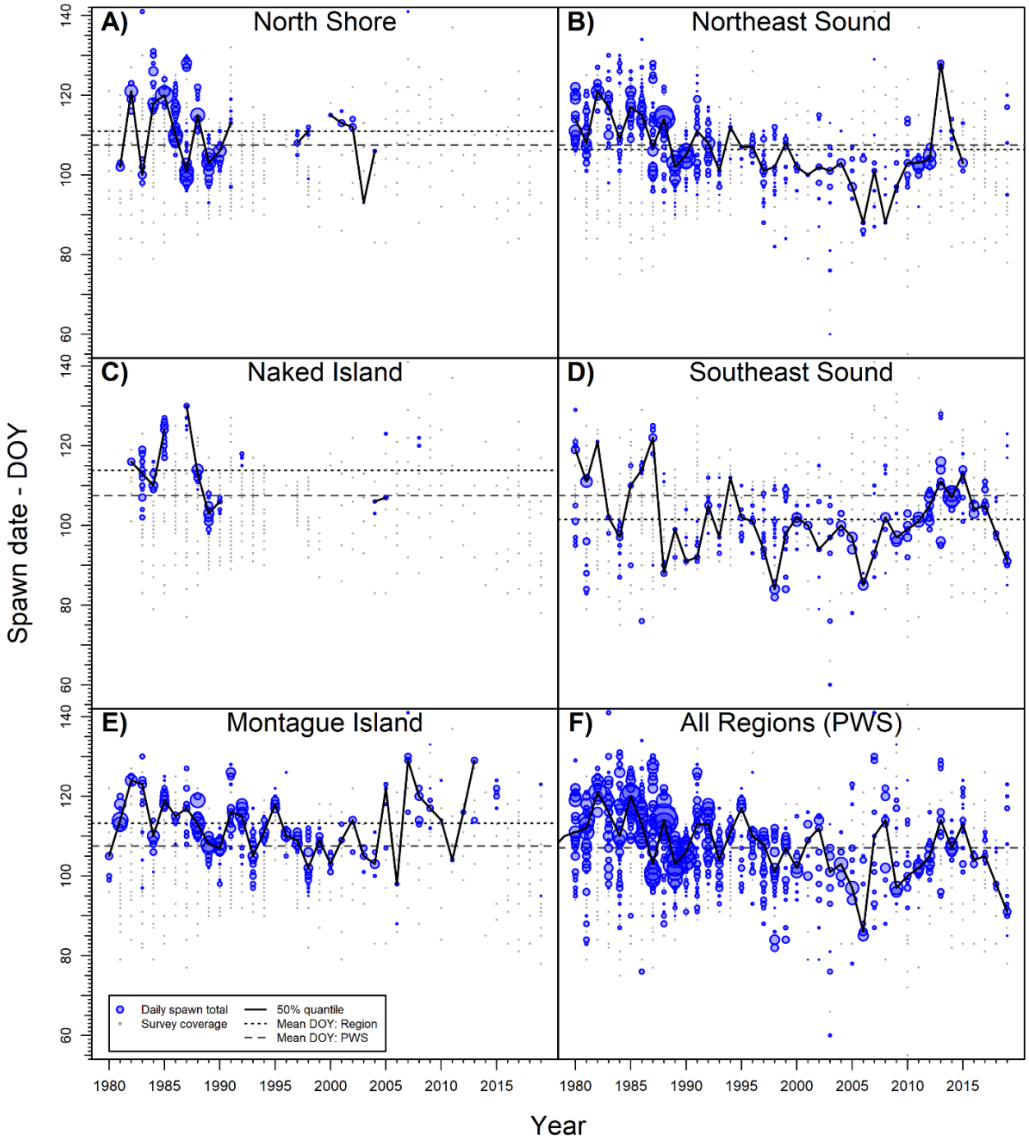

Figure 3-8. Distribution of spawn timing (day-of-year, DOY) from 1980 to 2019 by (A-E) region and (F) for all regions within Prince William Sound (PWS) combined. Daily spawn total is scaled by total mile-days of milt observed within each region. Each plot shows a time series of the DOY when 50% of total spawn was observed for each year (50% quantile), and mean time series values for the region (Mean DOY: Region) and all regions combined (Mean DOY: PWS).

The duration of the spawning season ranged from as few as 4 days (2016) to nearly two months (59 days, 1986). The first observed spawn event of the season occurred as early as 1 March (2003) and as late as 26 April (1982), while the last spawn event of the season ranged from 15 April (2005, 2011) to 21 May (1983, 2007). The mean day of year (DOY ± SE) when 50% of total spawn was observed (hereafter peak spawn date) in all PWS regions was 17 April (107 ± 1.2 d). The peak spawn date was earliest in the Southeast Shore region (12 April, 101.5 ± 1.4 d), and mostly progressed counter-clockwise across PWS from the Northeast Shore (16 April, 106.3 ± 1.4 d), North Shore (21 April, 110.9 ± 2.4 d), Naked Island (24 April, 113.8 ± 2.3 d), and Montague Island (23 April, 113.2 ± 1.3 d) regions.

The two best supported MARSS models (models with $\mathbf{Z}_2$ and $\mathbf{Z}_{13}$ spawning area configurations) estimated that there was one spawn timing trajectory for regions in western PWS (Montague Island, Naked Island, and North Shore regions), and either one or two trajectories for the Southeast Shore and Northeast Shore regions in eastern PWS (Table 3-3). Both of these models (hereafter the $\mathbf{Z}_2$ and $\mathbf{Z}_{13}$ models) had process errors (**Q**) that were correlated with equal variances and estimated a stationary autoregressive process (**B**). Diagnostic plots indicated that residuals for all MARSS models in which process errors were independent of other states (with either equal or unique variances) remained autocorrelated in time (not shown) and were therefore rejected. AIC_C values for all random walk models (i.e., **B** fixed at 1) were consistently higher than those with the same spawning area configuration that estimated **B** (Table 3-3).

The $\mathbf{Z}_2$ and $\mathbf{Z}_{13}$ models show there were spatial differences in spawn timing processes between regions in eastern and western PWS. Comparison of estimated **B** coefficients (Table 3-4) between states indicated that the autoregressive process was weaker for western PWS regions in both models ($\mathbf{Z}_2$: $b_{\mathbf{x}_1}$ = 0.25; $\mathbf{Z}_{13}$: $b_{\mathbf{x}_1}$ = 0.27) than in eastern PWS regions ($\mathbf{Z}_2$: $b_{\mathbf{x}_2}$ = 0.68; $\mathbf{Z}_{13}$: $b_{\mathbf{x}_2}$ = 0.61, $b_{\mathbf{x}_3}$ = 0.79); this suggests there was a process with stronger autocorrelation influencing spawn timing in eastern PWS. The effect of these regional differences in **B** coefficients on spawn timing trajectories is most apparent between 1980 to 2006 when a shift in earlier spawning occurred at different rates in eastern and western PWS regions (Figure 3-9). During this 27-year period, spawn timing shifted earlier in the season by approximately 25 ($\mathbf{Z}_2$ model) to 30 ($\mathbf{Z}_{13}$ model) days in eastern PWS regions, while spawn timing was more variable in western PWS and shifted earlier by only 15 days in both models. Between 2007 and 2013, spawn timing shifted back later in the season in all regions before returning to the long-term mean spawn time by 2019 (Figure 3-9).

Table 3-3. Model performance based on Akaike information criterion corrected for small sample size (AICc). The Z matrix for each spawning area configuration (numbered Z_1 to Z_{14}) indicates corresponding states (x_{1-5}) among the region time series in western or eastern Prince William Sound (W. PWS, E. PWS): MI = Montague Island; SE = Southeast Shore; NE = Northeast Shore; NS = North Shore; NI = Naked Island. Results for three model structures are shown for each Z matrix, including ΔAICc values that are relative to the best model (AICc), and the number of parameters (P).

						Q = equal var. and cov.					
Spawning area state(s) ($\mathbf{x}_m$)						**B** = 1				**B** = unique	
W. PWS				E. PWS		**u** = zero		**u** = unique		**u** = zero	
Num	MI	NS	NI	SE	NE	ΔAIC_c	P	ΔAIC_c	P	ΔAIC_c	P
$\mathbf{Z}_1$	$\mathbf{x}_1$	$\mathbf{x}_1$	$\mathbf{x}_1$	$\mathbf{x}_1$	$\mathbf{x}_1$	15.0	7	17.3	8	**11.2**	8
$\mathbf{Z}_2$	$\mathbf{x}_1$	$\mathbf{x}_1$	$\mathbf{x}_1$	$\mathbf{x}_2$	$\mathbf{x}_2$	10.6	9	9.1	11	**0**	11
$\mathbf{Z}_3$	$\mathbf{x}_1$	$\mathbf{x}_2$	$\mathbf{x}_1$	$\mathbf{x}_2$	$\mathbf{x}_2$	16.2	9	14.6	11	8.2	11
$\mathbf{Z}_4$	$\mathbf{x}_1$	$\mathbf{x}_2$	$\mathbf{x}_2$	$\mathbf{x}_1$	$\mathbf{x}_1$	18.5	9	17.7	11	11.6	11
$\mathbf{Z}_5$	$\mathbf{x}_1$	$\mathbf{x}_2$	$\mathbf{x}_2$	$\mathbf{x}_1$	$\mathbf{x}_2$	19.7	9	24.0	11	17.3	11
$\mathbf{Z}_6$	$\mathbf{x}_1$	$\mathbf{x}_2$	$\mathbf{x}_1$	$\mathbf{x}_1$	$\mathbf{x}_2$	19.7	9	22.9	11	15.3	11
$\mathbf{Z}_7$	$\mathbf{x}_1$	$\mathbf{x}_2$	$\mathbf{x}_2$	$\mathbf{x}_2$	$\mathbf{x}_2$	18.3	9	17.4	11	10.1	11
$\mathbf{Z}_8$	$\mathbf{x}_1$	$\mathbf{x}_1$	$\mathbf{x}_1$	$\mathbf{x}_2$	$\mathbf{x}_1$	19.7	9	20.6	11	9.6	11
$\mathbf{Z}_9$	$\mathbf{x}_1$	$\mathbf{x}_1$	$\mathbf{x}_1$	$\mathbf{x}_1$	$\mathbf{x}_2$	17.9	9	20.0	11	9.3	11
$\mathbf{Z}_{10}$	$\mathbf{x}_1$	$\mathbf{x}_2$	$\mathbf{x}_1$	$\mathbf{x}_3$	$\mathbf{x}_2$	21.2	10	19.3	13	9.9	13
$\mathbf{Z}_{11}$	$\mathbf{x}_1$	$\mathbf{x}_2$	$\mathbf{x}_2$	$\mathbf{x}_1$	$\mathbf{x}_3$	21.6	10	20.3	13	10.0	13
$\mathbf{Z}_{12}$	$\mathbf{x}_1$	$\mathbf{x}_2$	$\mathbf{x}_2$	$\mathbf{x}_3$	$\mathbf{x}_2$	22.3	10	21.5	13	–	13
$\mathbf{Z}_{13}$	$\mathbf{x}_1$	$\mathbf{x}_1$	$\mathbf{x}_1$	$\mathbf{x}_2$	$\mathbf{x}_3$	16.4	10	14.0	13	**0.9**	13
$\mathbf{Z}_{14}$	$\mathbf{x}_1$	$\mathbf{x}_2$	$\mathbf{x}_3$	$\mathbf{x}_4$	$\mathbf{x}_5$	25.4	12	20.5	17	7.0	17

Note: Process errors (**Q**) were estimated with equal variances that were correlated (equal var. and cov.). The diagonal of the **B** matrix was set to 1 (i.e., random walk) or estimated for each state (unique). Bias (**u**) was either set to zero or estimated for each of the random walk models (unique). Bold ΔAIC_c values indicate the three models shown in Figure 3-9. – indicates models that did not converge indicated.

The advantage of estimating separate states for true spawn timing for the eastern and western PWS regions is apparent when compared with the simplest model that estimated one state for all regions ($\mathbf{Z}_1$ model in Table 3-3). While the estimated process for the one-state model shows similar shifts in spawn timing in 2006 and 2013, the regional differences detected in the two models that split PWS into eastern and western regions related to the rate of change and interannual variability are averaged out. For example, the $\mathbf{Z}_1$ model estimated that true spawn timing shifted earlier in the season by approximately 17 days between 1980 to 2006 (Figure 3-9), similar to the 15-day shift in the western PWS regions, but that the estimated strength of the autoregressive process was more similar to the eastern PWS regions ($\mathbf{Z}_1$: $b_{\mathbf{x}_1}$ = 0.59, Table 3-4). In addition to the loss of these regional differences, observation variances for all time series were higher in the $\mathbf{Z}_1$ model compared to estimates from the $\mathbf{Z}_2$ and $\mathbf{Z}_{13}$ models (Table 3-4).

Table 3-4. Parameter estimates (standard errors) for models in bold in Table 3-3 identified by their respective Z matrix configuration.

	Model form		
Coefficient	$\mathbf{Z}_1$	$\mathbf{Z}_2$	$\mathbf{Z}_{13}$
Observation variance (**R**)			
r_{MI}	41.72 (11.71)	28.53 (10.12)	31.97 (10.03)
r_{SE}	45.79 (12.26)	41.55 (11.68)	38.31 (11.9)
r_{NE}	36.58 (10.49)	27.02 (8.81)	25.51 (9.14)
r_{NS}	111.36 (38.21)	79.75 (28.42)	84.02 (29.39)
r_{NI}	32.82 (16.13)	29.55 (15.46)	30.05 (15.14)
AR strength (**B**)			
$b_{\mathbf{x}_1}$	0.59 (0.19)	0.25 (0.24)	0.27 (0.25)
$b_{\mathbf{x}_2}$		0.68 (0.12)	0.61 (0.13)
$b_{\mathbf{x}_3}$			0.79 (0.09)
Process variance-covariance (**Q**)			
q_{diag}	15.36 (7.08)	20.88 (7.7)	18.51 (7.38)
$c_{offdiag}$		17.99 (7.08)	17.51 (6.5)
Estimated state value $\mathbf{x}_t$ at time 0			
$\mu_{\mathbf{x}_1}$	9.79 (9.5)	-31.53 (42.25)	-30.25 (40.17)
$\mu_{\mathbf{x}_2}$		16.59 (9.45)	28.57 (14.13)
$\mu_{\mathbf{x}_3}$			9.28 (7.65)

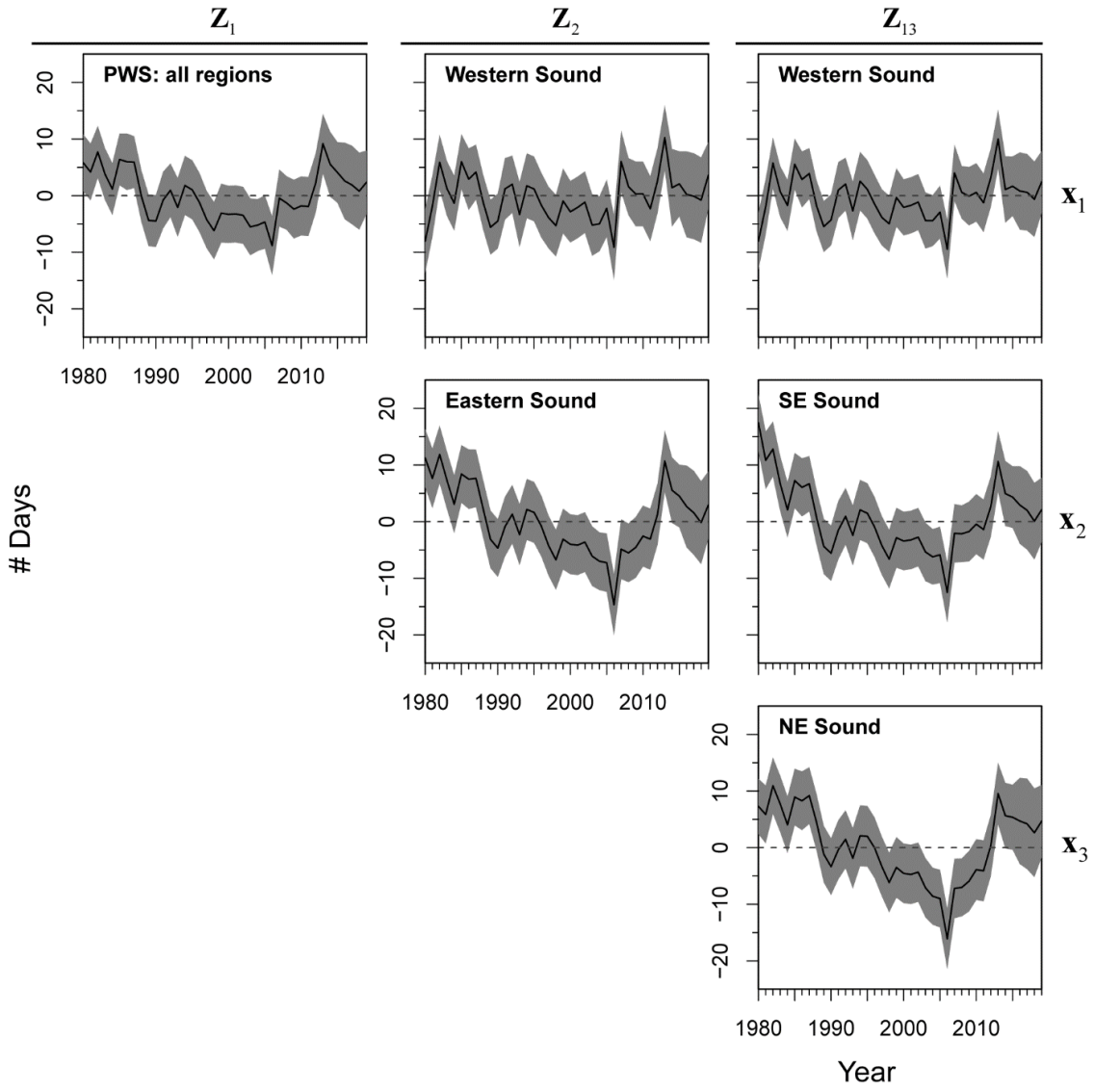

Figure 3-9. Estimated spawn timing trends (x_m, solid line) with 95% confidence intervals (shaded area) for the MARSS models in bold in Table 3-3. Estimated trends (i.e., states) for each time series are centered by their mean for all years (dashed line) to indicate earlier/later (-/+ number of days) spawning by year. Results for each model are shown by column (labels indicate the model's respective Z matrix). Each row shows the model's estimated state(s) (x_m) for regions grouped in unique spawning area configurations (refer to Table 3-3).

DISCUSSION

Herring no longer use the primary spawning areas in PWS that were used as the population reached peak abundance in the 1980s. If the spatial extent of spawning areas is linked to the size of the population and follows the theory of the basin model (MacCall 1990), declines in population abundance would have been expected to result in contraction of spawning distributions towards one or more of the PWS regions that were primarily used in the 1980s (i.e., Montague Island, North Shore, or Northeast Shore). Instead, spawning distributions contracted

towards the Southeast Shore region, the area with the lowest reproductive activity at the high point in population size. Furthermore, major declines in spawn activity within the primary areas occurred prior to the population collapse (North Shore, Northeast Shore) and more recent abundance declines in the late-1990s and early-2010s (Montague Island). These findings indicate that changes in spawning distributions within PWS may be contributing to, rather than resulting from, abundance declines.

Major shifts in spawning distributions may be linked to spatial changes in population demographics. The rapid increase in population abundance during the 1980s primarily resulted from the combined production of the 1980, 1981, and 1984 cohorts. Spawning production declined as these cohorts aged out of the population, particularly in the northern regions of PWS. It appears that 1991 was a critical year for the population, during which the 1988 cohort recruited to the spawning population and first selected spawning areas. Preliminary examination of age composition data for each region indicates that the 1988 cohort primarily spawned in the Montague Island region in 1991, but not in the northern regions where the 1984 cohort remained the dominant year class. The following year, no spawning was observed in the North Shore region (the first of five consecutive years with no activity), while spawning increased in both the Montague Island and Northeast Shore regions where the 1988 cohort was the dominant year class. If the assumption that younger fish follow older fish to first select spawning habitat is valid (MacCall et al. 2018), we speculate that productive spawning areas in the North Shore region were abandoned due to a failure of the 1988 cohort to utilize these grounds.

The second major shift in spawning distributions towards the Southeast Shore region in the late-1990s may also be linked to poor recruitment and localized effects of the fishery in other regions. Spawning declined until the mid-1990s as the 1988 cohort aged out of the population without any new strong cohorts entering the population. Despite a brief increase in spawning from 1997 to 1998, spawning declined to record lows by 2001 in the Montague Island and Northeast Shore regions while increasing in the Southeast Shore region. The collapse of spawning activity in the Montague Island region is notable because it followed the last two years of the fishery, during which landings were concentrated within this region. Although the total allowable catch in 1997 and 1998 may have been deemed sustainable for the overall population, the concentration of harvest in one region potentially exceeded what local spawning aggregations could withstand (Okamoto et al. 2018). The effects of this localized depletion may have been amplified due to the overall low population size and precipitated the collapse of region's spawning aggregations (Essington et al. 2015).

These two major spatial reorganizations of spawning areas have potentially inhibited recruitment by shifting reproductive activity from source areas to sinks. Following the *Exxon Valdez* oil spill, the Sound Ecosystem Assessment program investigated larval dispersal and mortality rates of herring during critical life stages in their first year from 1995 to 1998 (see synthesis of this work in Norcross et al. 2001). Simulated larval dispersal trajectories indicated that herring larvae released from the Montague Island, North Shore, and Northeast Shore regions were widely dispersed to all areas of PWS, except to the Southeast Shore region (see Figure 3 in Norcross et al. 2001). In contrast, larvae released from the Southeast Shore region were mostly retained locally, with some being dispersed to the Northeast Shore and Naked Island regions. Energetics-based estimates of survival rates of herring over their first winter were highest in bays and fjords in the North Shore and Montague Island regions and lowest in the Southeast Shore region. The

Sound Ecosystem Assessment program attributed higher over-winter survival rates primarily to food availability, indicating that the supply of higher quality prey from the Gulf of Alaska continental shelf (hereafter shelf) in summer and fall was critical for supporting growth and energy storage demands of juvenile herring. These findings are supported by more recent stable isotope analyses that show juvenile herring in the northern and western areas of PWS with isotope signatures reflecting carbon originating from the shelf were energetically in better condition (i.e., more likely to survive) compared to herring in the Southeast Shore region (Gorman et al. 2018). Based on the high retention of larvae spawned locally in an area with lower prey quality and over-winter survival rates of age-0 herring, the Southeast Shore region has characteristics of sink habitat, in which reproduction is insufficient to compensate for local mortality rates (Pulliam 1988). The PWS population size has fallen to its lowest levels as spawning has contracted to the Southeast Shore region, signifying that future recruitment success is more likely to occur following significant increases in spawning in other areas of PWS for the population to recover.

In addition to spatial shifts in spawning patterns, there is clear evidence that spawn timing trends have coincided with large-scale temperature anomalies. Following a two-decade period in which peak spawning gradually shifted earlier in the season by two to four weeks, spawn timing abruptly reverted back to later in the season by three to four weeks within a 6-year period. This abrupt shift coincided with a large-scale transition in PWS and the Gulf of Alaska from an extended period of warm (2001 to 2006) to cold (2007 to 2013) sea temperatures (cf. Figure 14 in Campbell 2018). A second shift in spawn timing trends occurred between 2013 and 2014, as earlier spawning in PWS from 2014 to 2018) coincided with the onset of the multi-year (2014 to 2016) marine heatwave in the Northeast Pacific (Bond et al. 2015, Di Lorenzo and Mantua 2016). These observed differences between earlier and later spawning during warm and cold years are consistent with expected effects that temperature has on gonad maturation rates of herring (Hay 1985, Ware and Tanasichuk 1989).

There are indications that demographic changes are also contributing to abrupt shifts in peak spawn timing. The 2006-07 shift coincided with a major change in the population's age structure as the 2004 cohort replaced the 1999 cohort as the dominant year class. A similar shift from earlier-to-later peak spawning occurred between 1990 and 1991 as the 1988 cohort replaced the 1984 cohort as the dominant year class. These age-related differences in spawn timing are consistent with long-term observations for herring populations in British Columbia (Hay 1985) and the Atlantic (Lambert 1987).

Major shifts in spawn timing trends were coincident in the eastern and western regions of PWS, but spatial differences in the magnitude of the long-term trends between these hydrologically distinct areas indicate that other environmental processes are influencing spawning behavior. Identifying these processes is the focus of ongoing work in collaboration with Gulf Watch Alaska partners, in addition to conducting a more in-depth examination of how temperature variability and changes in population demographics (e.g., age structure, condition factor) influence spatial and temporal shifts in spawning.

CONCLUSION

This study shows substantial changes in spatial and temporal patterns of herring spawning in PWS have occurred over the past four decades, and that these changes are likely contributing to

the population's lack of recovery. Spatial reorganization of spawning areas prior to the population collapse in 1993 coincided with the end of a large cohort and failure of younger generations to utilize productive spawning habitat in northern PWS. Poor recruitment and potential fishery-related effects on spawning aggregations within the Montague Island region in the late-1990s preceded a second major shift in spawning distributions that led to the current consolidation of spawning mostly within the Southeast Shore region. The concentration of spawning in the Southeast Shore region has coincided with declines in population abundance to current record lows. Previous work conducted during the Sound Ecosystem Assessment program and more recently by the Herring Research and Monitoring program suggests there is higher larval retention but lower prey quality and survival rates of juvenile herring in the Southeast Shore region, raising concerns that this region may be an ecological sink compared to other areas of PWS. In addition, major shifts in spawn timing have coincided with large-scale changes in ocean temperatures, indicating the population is also responding to external perturbations in their environment. The current state of the population (i.e., low abundance, spatially constrained spawning habitat, and lack of a broad age structure that extends the spawning period) suggests its potential for reproductive success is greatly reduced. An expansion of spawning to other areas of PWS will likely be a necessary first step to increase the population's capacity to broadly release batches of eggs across space and time to increase opportunities for optimizing survival of offspring during critical early life stages in a heterogeneous and dynamic environment.

ACKNOWLEDGEMENTS

This study was possible thanks to the dedicated efforts of the pilots and ADF&G staff who have conducted the aerial survey since 1973, as well as because of those who digitized survey data from historical maps. We thank ADF&G staff S. Dressel, M. Foster, K. Hebert, S. Moffitt, and T. Otis, along with T. Francis (Puget Sound Institute, U. of Washington), S. Pegau (Prince William Sound Science Center), O. Shelton (NOAA Northwest Fisheries Science Center, NWFSC), E. Ward (NOAA-NWFSC), and members of the Herring Research and Monitoring program for their insightful conversations on herring that improved the study design. Special thanks to A. MacCall for inspiring our research questions, and J. Trochta for sharing outputs and figures from the stock assessment model. Funding was provided by the *Exxon Valdez* Oil Spill Trustee Council. Any use of trade, firm, or product names is for descriptive purposes only and does not imply endorsement by the U.S. Government or State of Alaska. The findings and conclusions of this paper do not necessarily represent the views of the U.S. Geological Service or ADF&G.

REFERENCES

Bochenek, R. J. 2010. PWS herring data portal. *Exxon Valdez* Oil Spill Restoration Project Final Report, Axiom Consulting & Design, Anchorage, Alaska.

Bond, N. A., M. F. Cronin, H. Freeland, and N. Mantua. 2015. Causes and impacts of the 2014 warm anomaly in the NE Pacific. Geophysical Research Letters 42:3414–3420.

Brady, J. A. 1987. Distribution, timing and relative biomass indices for Pacific herring as determined by aerial surveys in Prince William Sound 1978 to 1987. Prince William Sound Data Report, Alaska Department of Fish and Game, Division of Commercial Fisheries, Cordova, Alaska.

Burnham, K. P., and D. R. Anderson. 2002. Model Selection and Multimodel Inference: A Practical Information-Theoretic Approach. 2nd edition. Springer, New York, New York, USA.

Campbell, R. W. 2018. Hydrographic trends in Prince William Sound, Alaska, 1960–2016. Deep Sea Research Part II 147:43–57.

Corten, A. 2002. The role of "conservatism" in herring migrations. Reviews in Fish Biology and Fisheries 11:339–361.

Cowan, Jr., J. H., and R. F. Shaw. 2002. Recruitment. Pages 88–111 *in* L. A. Fuiman and R. G. Werner, editors. Fishery Science: The Unique Contributions of Early Life Stages. John Wiley & Sons.

Cushing, D. H. 1990. Plankton production and year-class strength in fish populations: an update of the match/mismatch hypothesis. Advances in Marine Biology 26:249–293.

Deriso, R. B., M. N. Maunder, and W. H. Pearson. 2008. Incorporating covariates into fisheries stock assessment models with application to Pacific herring. Ecological Applications 18:1270–1286.

Di Lorenzo, E., and N. Mantua. 2016. Multi-year persistence of the 2014/15 North Pacific marine heatwave. Nature Climate Change 6:1042–1047.

Essington, T. E., P. E. Moriarty, H. E. Froehlich, E. E. Hodgson, L. E. Koehn, K. L. Oken, M. C. Siple, and C. C. Stawitz. 2015. Fishing amplifies forage fish population collapses. Proceedings of the National Academy of Sciences 112:6648–6652.

Flostrand, L. A., J. F. Schweigert, K. S. Daniel, and J. S. Cleary. 2009. Measuring and modelling Pacific herring spawning-site fidelity and dispersal using tag-recovery dispersal curves. ICES Journal of Marine Science 66:1754–1761.

Gorman, K. B., T. C. Kline, M. E. Roberts, F. F. Sewall, R. A. Heintz, and W. S. Pegau. 2018. Spatial and temporal variation in winter condition of juvenile Pacific herring (*Clupea pallasii*) in Prince William Sound, Alaska: oceanographic exchange with the Gulf of Alaska. Deep Sea Research Part II 147:116–126.

Haught, S., and S. Moffitt. 2018. ADFG Surveys: aerial survey route, biomass, age sex length, and spawn. Alaska Ocean Observing System. Gulf of Alaska Data Portal. Available from https://portal.aoos.org. [Accessed 5 Nov 2018].

Hay, D. E. 1985. Reproductive Biology of Pacific Herring (*Clupea harengus pallasi*). Canadian Journal of Fisheries and Aquatic Sciences 42:s111–s126.

Hay, D. E., P. B. McCarter, and K. S. Daniel. 2001. Tagging of Pacific herring Clupea pallasi from 1936-1992: a review with comments on homing, geographic fidelity, and straying. Canadian Journal of Fisheries and Aquatic Sciences 58:1356–1370.

Hay, D. E., P. B. McCarter, K. S. Daniel, and J. F. Schweigert. 2009. Spatial diversity of Pacific herring (*Clupea pallasi*) spawning areas. ICES Journal of Marine Science 66:1662–1666.

Holmes, E. E. 2013. Derivation of an EM algorithm for constrained and unconstrained multivariate autoregressive state-space (MARSS) models. arXiv:1302.3919 [stat.ME].

Holmes, E. E., E. J. Ward, and M. D. Scheuerell. 2014. Analysis of multivariate time-series using the MARSS package. NOAA Fisheries, Northwest Fisheries Science Center, 2725 Montlake Blvd. E., Seattle, WA 98112, USA.

Holmes, E. E., E. J. Ward, and K. Wills. 2012. MARSS: Multivariate autoregressive state-space models for analyzing time-series data. The R Journal 4:11–19.

Holmes, E., E. Ward, M. Scheuerell, and K. Wills. 2018. MARSS: Multivariate Autoregressive State-Space Modeling. R package version 3.10.10

Houde, E. D. 2016. Recruitment variability. Pages 98–187 *in* T. Jakobsen, M. J. Fogarty, B. A. Megrey, and E. Moksness, editors. Fish Reproductive Biology. 2nd edition. Wiley-Blackwell, Oxford, UK.

Hulson, P.-J. F., S. E. Miller, T. J. Quinn, G. D. Marty, S. D. Moffitt, and F. Funk. 2008. Data conflicts in fishery models: incorporating hydroacoustic data into the Prince William Sound Pacific herring assessment model. ICES Journal of Marine Science 65:25–43.

Keeling, B., M. Hessing-Lewis, C. Housty, D. K. Okamoto, E. J. Gregr, and A. K. Salomon. 2017. Factors driving spatial variation in egg survival of an ecologically and culturally important forage fish. Aquatic Conservation: Marine and Freshwater Ecosystems 27:814–827.

Lambert, T. C. 1987. Duration and intensity of spawning in herring Clupea harengus as related to the age structure of the mature population. Marine Ecology Progress Series 39:209–220.

Ljungström, G., T. B. Francis, M. Mangel, and C. Jørgensen. 2018. Parent-offspring conflict over reproductive timing: ecological dynamics far away and at other times may explain spawning variability in Pacific herring. ICES Journal of Marine Science 76:559–572.

MacCall, A. D. 1990. Dynamic geography of marine fish populations. Washington Sea Grant Program Seattle, Washington.

MacCall, A. D., T. B. Francis, A. E. Punt, M. C. Siple, D. R. Armitage, J. S. Cleary, S. C. Dressel, R. R. Jones, H. Kitka, L. C. Lee, P. S. Levin, J. McIsaac, D. K. Okamoto, M. Poe, S. Reifenstuhl, J. O. Schmidt, A. O. Shelton, J. J. Silver, T. F. Thornton, R. Voss, and J. Woodruff. 2018. A heuristic model of socially learned migration behaviour exhibits distinctive spatial and reproductive dynamics. ICES Journal of Marine Science 76:598–608.

Muradian, M. L. 2015. Modeling the population dynamics of herring in the Prince William Sound, Alaska. Thesis, University of Washington, Seattle, WA.

Muradian, M. L., T. A. Branch, S. D. Moffitt, and P.-J. F. Hulson. 2017. Bayesian stock assessment of Pacific herring in Prince William Sound, Alaska. PLOS ONE 12:e0172153.

Norcross, B. L., E. D. Brown, R. J. Foy, M. Frandsen, S. M. Gay, T. C. Kline, D. M. Mason, E. V. Patrick, A. J. Paul, and K. D. E. Stokesbury. 2001. A synthesis of the life history and ecology of juvenile Pacific herring in Prince William Sound, Alaska. Fisheries Oceanography 10:42–57.

Okamoto, D. K., M. Hessing-Lewis, J. F. Samhouri, A. O. Shelton, A. Stier, P. Levin, and A. K. Salomon. 2018. Spatial variation in exploited metapopulations obscures risk of collapse. bioRxiv 315481.

Payne, L. X., D. E. Schindler, J. K. Parrish, and S. A. Temple. 2005. Quantifying Spatial Pattern with Evenness Indices. Ecological Applications 15:507–520.

Pearson, W. H., R. B. Deriso, R. A. Elston, S. E. Hook, K. R. Parker, and J. W. Anderson. 2012. Hypotheses concerning the decline and poor recovery of Pacific herring in Prince William Sound, Alaska. Reviews in Fish Biology and Fisheries 22:95–135.

Pielou, E. C. 1966. The measurement of diversity in different types of biological collections. Journal of Theoretical Biology 13:131–144.

Pulliam, H. R. 1988. Sources, Sinks, and Population Regulation. The American Naturalist 132:652–661.

Quinn, T. J., G. D. Marty, J. Wilcock, and M. Willette. 2001. Disease and population assessment of Pacific herring in Prince William Sound, Alaska. Pages 363–379 *in* F. Funk, J. Blackburn, D. Hay, A. J. Paul, and R. Stephanson, editors. Herring: expectations for a new millennium. University of Alaska Sea Grant, Anchorage, AK.

R Core Development Team. 2015. R: A Language and Environment for Statistical Computing. R Foundation for Statistical Computing, Vienna, Austria. Available from http://www.R-project.org.

Rooper, C. N., L. J. Haldorson, and T. J. Quinn II. 1999. Habitat factors controlling Pacific herring (*Clupea pallasi*) egg loss in Prince William Sound, Alaska. Canadian Journal of Fisheries and Aquatic Sciences 56:1133–1142.

Russell, C. W., J. Botz, S. Haught, and S. Moffitt. 2017. 2016 Prince William Sound Area Finfish Management Report. Alaska Department of Fish and Game, Anchorage, AK.

Schindler, D. E., R. Hilborn, B. Chasco, C. P. Boatright, T. P. Quinn, L. A. Rogers, and M. S. Webster. 2010. Population diversity and the portfolio effect in an exploited species. Nature 465:609–612.

Shannon, C. E., and W. Weaver. 1949. The mathematical theory of communication. University of Illinois Press, Urbana, Illinois, USA.

Shelton, A. O., T. B. Francis, G. D. Williams, B. Feist, K. Stick, and P. S. Levin. 2014. Habitat limitation and spatial variation in Pacific herring egg survival. Marine Ecology Progress Series 514:231–245.

Shepherd, S., and S. Haught. 2019. Pacific herring aerial surveys and age, sex, and size processing in the Prince William Sound Area, 2018–2021. Regional Operational Plan CF.2A.2019.05, Alaska Department of Fish and Game, Division of Commercial Fisheries, Cordova, Alaska.

Sinclair, M., and M. J. Tremblay. 1984. Timing of Spawning of Atlantic Herring (Clupea harengus harengus) Populations and the Match–Mismatch Theory. Canadian Journal of Fisheries and Aquatic Sciences 41:1055–1065.

Siple, M. C., and T. B. Francis. 2016. Population diversity in Pacific herring of the Puget Sound, USA. Oecologia 180:111–125.

Thorne, R. E., and G. L. Thomas. 2008. Herring and the "*Exxon Valdez*" oil spill: an investigation into historical data conflicts. ICES Journal of Marine Science 65:44–50.

Ward, E. J., M. Adkison, J. Couture, S. C. Dressel, M. A. Litzow, S. Moffitt, T. H. Neher, J. Trochta, and R. Brenner. 2017. Evaluating signals of oil spill impacts, climate, and species interactions in Pacific herring and Pacific salmon populations in Prince William Sound and Copper River, Alaska. PLOS ONE 12:e0172898.

Ward, E. J., H. Chirakkal, M. González-Suárez, D. Aurioles-Gamboa, E. E. Holmes, and L. Gerber. 2010. Inferring Spatial Structure from Time-Series Data: Using Multivariate State-Space Models to Detect Metapopulation Structure of California Sea Lions in the Gulf of California, Mexico. Journal of Applied Ecology 47:47–56.

Ware, D. M., and R. W. Tanasichuk. 1989. Biological basis of maturation and spawning waves in Pacific herring (*Clupea harengus pallasi*). Canadian Journal of Fisheries and Aquatic Sciences 46:1776–1784.

Ware, D., and J. Schweigert. 2001. Metapopulation structure and dynamics of British Columbia herring. Canadian Stock Assessment Secretariat Research Document 2001/127, Nanaimo, BC, Canada.

Table A1. Number of days sampled during Alaska Department of Fish & Game aerial surveys by year and region: PWS = any area within Prince William Sound; MI = Montague Island; SE = Southeast Shore; NE = Northeast Shore; NS = North Shore; NI = Naked Island; KI = Kayak Island.

Year	Date Range	PWS	MI	SE	NE	NS	NI	KI
1973[1]	17 April-4 June	13	5	0	8	2	0	0
1974	5 April-1 July	14	6	1	14	7	0	0
1975[1]	12 April-28 April	10	3	3	9	0	0	0
1976	5 April-30 April	14	5	4	12	5	0	0
1977	31 March-11 May	13	3	2	10	1	0	0
1978	11 April-14 June	13	2	2	12	4	0	0
1979	7 April-12 June	18	1	11	18	7	0	0
1980	3 April-8 May	21	7	17	15	11	0	0
1981	20 March-5 May	33	22	26	31	13	0	0
1982	25 March-14 May	27	18	17	26	14	6	1
1983	23 March-21 May	32	26	9	23	19	23	0
1984	15 March-10 May	42	23	25	36	30	20	0
1985	24 March-7 May	30	19	20	25	22	22	0
1986	17 March-14 May	35	20	23	34	27	22	0
1987	18 March-10 May	33	20	26	31	26	25	0
1988	25 March-1 May	24	18	12	22	22	17	0
1989	25 March-27 April	25	20	23	21	22	23	0
1990	31 March-23 April	22	20	12	20	21	19	0
1991	30 March-12 May	33	26	25	29	28	25	0
1992	1 April-27 April	23	18	17	20	16	17	0
1993	1 April-27 April	19	19	16	19	19	19	0
1994	31 March-29 April	25	25	18	17	15	16	0
1995	6 April-2 May	16	10	8	7	0	0	0
1996	2 April-10 May	15	11	11	10	3	1	0
1997	29 March-22 April	21	19	18	19	13	12	0
1998	23 March-22 April	18	15	17	15	13	11	0
1999	25 March-28 April	17	15	15	15	5	5	0
2000	3 April-27 April	10	9	10	8	2	2	0
2001	20 March-26 April	11	10	11	10	5	5	0
2002	20 March-2 May	10	6	10	9	6	6	0
2003	1 March-23 April	10	6	10	10	4	4	0
2004	23 March-20 April	6	5	6	6	5	5	0
2005	19 March-3 May	11	8	11	8	6	7	0
2006	26 March-1 May	13	11	12	13	7	10	0
2007	28 March-21 May	15	9	14	13	7	8	2
2008	19 March-6 May	14	10	12	9	6	8	3
2009	1 April-18 May	17	12	15	11	7	9	2

Year	Date Range	PWS	MI	SE	NE	NS	NI	KI
2010	24 Feb-4 May	21	8	19	18	5	6	2
2011	18 March-17 May	13	6	13	13	3	3	0
2012	28 March-30 April	17	5	16	13	2	2	1
2013	2 April-9 May	18	7	18	16	4	3	1
2014	23 March-1 May	15	2	15	14	1	2	3
2015	24 March-4 May	19	9	18	12	3	3	3
2016	23 March-27 April	14	10	14	14	5	5	0
2017	22 March-6 May	22	15	22	21	8	12	3
2018	24 March-19 April	12	9	11	9	6	8	2
2019	19 March-3May	17	15	17	16	3	9	2

[1] Only includes days when spawning was observed

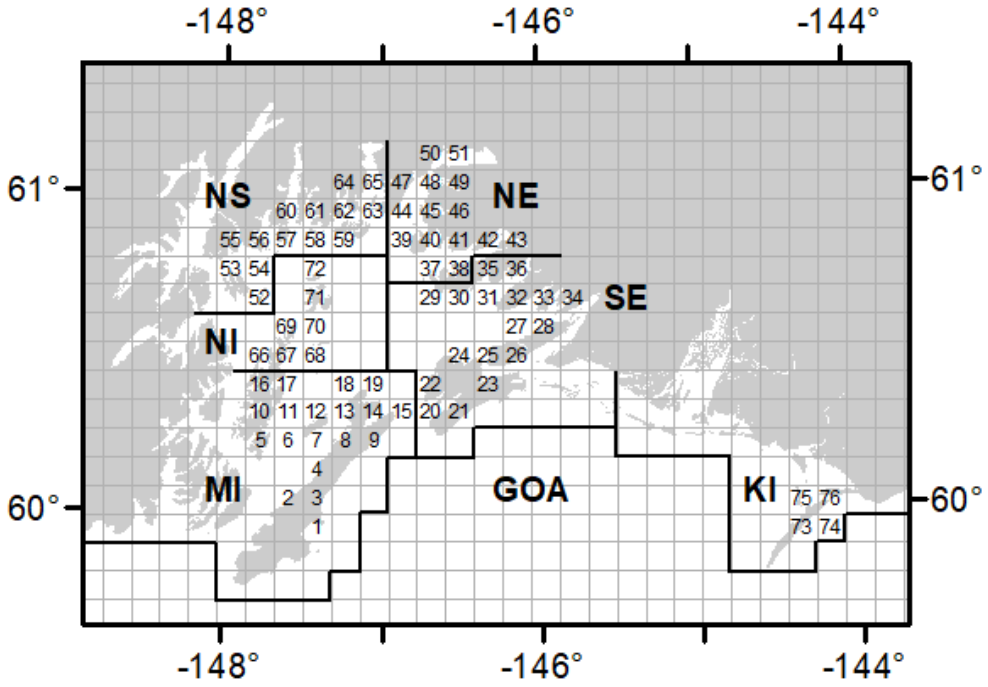

Figure A1. Boundaries for Prince William Sound regions (MI = Montague Island; SE = Southeast Sound; NE = Northeast Sound; NS = North Shore; NI = Naked Island; KI = Kayak Island) and the Gulf of Alaska (GOA) adapted from Appendix G4. in Russell et al. (2017). Numbered 10×10 km grid cells indicate areas within each region where herring spawning was observed between 1973 to 2017, and correspond with the x-axis in Figure 3-4A in the manuscript.

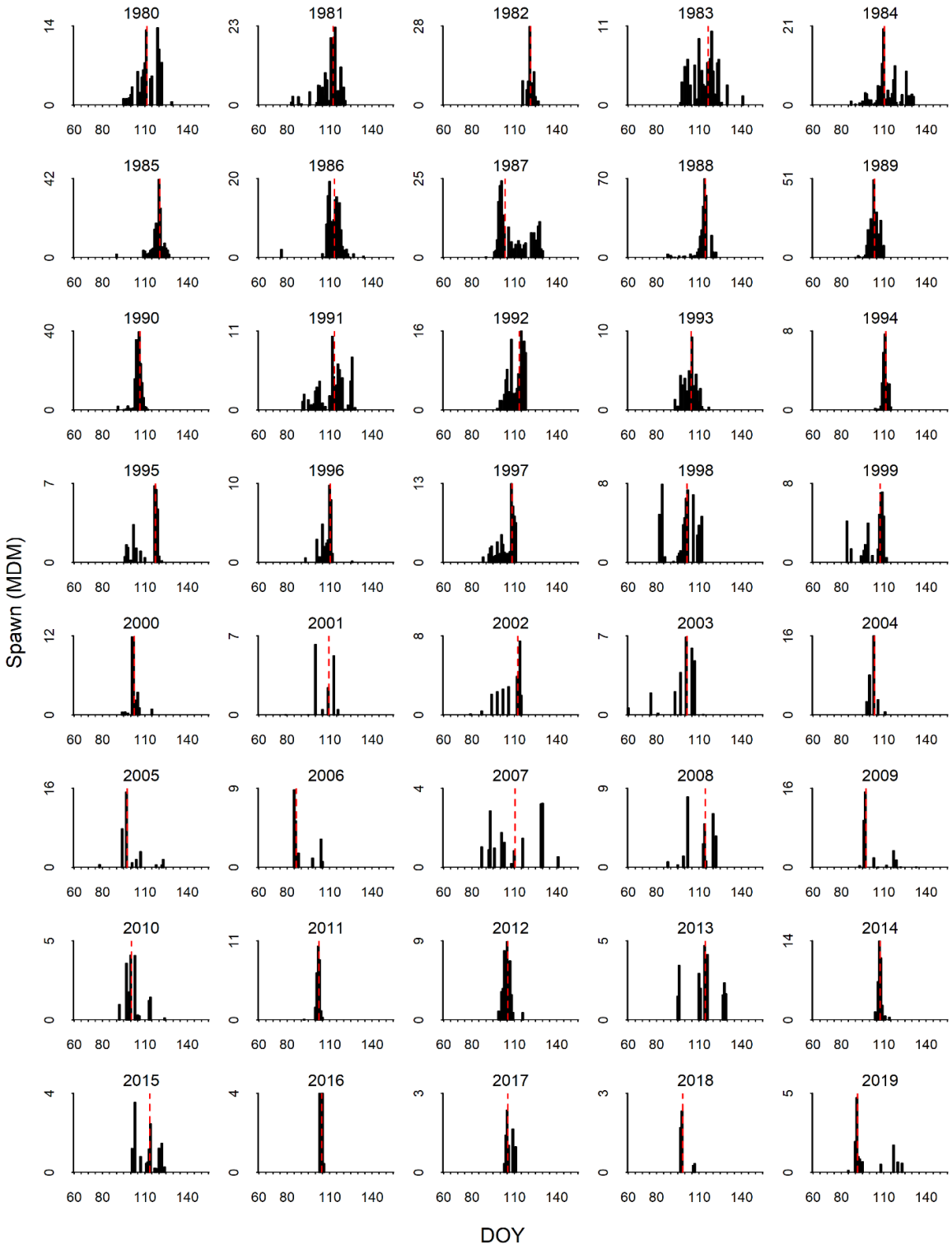

Figure A2. Histograms of annual spawning (mile-days of milt, MDM) for all regions combined from 1980 to 2019. The red dashed line indicates the date when 50% of total spawn was observed for each year.

CHAPTER 4 ANNUAL HERRING MIGRATION CYCLE

Mary Anne Bishop[1] and Jordan Bernard[1]

[1] *Prince William Sound Science Center, Cordova, AK*

INTRODUCTION

Our 2013 pilot project established that after spawning, a majority of adult, acoustic-tagged Pacific herring (*Clupea pallasii*) moved from the spawning grounds in Prince William Sound (PWS), where spawning ground acoustic arrays were located, to the entrances to the Gulf of Alaska (GOA), where the Ocean Tracking Network acoustic arrays (hereafter referred to as the entrance arrays) were located (Eiler and Bishop 2016, Bishop and Eiler 2018). Our conclusions were limited in scope, however, because tag life was < 9 months and because the entrance arrays consisted of single lines, precluding information on the direction of movements. Since the 2013 pilot study, we have deployed additional receivers that provide data on movement direction and have deployed two tags types, with battery lives of 9 and 25 months, respectively. Here we summarize our results from an analysis of herring movements over a two-year period (April 2017 through March 2019) based on herring tagged in PWS during 2017 and 2018.

OBJECTIVES

1) Document location, timing, and direction of Pacific herring seasonal migrations between PWS and the GOA.
2) Relate large-scale movements to year class and body condition of tagged individuals.
3) Determine seasonal residency time within PWS, at the entrances to PWS, and in the GOA.

METHODS

In February 2017, we deployed a second line of receivers at each of the four Southwest Passages, as well as a second line of four receivers each at Hinchinbrook Entrance and Montague Strait arrays. Because most detections occur near the shoreline, two receivers were placed at each end of Hinchinbrook Entrance and Montague Strait arrays. Receiver arrays were also deployed on the spawning grounds as well as in other suspected PWS post spawning habitat (Figure 4-1). Data were uploaded from receiver arrays at the entrances to the GOA in February (2018 & 2019) and September (2017-2019; partial upload only), and from spawning grounds arrays between April and June (2017-2019).

For these analyses, we defined two seasons for each 12-month period: spring/summer (1 April – 31 August; 5 months) and fall/winter (1 September – 31 March; 7 months). We developed an Arnason-Schwarz (AS) multistate model (Schwarz and Arnason 1993), a generalization of the Cormack-Jolly-Seber mark-recapture model, to estimate the probability at which PWS herring move between geographic locations while accounting for uncertainty of fish locations and mortality rates in the PWS and GOA (Figure 4-2). We implemented a Bayesian version of the AS model where fish direction information recorded at the entrance arrays was incorporated into

the model by using informative priors on the movement probabilities at the entrance arrays. The computation was carried out using R (R Core Team 2013) and JAGS (Plummer 2003).

A logit link function was used to model movement probabilities as a function of categorical variables. Variables considered included sex, spawn state at the time of tagging (spawned, not yet spawned), standard length, weight, condition (defined as weight*length^{-3}*1000), and tag-burden (tag weight/fish weight). We combined the 2017 and 2018 data and used the median as the break point to separate the variables standard length, weight, condition, and tag-burden into two categories each.

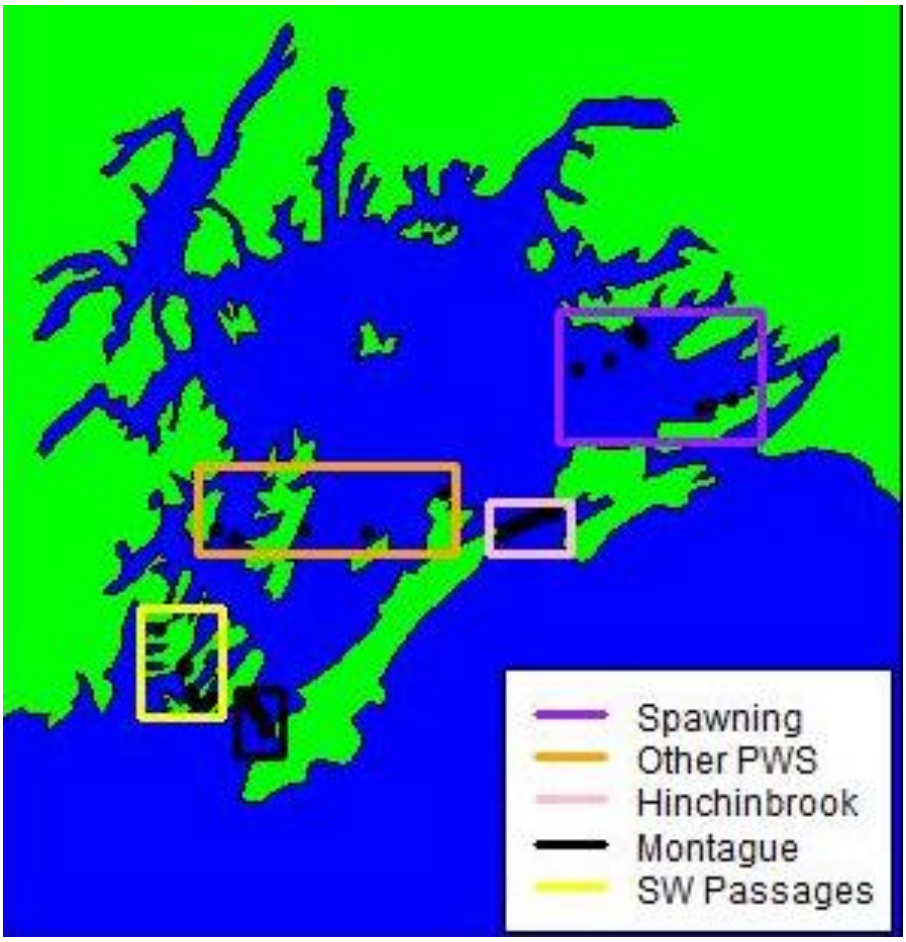

Figure 4-1. Location of Prince William Sound acoustic arrays. Hinchinbrook Entrance, Montague Strait, and the four Southwest Passages are collectively referred to as the entrance.

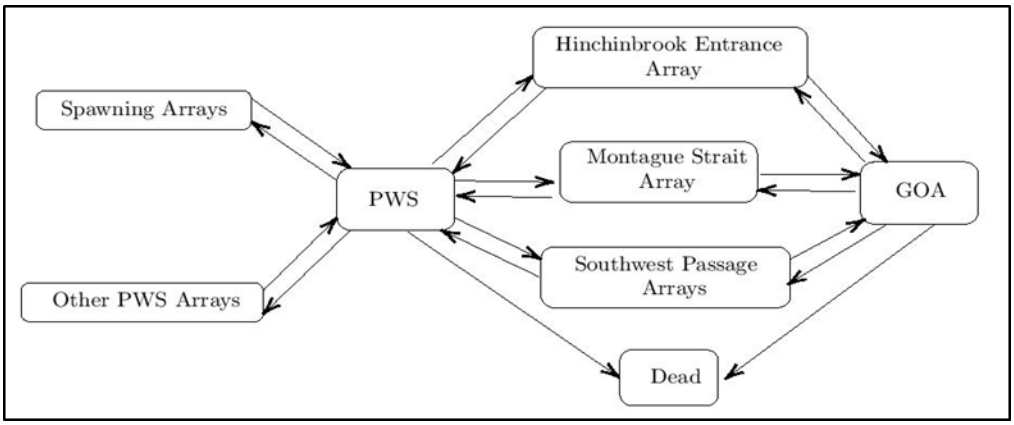

Figure 4-2. Schematic of multistate model used to describe adult herring movements. Eight model states (shown in rectangles) describe the possible location of a fish and whether or not it is alive. Arrows between geographic locations represent movement probabilities, while arrows pointing to the "dead" state represent mortality probabilities.

Mean residency times were estimated at the entrance arrays, spawning ground arrays (fall/winter season only) and in the GOA. The residency times at the entrance and spawning ground arrays were based on the time of first and last detection. Fish that went undetected for a period of >24h were considered to have departed an entrance or spawning ground array. To estimate residency time in the GOA we considered only fish with PWS-GOA directional detections that were then undetected for >7 d, followed by a detected return at the outside of an entrance array receiver.

To estimate seasonal mortality in PWS and the GOA we used an unconstrained version of the multi-state AS model. Because permanent immigration into the GOA cannot be distinguished from mortality, and because we would expect permanent immigration to be relatively low, we refer to our estimate as the GOA mortality rate.

RESULTS AND DISCUSSION

We tagged herring during April 2017 (n = 124) and 2018 (n = 202) in and around the spawning grounds at Port Gravina (2017 and 2018) and Hawkins Island (2018; Table 4-1).

Table 4-1. Total by sex, tagging location and year of acoustic-tagged herring, 2017-2019.

Month/Year	Location	Male	Female	Unknown
Apr 2017	Port Gravina	62	59	3
Apr 2018	Port Gravina/Cedar Bay – Canoe Pass	128	69	5
Apr 2019	Port Gravina/Canoe Pass/Double Bay/Rocky Bay	92	63	10
	Total	282	191	18

SEASONAL MIGRATION BETWEEN PWS AND GOA

We modeled movement probabilities between PWS and the GOA. At both Hinchinbrook Entrance and Montague Strait, herring were more likely to migrate from PWS to GOA during the spring/summer season, while during the fall/winter season herring were more likely to migrate from GOA to PWS. At the Southwest Passages, similar patterns were not observed, suggesting that the migration pathways run primarily through Hinchinbrook Entrance and Montague Strait (Figure 4-3). Seasonally, fish were most likely to leave PWS through Hinchinbrook Entrance during spring/summer season (Figure 4-4) whereas fish were more likely to return to PWS during the fall/winter season using Montague Strait.

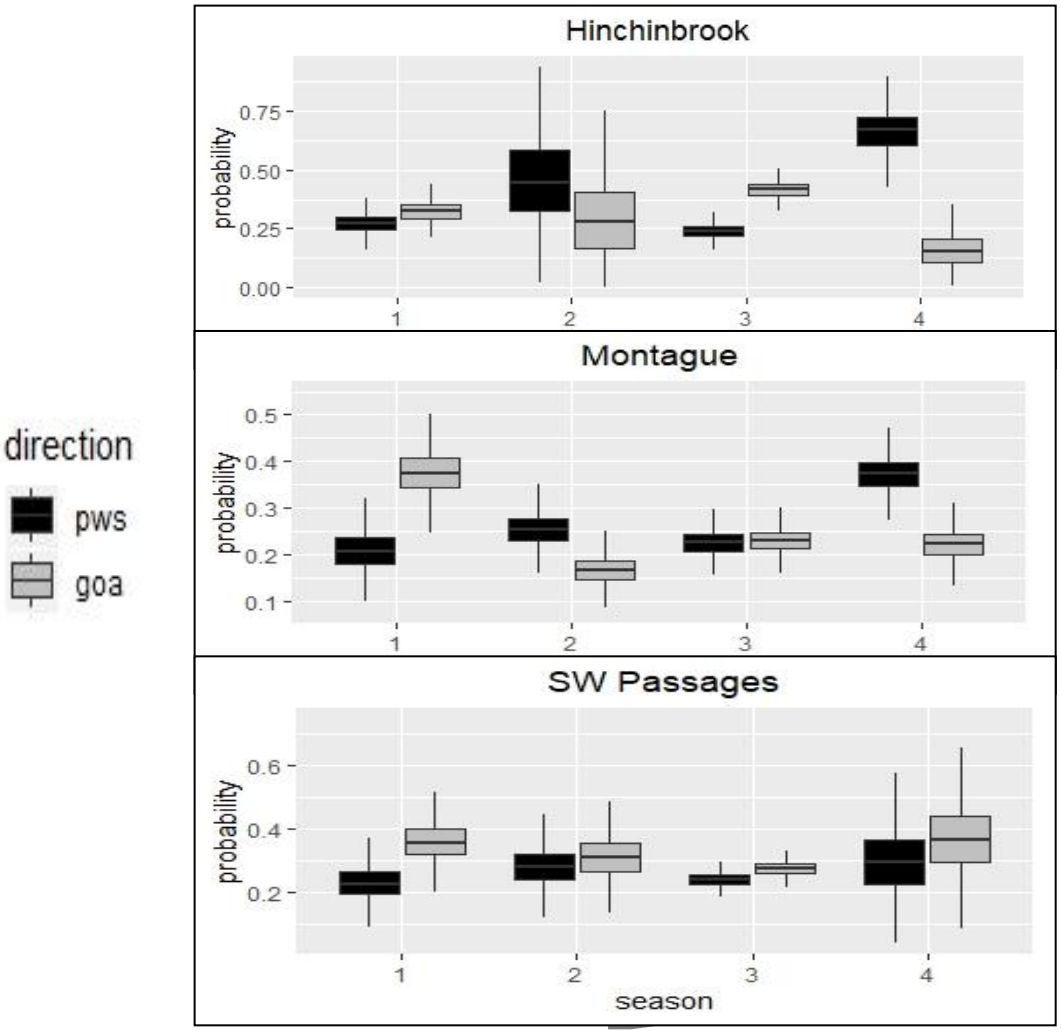

Figure 4-3. Movement probabilities by season, array, and direction, April 2017-March 2019. Black = Gulf of Alaska (GOA) to Prince William Sound (PWS); light gray = PWS to GOA. At Hinchinbrook Entrance and Montague Strait during spring/summer (April-August; seasons 1 & 3), fish are more likely to move from PWS to GOA than from GOA to PWS. During fall/winter (September-March; seasons 2 & 4), the trend reverses. This oscillatory trend is indicative of seasonal migration did not occur at the Southwest Passages.

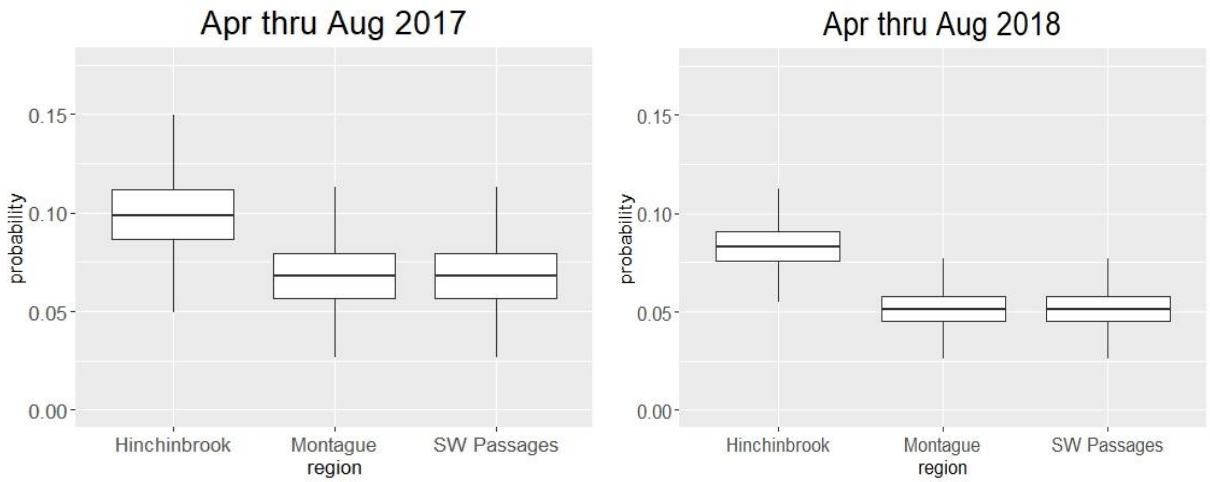

Figure 4-4. Probability of moving from Prince William Sound to the Gulf of Alaska by entrance array during spring/summer season (1 April- 31 August). Both years, fish were more likely to leave Prince William Sound through Hinchinbrook Entrance.

To better describe the phenology of herring migration, we used a kernel density plot to visualize the direction of movements over the two-year period (Figure 4-5). The plot shows that most of the PWS-GOA and GOA-PWS detections occurred between April and August. This is because some fish mingle around the entrance arrays, in particular at the Southwest Passages and log both PWS-GOA and GOA-PWS detections (Figure 4-6).

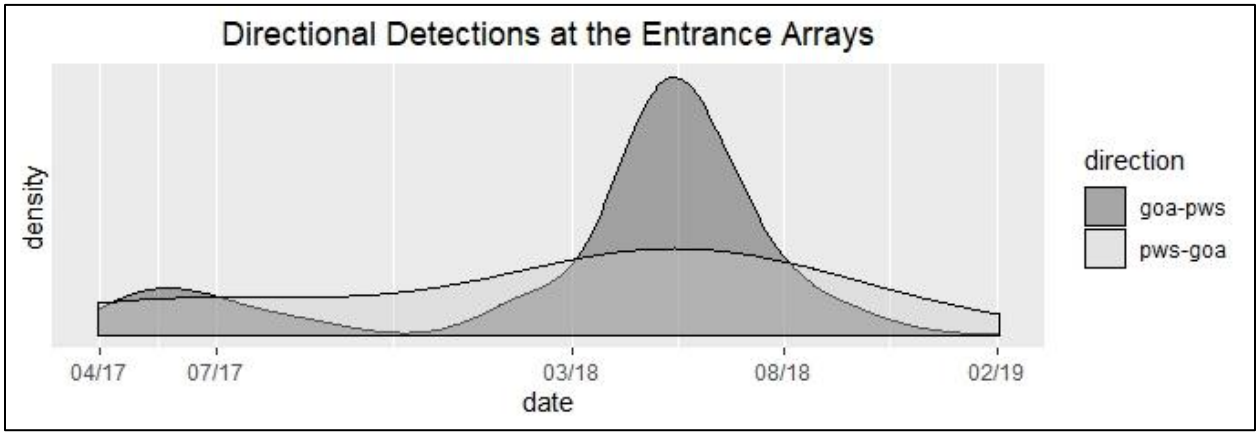

Figure 4-5. Kernel density estimate of movement direction at Prince William Sound entrance arrays (Hinchinbrook Entrance, Montague Strait, and Southwest Passages), April 2017-February 2019. GOA = Gulf of Alaska; PWS = Prince William Sound.

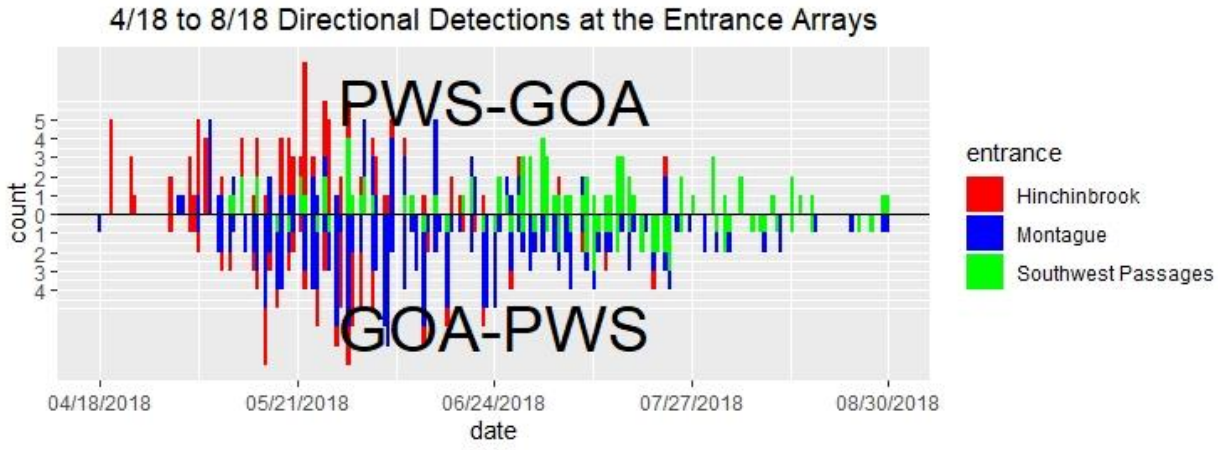

Figure 4-6. Exit from and returns to Prince William Sound by entrance array, spring/summer season 2018.

Effect of length, weight, and condition on migration

Our analyses indicated that neither sex nor spawning state had a significant effect on movement rates, however, length, weight, and condition did have significant effects. These three variables are deeply correlated, and results were similar across the three variables. Using the median weight for the first two tag years to separate heavy and light fish, we found that during spring/summer season, heavier herring were more likely to move to the entrance arrays (Figure 4-7). Likewise, longer, heavier fish in good condition were determined to be the most likely to migrate between PWS and the GOA. Lighter fish, on the other hand, were more likely to return to the PWS spawning areas during the fall/winter season (Figure 4-7).

Residency times at PWS arrays

Within PWS, the longest residency times at the entrance arrays occurred during the spring/summer season. Longest residencies were recorded during spring/summer 2017 at Prince of Wales and Elrington, two adjacent Southwest Passages, when estimated mean residency was 59.2 h and 34.8 h, respectively (

Table 4-2). On the spawning grounds during winter, average residency time was 3.2h (n = 4 fish) the first winter (September 2017 – March 2018) when there were only receivers at Gravina array; average residency time was 15.0 h (n = 33 fish) the second winter (September 2018 – March 2019) when there were additional arrays at Redhead and Hawkins Island.

Figure 4-7. Left: Effect of weight on Prince William Sound (PWS) to entrance array movement probability. Negative β estimates show that heavy fish are more likely to move from PWS to Montague Strait during spring/summer season. Similar trends were found at Hinchinbrook Entrance and the Southwest Passages. Right: Effect of weight on PWS to spawning ground movement probability. Positive β estimates show that during fall/winter season lighter fish are more likely than heavier fish to move from PWS to the spawning grounds.

Table 4-2. Estimated mean residency time (h) at entrance to Gulf of Alaska receiver arrays by season, April 2017 – March 2019. Number of individual fish denoted in parentheses. Fish were considered having departed from an array if no detections occurred for 24h.

Array	Apr-Aug 2017	Sep 2017-Mar 2018	Apr-Aug 2018	Sep 2018-Mar 2019
Hinchinbrook	11.0 (47)	0.2 (2)	7.7 (115)	1.0 (29)
Montague	13.4 (30)	5.9 (15)	16.8 (63)	12.3 (46)
Southwest Passages				
LaTouche	1.7 (4)	-	5.5 (19)	-
Elrington	34.8 (14)	22.1 (10)	25.0 (33)	17.4 (2)
Prince of Wales	59.2 (5)	42.0 (1)	44.3 (22)	28.4 (1)
Bainbridge	-	-	5.1 (4)	-

RESIDENCY IN GOA AND EFFECT OF SEX AND WEIGHT

Residency time in the GOA was estimated at 39.7 d for fish exiting from Hinchinbrook Entrance, 47.7 d for fish exiting through Montague Strait, and 31.2 d for fish exiting through the Southwest Passages. Fish exiting through Hinchinbrook Entrance and returning to PWS via Montague Strait had the longest GOA residency times (64.9 d, n = 6; Figure 4-8). One-third (n = 42) of the GOA 126 residency events involved fish exiting from and returning along the western shoreline of Montague Strait. Of the 126 occurrences where we could estimate residency time, 17 (14%) were

in the GOA for >3 months (max = 295 d) and 10 of the 17 fish (59%) returned during either January of February (Figure 4-9).

We used linear regression to understand the factors influencing residency time in the GOA. Variables examined included exit array, as well as fish length, weight, condition, sex, and spawning state. At the $\alpha = 0.10$, only weight ($p = 0.04$) was significant. Fish weight had a positive linear effect on residency time. An increase in 1.0 g weight was associated with a 0.34 d increase in residency (90% CI = 0.06 - 0.62).

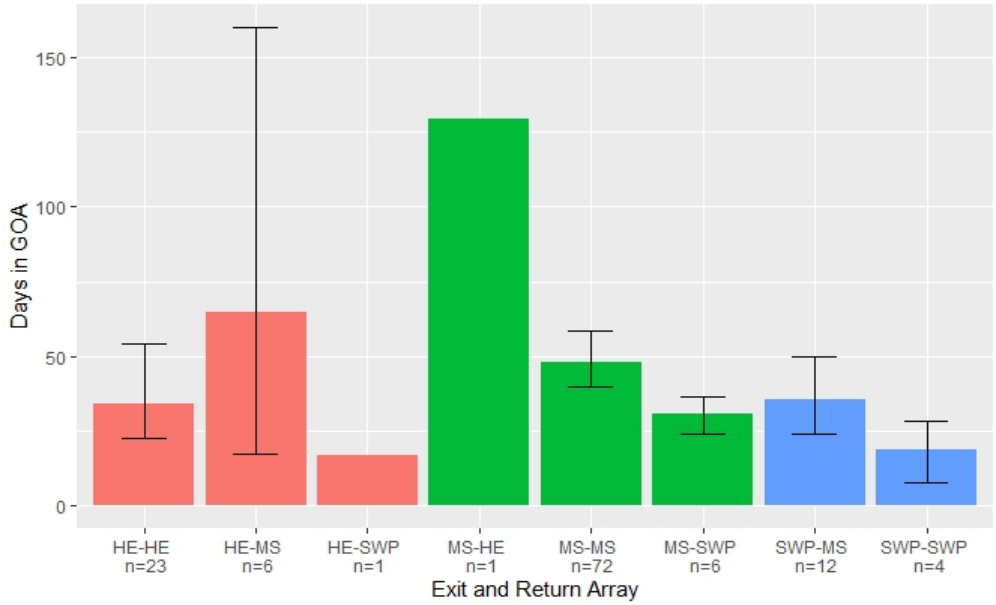

Figure 4-8. Estimated mean residency time (d) and 90% confidence interval for fish exiting to and remaining in the Gulf of Alaska > 7 d, followed by a return to Prince William Sound. Residency estimate shown by exit and return entrance arrays. Arrays: HE = Hinchinbrook Entrance, MS = Montague Strait, SWP = Southwest Passages. n = total exit/return where residency could be estimated for a total of 69 individual fish.

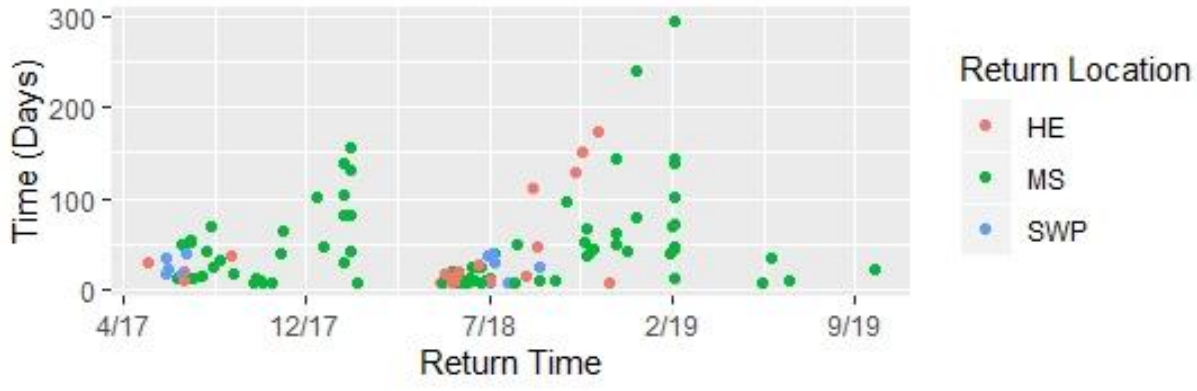

Figure 4-9. Residency time (d) in the Gulf of Alaska calculated as a function of return date to Prince William Sound and return entrance array. HE = Hinchinbrook Entrance, MS = Montague Strait, and SWP = Southwest Passages. Note the tendency of fish with longer stays to return to the Sound during winter months (December-February).

Mortality rates for tagged fish in PWS and GOA

Using 90 percent credible intervals, the seasonal mortality rates between PWS and the GOA were not significantly different and showed similar trends. Mortality was higher during the spring/summer season than during the fall/winter season (Figure 4-10), although the seasonal effect was significant only for PWS. Notably, during spring/summer 2017, the PWS weekly mortality rate was estimated to be 0.15, which is much higher than we would expect given the lifespan of the fish. In contrast, the following spring/summer season, PWS mortality dropped to 0.09, and was similar to the GOA mortality rate.

To determine if mortality varied within the spring/summer season, we split each spring/summer season in half and reran the model. We found that higher mortality tended to occur during the first one-half of the season (1 April – 15 June; Figure 4-11). We suggest that the higher mortality rate observed during the first one-half of the spring/summer season may be due to two factors: a) negative effects of tagging; and b) higher predation rate by marine mammals as a result of converging herring schools on the spawning grounds.

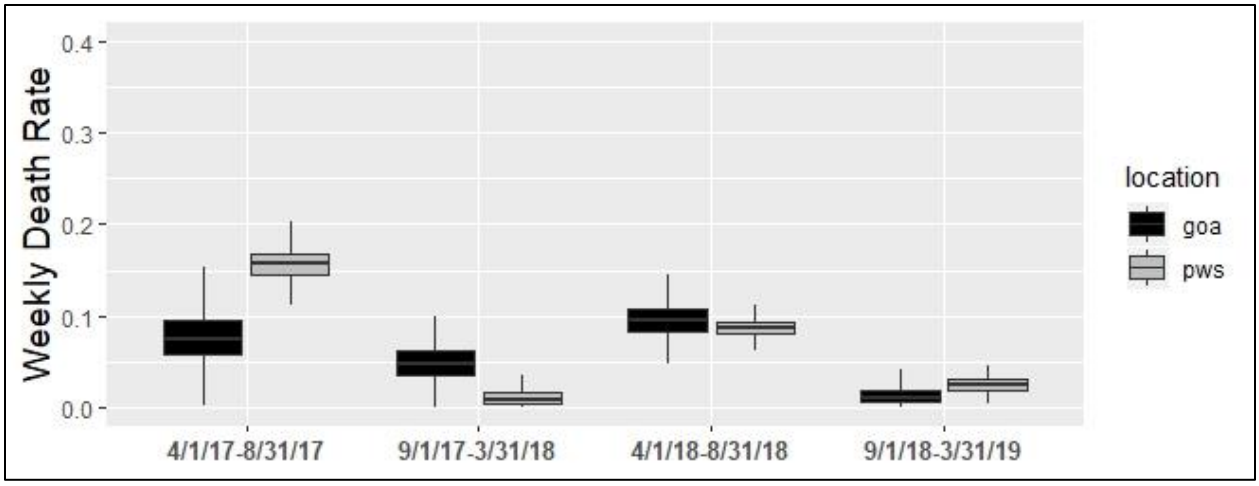

Figure 4-10. Average weekly mortality rate for acoustic-tagged herring in Prince William Sound (PWS) and the Gulf of Alaska (GOA) by season. April 2017 – March 2019.

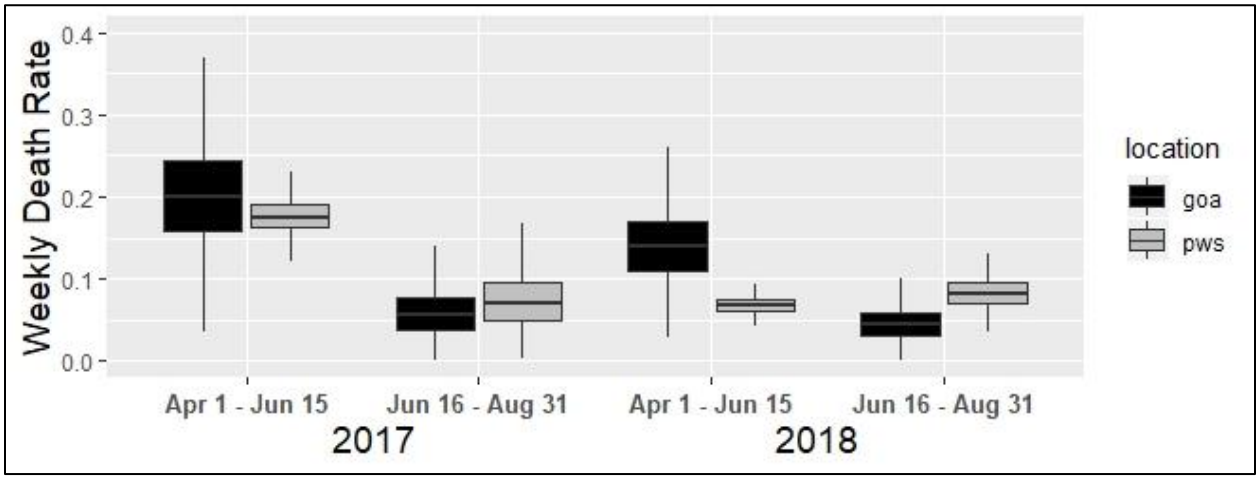

Figure 4-11. Average weekly mortality rate for acoustic-tagged herring in Prince William Sound (PWS) and the Gulf of Alaska (GOA) during the first (1 April – 15 June) and second (16 June – 31 August) one-half of the spring/summer season.

REFERENCES

Bishop, M.A. and J. Eiler. 2018. Migration patterns of spring-spawning Pacific Herring in Alaska's Prince William Sound. Deep-Sea Research II 147:108-115.

Eiler, J. and M.A. Bishop. 2016. Determining the post-spawning movements of Pacific herring, a small pelagic forage fish sensitive to handling, with acoustic telemetry. Transactions of American Fisheries Society. 145:2, 427-439, DOI: 10.1080/00028487.2015.1125948

Plummer, M., 2003, March. JAGS: A program for analysis of Bayesian graphical models using Gibbs sampling. In Proceedings of the 3rd international workshop on distributed statistical computing (Vol. 124, No. 125, p. 10).

R Core Team, 2013. R: A language and environment for statistical computing.

Schwarz, C.J. and Arnason, A.N., 1996. A general methodology for the analysis of capture-recapture experiments in open populations. Biometrics, pp.860-873.

This page intentionally left blank.

CHAPTER 5 HERRING DISEASE SYNTHESIS

Paul Hershberger[1] and Maya Groner[2]

[1] *USGS, Marrowstone Marine Field Station, WA*
[2] *Prince William Sound Science Center, Cordova, AK*

INTRODUCTION

Boom-bust cycles, or periodic oscillations in biomass and abundance, commonly occur among Clupeid populations throughout the world (Baukun 2006). The proximate and ultimate drivers of these cycles can be grouped into top-down (e.g. predation, disease, harvest) or bottom-up (e.g. food availability) factors. The hypothesis that disease contributed to the biomass decline in Prince William Sound (PWS) during the early 1990s is supported by concomitant observations involving large numbers of diseased Pacific herring (*Clupea pallasii*) among the returning survivors (Marty et al 1998). Since this decline, a new (lower) herring population size steady state established in PWS, and it is hypothesized that endemic diseases are preventing its recovery to the former (higher) steady state.

As a result of these observations, the Herring Disease Program (HDP) was created and nested within the Herring Research and Monitoring Program, with the goals of understanding and mitigating the impacts of infectious and parasitic diseases to the PWS herring population. Historically, our understanding of disease impacts on populations of wild marine fishes has been limited by an investigative approach that relied exclusively on correlations and inferences from field survey efforts. Although this approach can be effective at documenting trends in infection / disease prevalence and severity, it is unable to demonstrate cause-and-effect relationships between disease and population impacts. The HDP seeks to understand the proximate and ultimate drivers that influence disease outbreaks by expanding beyond this traditional approach and integrating active laboratory and field experimentation. The following sections synthesize some of the recent findings of the HPD and describe how these results can be used to forecast disease risk and inform management decisions to mitigate disease impacts.

VIRAL HEMORRHAGIC SEPTICEMIA VIRUS (VHS VIRUS)

Although viral hemorrhagic septicemia (VHS) virus has occurred in the Pacific Northwest for centuries (Einer-Jensen et al. 2004), enhanced surveillance efforts were largely responsible for its first isolation in the region during the late 1980's - from asymptomatic, adult Pacific salmonids (Brunson et al. 1989, Stewart et al. 1990, Eaton et al. 1991). Subsequent studies confirmed that the newly isolated virus was genetically distinct from strains previously known to occur in Europe (Batts et al. 1993), which severely impacted the farmed rainbow trout (*Onchorhynchus mykiss*) industry. It was quickly determined that the North America strain (Genogroup IVa) demonstrated little pathogenicity to Pacific salmonids (Winton et al. 1991, Gross et al. 2019). Consequently, initial concern for the presence of the endemic virus waned - until the virus was isolated from clinically diseased, dead and dying, marine fishes including Pacific cod *Gadus macrocephalus*), Pacific hake (*Merluccius productus*), walleye pollock (*Theragra chalcogramma*), and Pacific herring in Alaskan waters (Meyers et al. 1999, Hedrick et al. 2003).

It is now known that VHS virus (Genogroup IVa) is highly virulent to many species of marine fishes and it periodically causes epizootics and resulting fish kills throughout the Pacific Northwest (Garver et al. 2013). Efforts within the HDP have identified a series of guiding principles that govern the epizootiology of VHS virus (Hershberger et al. 2016a):

Principle #1: Pacific herring are highly susceptible to VHS

Recurring epizootics of VHS are responsible for fish kills in Pacific herring and other forage fishes (Garver et al. 2013). Indeed, ongoing studies in 2018 and 2019 indicate that annual VHS epizootics consistently occur among some age 0 herring aggregations in nearshore habitats (e.g. Port Angeles Harbor, WA; Hershberger new data, unpublished). These observations are further supported by controlled laboratory studies which indicate that naïve Pacific herring are highly susceptible to direct mortality from VHS (Kocan et al. 1997; Hershberger et al. 2007, 2010a). Therefore, Pacific herring are considered an exceptionally susceptible host species, with waterborne exposure levels as low as 10^1 virus particles (plaque-forming units, PFU) / mL capable of initiating epizootics. Additionally, the virus is capable of infecting and killing previously-naïve Pacific herring when injected into the body cavity at a calculated dose of 0.07 PFU / fish, a level below the detection threshold of a standard viral plaque assay (Hershberger et al. 2011).

Principle #2: Pacific herring are super-shedders of VHS virus

After exposure to the virus and successful establishment of infection, Pacific herring and other species shed copious amounts of VHS virus into the water (Hershberger et al. 2010b). In lab settings, shed VHS virus can be detected in the water as early as 4-5 days post-exposure, prior to the onset of host mortality from the resulting disease. Viral shedding peaks 6-10 days post-exposure and high levels of shed virus are no longer detectable after 16 days. During the shedding peak, each diseased herring sheds an average of 500 million virus particles into the water each day. The progression of viral shedding is temperature-dependent, with lower temperatures generally resulting in higher shedding rates and delayed peaks in viral shedding (Hershberger et al. 2013). In the wild, an abundance of super-shedders in a population likely results in the rapid amplification of exogenous virus, thereby providing a critical viral amplification step in the irreversible cascade of events that culminate in a VHS outbreak (Hershberger et al. 2016a). Ongoing studies indicate that herring continue to shed low levels of VHS virus well-after this acute and transient viral shedding period, with waterborne virus detected in laboratory settings at least 6 months post exposure and well after the occurrence of an outbreak (Hershberger new data, unpublished). Viral shedding is exacerbated by decreasing water temperatures during this long-term chronic shedding period.

Principle #3: Pacific herring are a natural reservoir for VHS virus

The involvement of Pacific herring and other highly susceptible fishes including Pacific sardines (*Sardinops sagax caerulea*), walleye pollock, and Pacific sand lance (*Ammodytes personatus*) as natural reservoirs for VHS virus in the Northeast Pacific was recently recognized by combining lines of evidence from field observations, manipulations of wild herring, and controlled laboratory studies. Although sensitive VHS virus diagnostic techniques typically fail to detect VHS virus-positive tissue samples during wild fish surveys,

the confinement of wild herring into net pens or laboratory tanks supplied with specific pathogen free water often results in rapid escalation of VHS epizootics (Hershberger et al. 1999, Kocan et al. 2001a). This observation indicates that VHS virus is maintained covertly in populations of wild Pacific herring at extremely low prevalence and intensity levels; however, the virus can quickly amplify in the same population in response to exacerbating conditions such as capture, handling, transport, and/or confinement. Indeed, an ongoing study has been able to demonstrate the persistence of low viral loads in the gills and the recurrence of low levels of VHS virus in the kidney / spleen tissues of survivors at least two years post-exposure; this low-level viral recurrence is exacerbated by decreasing water temperatures. The mechanism(s) of long-term viral persistence in these populations involves a combination of chronic infections among neurotropic carriers (Lovy et al. 2012) and low-level replication /shedding in gill and other epithelial cells among the among immune individuals (Hershberger et al. 2010a).

Principle #4: Co-factors influence the potential for VHS epizootics

Several host and environmental factors influence the risk of VHS outbreaks, including water temperatures, weather / climatic patterns, diet, and conditions that impact infection pressures, including water exchange rates, gregarious host behaviors, and proximity to VHS virus reservoir species. The susceptibility of Pacific herring to VHS is inversely related to ambient seawater temperature, as cooler temperatures result in higher mortalities, greater viral shedding, and longer viral persistence in the tissues of survivors (Hershberger et al. 2013). Once shed into the water, the stability of exogenous VHS virus increases with the amount of proteinaceous material in the water, decreasing salinity, decreasing ambient temperatures, and decreased ultraviolet irradiation (Kocan et al. 2001b, Oye and Rimstad 2001, Hawley and Garver 2008). Although the effects of natural diet items on host susceptibility remain uninvestigated, the provision of various commercially available pelleted feeds to captive herring results in host susceptibility differences, possibly due to the inclusion of immunostimulants as feed ingredients (Beaulaurier et al. 2012). Tidal and wind-driven water circulation patterns can influence the titer of waterborne VHS virus within fjords and embayments where limited water exchange may occur; additionally, advection currents from an area with a localized epizootic may result in expansion of localized epizootics to much broader areas (Foreman et al. 2015; Salama and Rabe 2013). Finally, certain predator-avoidance behaviors of Pacific herring and other pelagic forages fishes, particularly the coalescence of schools and shoals into extremely tight aggregations, are conducive to transmission of VHSV.

Principle #5: Acquired Resistance is a critical determinant of VHS potential

Although immunologically naïve Pacific herring are highly susceptible to VHS, survivors of the disease develop a long-lived adaptive immunity that results in resistance to the disease. VHS progression in susceptible Pacific herring can be extremely rapid, with detectable levels of virus occurring in the tissues of exposed herring as early as 2 days post-exposure, and mortality from the disease occurring as early as 4 days post-exposure (Kocan et al. 1997; Hershberger et al. 2010a). As noted in previous sections, the pace, intensity, and outcome of the disease are highly dependent on several variables including exposure level and duration, temperature, diet, water exchange rate, and other factors factors (Hershberger et al. 2011a,

2013). Regardless of the disease progression and magnitude, survivors of active case of VHS develop solid resistance to future recurrences of the disease even after their subsequent exposure to high levels of virus. Therefore, the potential for VHS epizootics typically decreases with the host age; not as a result of an increased innate immune response; rather because older cohorts are more likely to have survived prior infection and developed acquired immunity. This acquired resistance supersedes all other disease co-factors, and a resistant population will not experience a VHS epizootic even if all other disease co-factors are present. However, situations can occur where older age cohorts remain naïve to the virus and retain their susceptibility to the disease; indeed, VHS epizootics occur in wild adult herring (Garver et al. 2013) and lifelong susceptibility is seen in laboratory colonies of adult Pacific herring that were reared under specific pathogen-free conditions. Often, some proportion of the adult population is immune, while the remaining proportion retains susceptibility; the relative proportions of these immune and susceptible fractions determines the levels of protective herd immunity within any herring population.

VHS FORECASTING AND MANAGEMENT IMPLICATIONS

Information from these newly articulated principles can be integrated into tools capable assessing prior population-level impacts and forecasting future disease risk (Hershberger et al. 2016a). In this context, Principle #5 is the most informative, as the immune status of individuals and populations supersedes all the principles. For example, a population of immune individuals will not experience an epizootic, even if all other disease co-factors occur simultaneously (i.e. exposure to virus, cool temperatures, elevated infection pressures, etc.). Further, with annual immunological monitoring of herring population across year classes, we can deduce if, and when, epizootics occurred. This deduced exposure history can then be paired with population assessments to assess whether the epizootic was associated with a concomitant reduction in biomass or abundance.

Because of the forecasting and hindcasting potential offered by Principle #5, considerable effort was undertaken to develop laboratory tools capable of assessing the VHS virus exposure history of wild Pacific herring. Several enzyme-linked immunosorbent assays were developed, but the assays were quite onerous and data reproducibility was not optimal (Wilson et al. 2014 and Hershberger unpublished). Therefore, we developed a plaque neutralization test (PNT) that offers a quantitative assessment of VHSV neutralizing antibody titers in Pacific herring; the assay works well and produces highly reproducible results (Hart et al. 2017). Using this PNT, we processed archived plasma samples collected during the past 10 years in PWS and Sitka Sound. We also started validating the PNT using wild herring with known VHSV exposure histories. During the validation process, we discovered that slight adjustments to the PNT methods can significantly increase the sensitivity of the assay (Hershberger unpublished). For example, by inactivating all endogenous complement in the herring test sera and adding back known amounts of clean exogenous complement, we effectively increase the mean titers of detectable antibodies in wild herring from 80 neutralizing units (old methods) to 1,331 neutralizing units (new methods). We are in the final stages of validating these new methods using wild herring with known exposure histories (expected completion 30 November 2019); after which, the new methods will be re-applied to all archived plasma samples from PWS and Sitka Sound (anticipated completion March 2020). These historical antibody data, linked to each herring year class, will then be incorporated into a revised Age-Structured-Assessment (ASA) population

model to deduce whether any epizootics occurred concomitantly with changes in population abundance or biomass.

ICHTHYOPHONUS SP.

Ichthyophonus is perhaps the most ecologically and economically significant pathogen of wild marine fishes throughout the world, based on its low host specificity, broad geographic range, and recurring association with epizootics that result in massive fish kills and population-level impacts. Recurring epizootics have been documented in Atlantic herring (*Clupea harengus*) populations throughout the coastal regions of the Atlantic Ocean, Chinook salmon (*O. tshawytscha*) in the Yukon River, yellowtail flounder (*Pleuronectes ferruginea*) in the western North Atlantic, and American shad (*Alosa sapidissima*) in the Columbia River (reviewed in Burge et al. 2014). *Ichthyophonus* is also endemic in Pacific herring, where it typically occurs in high infection prevalence with varying intensities (Hershberger et al. 2002 & 2016b).

The widespread distribution of *Ichthyophonus* in Pacific herring throughout the west coast of North America provides some indication of the mechanisms involved in the perpetuation and transmission of the parasite. Natural route(s) of *Ichthyophonus* transmission in Pacific herring remain unresolved and laboratory studies have been largely unsuccessful at demonstrating transmission by host cohabitation, immersion in parasite isolates, or feeding with infected tissues or isolates (Gregg et al. 2012). Additionally, molecular-based efforts to identify an intermediate host parasite in zooplankton community herring have been largely unsuccessful; analogous efforts to detect the parasite in sea lice (*Caligus clemensii*) grazing on surface lesions of herring demonstrating gross signs of ichthyophoniasis were also unsuccessful (Hershberger new data, unpublished). Collectively, these results fail to provide any evidence that the parasite passes through an intermediate or paratenic invertebrate host. Therefore, our investigations into transmission routes have shifted towards the possibility of direct transmission mechanisms, including the possibility of transmission via the consumption of infected walleye pollock and herring eggs.

Over broad spatial and temporal scales, the prevalence of *Ichthyophonus* infections typically increases with herring size and age (Hershberger et al. 2002 and 2016b, Marty et al. 2003). This zoographic pattern is consistent with that of a chronic infection that accumulates in a population via recurring exposures throughout the lifetime of the host. The timing, location, and route of *Ichthyophonus* exposures to Pacific herring remain unknown; however, this accumulation hypothesis suggests that the clearance or elimination of the parasite from infected host tissues must be a rare event. As a result of this direct relationship between infection prevalence and host age, we started reporting infection prevalence data for individual age / size classes rather than as a single prevalence from a geographic stock / location.

Exceptions to this direct relationship between *Ichthyophonus* prevalence and Pacific herring age / size occur periodically throughout the Northeast Pacific. For example, *Ichthyophonus* hot spots occur among juvenile herring from Cordova Harbor (Hershberger new data, unpublished) and adult herring from North Hood Canal, WA (Hershberger et al. 2019). These anomalies were likely the result of site / regional-specific disease drivers and offer unique opportunities to target our investigations into parasite transmission routes. We hypothesize that the high prevalence in Cordova Harbor may be related to industrial activities on the waterfront. Similarly, the Hood

Canal hot spot may be due to density-dependent drivers, as this is currently the largest herring stock in Puget Sound (Hershberger et al. 2019).

Although *Ichthyophonus* typically persists in Pacific herring at chronic levels that accumulate in populations over time, several lines of evidence indicate that the parasite may periodically contribute to negative impacts on Pacific herring population dynamics. Laboratory exposures indicate that *Ichthyophonus* can be highly pathogenic to Pacific herring, with intraperitoneal injections resulting in host mortality with a mean day-to-death of 36d (Kocan et al. 1999). Massive epizootics and associated fish kills periodically occur in populations of adult Atlantic herring, often culminating in population-level impacts (reviewed in Burge et al. 2014). Similarly, the prevalence of *Ichthyophonus* decreased from 62.5% (5/8) to 19.6% (22/112) in the largest size class (>240mm) from Sitka Sound during 2007-2013 (Hershberger et al. 2016b). It is hypothesized that this size-specific decrease in *Ichthyophonus* prevalence resulted from selective mortality among the infected cohorts, as the heaviest infection intensities observed throughout this seven-year survey (2007-2013) occurred in Sitka Sound during 2012. Investigations are currently underway to understand whether the typical chronic *Ichthyophonus* infections shifted to a more acute form in Sitka Sound and resulted in disease mortality of the older age cohorts.

Interannual differences in *Ichthyophonus* infection prevalence occur periodically among different herring populations. For example, the infection decreased dramatically in recent years among all herring from Lower Cook Inlet and among the largest size cohorts in Sitka Sound (Hershberger et al. 2016b). We hypothesize that these changes resulted from proximate or ultimate mortality among the infected cohorts. Laboratory exposure studies provide no indication that, once infected, Pacific herring are capable of completely clearing *Ichthyophonus* infections; rather, infected individuals experience either acute mortality (Kocan et al. 1999) or survival with persistent infections (Hershberger 2012). Elevated mortality of infected cohorts could occur from selective predation on *Ichthyophonus*-infected cohorts if infected individuals with decreased swimming performance are more easily captured by predators. This predator selection hypothesis is supported by field observations during an *Ichthyophonus* epizootic, when 60-80% of Atlantic cod stomachs contained heavily-infected Atlantic herring (Kramer-Schadt et al. 2010).

A basic understanding of the natural transmission routes for *Ichthyophonus* will provide capacity to forecast the potential for future epizootics. For example, if it is determined that increased infection prevalence and intensity is associated with ovivory and punctuated exposures to infected eggs, then availability and spatial / temporal overlap of herring with these infected eggs would serve as an early warning sign for an oncoming epizootic.

Other Pathogens

As with all wild animals, Pacific herring are often infected with numerous other macro- and micro-parasites (Marty et al. 1998); most, such as *Vibrio* spp. (Hershberger et al. Submitted), anasakid nematodes, and liver and intestinal coccidians, are not particularly pathogenic under typical conditions. One exception is erythrocytic necrosis virus (ENV), which causes a viral erythrocytic necrosis (VEN). Herring are particularly susceptible to VEN, which can cause severe anemia and host death (Winton and Hershberger 2014). VEN epizootics recur in nearshore aggregations of Pacific herring (Meyers et al. 1986), possibly as a result of transient exposures to older Pacific herring age cohorts that are carriers of the virus (Hershberger et al.

2009). Several diagnostic techniques were developed to enhance our ability to detect and confirm the presence of ENV (Emmenegger et al. 2014, Purcell et al. 2016). The impacts of other common parasites remain unknown and require further investigations, including sea lice which sometimes occur at very high infection prevalence and density (Hershberger unpublished).

REFERENCES

Batts, W.N., C.K. Aeakawa, J. Bernard, J.R. Winton. 1993. Isolates of viral hemorrhagic septicemia virus from North America and Europe can be detected and distinguished by DNA probes. Diseases of Aquatic Organisms 17:67-71.

Baukun, A. 2006. *Wasp waist* populations and marine ecosystem dynamics: Navigating the "*predator pit*" topographies. Progress in Oceanography 68:271-288.

Beaulaurier, J., N. Bickford, J.L. Gregg, C.A. Grady, A. Gannam, J.R. Winton, P.K. Hershberger. 2012. Susceptibility of Pacific herring *Clupea pallasii* to viral hemorrhagic septicemia (VHS) is influenced by diet. Journal of Aquatic Animal Health. 24:43-48.

Burge, C.A., C.M. Eakin, C.S. Friedman, B. Froelich, P.K. Hershberger, E.E. Hofmann, L.E. Petes, K.C. Prager, E. Weil, B.L. Willis, S.E. Ford, C.D. Harvell. 2014. Climate change influences on marine infectious diseases: implications for management and society. Annual Review of Marine Science 6:249-277.

Brunson, R., K. True, J. Varney. 1989. VHS virus isolated at Makah National fish Hatchery. American Fisheries Society Fish Health Section Newsletter 17(2): 3 (Bethesda, MD).

Eaton, W.D., J. Heulett, R. Brunson, K. True. 1991. The first isolation in North America of infectious hematopoietic necrosis virus (IHNV) and viral hemorrhagic septicemia virus (VHSV) in coho salmon from the same watershed. Journal of Aquatic Animal Health 3:114-117.

Einer-Jensen, K., P. Ahrens, R. Forsberg, N. Lorenzen. 2004. Evolution of the fish rhabdovirus viral haemorrhagic secticaemia virus. Journal of General Virology 85:1167-1179.

Emmenegger, E.J., J.A. Glenn, J.R. Winton, W.N. Batts, J.L. Gregg, P.K. Hershberger. 2014. Molecular identification of erythrocytic necrosis virus (ENV) from the blood of Pacific herring (*Clupea pallasii*). Journal of Veterinary Microbiology 174:16-26.

Foreman, M.G.G., Guo, M., Garver, K.A., Stucchi, D., Chandler, P., Wan, D., Morrison, J., and Tuele, D. 2015. Modelling Infectious Hematopoietic Necrosis Virus Dispersion from Marine Salmon Farms in the Discovery Islands, British Columbia, Canada. *PLoS ONE* 10: 6. :e0130951. doi:10.1371/journal.pone.0130951.

Garver, K.A., G.S. Traxler, L.M. Hawley, J. Richard, J.P. Ross, J Lovy. 2013. Molecular epidemiology of viral hemorrhagic septicemia virus (VHSV) in British Columbia, Canada, reveals transmission from wild to farmed fish. Diseases of Aquatic Organisms 104:93-104.

Gregg J.L., C.A. Grady, C.S. Friedman, P.K. Hershberger. 2012. Inability to demonstrate fish-to-fish transmission of *Ichthyophonus* from laboratory-infected Pacific herring *Clupea pallasii* to naïve conspecifics. Diseases of Aquatic Organisms 99:139–44.

Gross, L., J. Richard, P. Hershberger, K. Garver. 2019. Low susceptibility of sockeye salmon *Oncorhynchus nerka* to viral hemorrhagic septicemia virus genotype IVa. Diseases of Aquatic Organisms 135:201-209.

Hart, L.M., M.K. Purcell, R. Powers, A. MacKenzie, P.K. Hershberger. 2017. Optimization of a plaque neutralization test to identify the exposure history of Pacific herring to viral hemorrhagic septicemia virus (VHSV). Journal of Aquatic Animal Health 29:74-82.

Hawley, L.M., K.A. Garver. 2008. Stability of viral hemorrhagic septicemia virus (VHSV0 in freshwater and seawater at various temperatures. Diseases of Aquatic Organisms 82:171-178.

Hedrick, R.P., W.N. Batts, S. Yun, G.S. Traxler, J. Kaufman, J.R. Winton. 2003. Host and geographic range extensions of the North American strain of viral hemorrhagic septicemia virus. Diseases of Aquatic Organisms 55:211-220.

Hershberger P.K. 2012. *Ichthyophonus* Disease (Ichthyophoniasis). *In*: Fish Health Section Blue Book: Suggested Procedures for the Detection and Identification of Certain Finfish and Shellfish Pathogens. American Fisheries Society.

Hershberger, P.K., N.E. Elder, C.A. Grady, J.L. Gregg, C.A. Pacheco, C. Greene, C. Rice and T.R. Meyers 2009. Prevalence of viral erythrocytic necrosis in Pacific herring and epizootics in Skagit Bay, Puget Sound, Washington. Journal of Aquatic Animal Health 21:1-7.

Hershberger, P.K., K.A. Garver, J.R. Winton. 2016a. Principles underlying the epizootiology of viral hemorrhagic septicemia in Pacific herring and other fishes throughout the North Pacific Ocean. Canadian Journal of Fisheries and Aquatic Sciences. 73: 53-859.

Hershberger, P.K., J.L. Gregg, L.M. Hart, S. Moffitt, R. Brenner, K. Stick, E. Coonradt, T. Otis, J.J. Vollenweider, K.A. Garver, J. Lovy, T.R. Meyers. 2016b. The parasite *Ichthyophonus* sp. in Pacific herring. Journal of Fish Diseases 39:395-410.

Hershberger, P.K., J.L. Gregg, C.A. Grady, R.M. Collins, J.R. Winton. 2010a. Susceptibility of three stocks of Pacific herring to viral hemorrhagic septicemia. Journal of Aquatic Animal Health. 22:1-7.

Hershberger, P., J. Gregg, C. Grady, R. Collins, J. Winton. 2010b. Kinetics of viral shedding provide insights into the epidemiology of viral hemorrhagic septicemia in Pacific herring. Marine Ecology Progress Series 400:187-193.

Hershberger, P.K., J.L. Gregg, C.A. Grady, L. Hart, S.E. Roon, J.R. Winton. 2011. Factors controlling the early stages of viral hemorrhagic septicemia epizootics: low exposure levels, virus amplification, and fish-to-fish transmission. Journal of Fish Diseases 34:893-899.

Hershberger, P.K., J. Gregg, C. Pacheco, J. Winton, J. Richard, G. Traxler. 2007. Larval Pacific herring, *Clupea pallasii* (Valenciennes), are highly susceptible to viral hemorrhagic septicemia and survivors are partially protected after their metamorphosis to juveniles. Journal of Fish Diseases 30:445-458.

Hershberger, P.K., R.M. Kocan, N.E. Elder, T.R. Meyers, and J.R. Winton. 1999. Epizootiology of viral hemorrhagic septicemia virus in herring from the closed pound spawn-on-kelp fishery. Diseases of Aquatic Organisms 37:23-31.

Hershberger, P.K., A.H. MacKenzie, J.L. Gregg, A. Lindquist, T. Sandell, M.L. Groner, D. Lowry. 2019. A Geographic Hot Spot of *Ichthyophonus* infection in the Southern Salish Sea, USA. Diseases of Aquatic Organisms 136:157-162.

Hershberger, P.K., M.K. Purcell, L.M. Hart, J.L. Gregg, R.L. Thompson, K.A. Garver, J.R. Winton. 2013. Influence of temperature on viral hemorrhagic septicemia (Genogroup IVa) in Pacific herring, *Clupea pallasii* Valenciennes. Journal of Experimental Marine Biology and Ecology 444:81-86.

Hershberger, P.K., K. Stick, B. Bui, C. Carroll, B. Fall, C. Mork, J.A. Perry, E. Sweeney, J. Wittouck, R.M. Kocan. 2002. Incidence of *Ichthyophonus hoferi* in Puget Sound fishes and its increase with age of adult Pacific herring. Journal of Aquatic Animal Health 14:50-56.

Hershberger, P.K., M.E.T. Stinson, B. Hall, A.J. MacKenzie, J.L. Gregg, W. Richards, J.R. Winton. *Submitted*. Pacific herring *Clupea pallasii* are not susceptible to vibriosis from *Vibrio anguillarum* or *V. ordalii* under laboratory conditions. Journal of Fish Diseases.

Kocan, R., M. Bradley, N. Elder, T. Meyers, W. Batts, J. Winton. 1997. North American strain of Viral hemorrhagic septicemia virus is highly pathogenic for laboratory-reared Pacific herring. Journal of Aquatic Animal Health. 9:279-290.

Kocan, R.M., P.K. Hershberger, N.E. Elder. 2001b. Survival of the North American strain of viral hemorrhagic septicemia virus (VHSV) in filtered seawater and seawater containing ovarian fluid, crude oil, and serum-enriched culture medium. Diseases of Aquatic Organisms. 44:75-78.

Kocan, R.M., P.K. Hershberger, N.E. Elder, J.R. Winton. 2001a. Epidemiology of viral hemorrhagic septicemia (VHS) among juvenile Pacific herring and Pacific sandlances in Puget Sound, Washington. Journal of Aquatic Animal Health. 13:77-85.

Kocan R., P. Hershberger, T. Mehl, N. Elder, M. Bradley, D. Wildermuth, K. Stick. 1999. Pathogenicity of *Ichthyophonus hoferi* for laboratory-reared Pacific herring (*Clupea pallasi*) and its early appearance in wild Puget Sound herring. Diseases of Aquatic Organisms 35:23-29.

Kramer-Schadt S., J.C. Holst, D. Skagen. 2010. Analysis of variables associated with the Ichthyophonus hoferi epizootics in Norwegian spring spawning herring, 1992-2008. Canadian Journal of Fisheries and Aquatic Sciences 67:1862-1873.

Lovy, J., N.L. Lewis, P.K. Hershberger, W. Bennett, K.A Garver. 2012. Viral tropism and pathology associated with viral hemorrhagic septicemia in larval and juvenile Pacific herring. Veterinary Microbiology 161:66-76.

Marty, G.D., E.F. Frieberg, T.R. Meyers, J. Wilcock, T.B. Farver, D.E. Hinton. 1998. Viral hemorrhagic septicemia virus, *Ichthyophonus hoferi*, and other causes of morbidity in Pacific herring *Clupea pallasi* spawning in Prince William Sound, Alaska, USA. Diseases of Aquatic Organisms 32:15-40.

Marty G.D., T.J. Quinn II, G. Carpenter, T.R. Meyers, N.H. Willits. 2003. Role of disease in abundance of a Pacific herring (*Clupea pallasi*) population. Canadian Journal of Fisheries and Aquatic Sciences 60:1258-1265.

Meyers T.R., A.K. Hauck, W.D. Blankenbeckler, T. Minicucci. 1986. First report of viral erythrocytic necrosis in Alaska, USA, associated with epizootic mortality in Pacific herring, *Clupea harengus pallasi* (Valenciennes). Journal of Fish Diseases 9:479–491.

Meyers, T.R., S. Short, K. Lipson. 1999. Isolation of the North American strain of viral hemorrhagic septicemia virus (VHSV) associated with epizootic mortality in two new marine host species of Alaskan Marine fish. Diseases of Aquatic Organisms 38:81-86.

Oye, A.K., E. Rimstad. 2001. Inactivation of infectious salmon anemia virus, viral haemorrhagic septicaemia virus, and infectious pancreatic necrosis virus in water using UVC irradiation. Diseases of Aquatic Organisms 48:1-5.

Purcell, M.K., S. Pearman-Gillman, R.L. Thompson, J.L Gregg, L.M. Hart. J.R. Winton, E.J. Emmenegger, P.K. Hershberger. 2016. Identification of the major capsid protein of erythrocytic necrosis virus (ENV) and development of quantitative real-time PCR assays for quantification of ENV DNA. Journal of Veterinary Diagnostic Investigation 28:382-391.

Salama, N.K.G., B. Rabe. 2013. Developing models for investigating the environmental transmission of disease-agents with open-cage salmon aquaculture. Aquacult. Env. Interact. 4:91-115.

Stewart, B.C., C. Olson, S. Lutz. 1990. VHS virus at Lummi Bay sea ponds, Bellingham, Washington. American Fisheries Society Fish Health Section Newsletter 18(1):2-3 (Bethesda, MD).

Wilson, A.E., T.L. Goldberg, S.V. Marquenski, W.J. Olson, R.F. Goetz, P.K. Hershberger, K.L. Toohey-Kurth. 2014. Development and evaluation of a blocking enzyme-linked immunosorbent assay and virus neutralization assay to detect antibodies to viral hemorrhagic septicemia. Clinical and Vaccine Immunology 21:435-442.

Winton, J.R., W.N. Batts, R.E. Deering, R. Brunson, K. Hopper, T. Nishizawa, C. Stehr. 1991. Characteristics of the first North American Isolates of viral hemorrhagic septicemia virus. In: Proceedings of the Second International Symposium on Viruses of Lower Vertebrates. Oregon State University Press, Corvallis. PP. 43-50.

Winton, J.R., P.K. Hershberger. 2014. Viral Erythrocytic Necrosis. *In*: Fish Health Section Blue Book: Suggested Procedures for the Detection and Identification of Certain Finfish and Shellfish Pathogens. American Fisheries Society. Accessible at: http://www.afs-fhs.org/perch/resources/14069231372.2.7ven2014.pdf